nature portfolio

Peer Review File

Evolution and heterogeneity of lethal metastatic bladder cancer subtypes

Corresponding Author: Dr Gavin Ha

Any redactions in this file are there to maintain patient confidentiality, the confidentiality of unpublished data, or to remove third-party material.

This file contains all reviewer reports in order by version, followed by all author rebuttals in order by version.

Version 0:

Reviewer comments:

Referee #1

(Remarks to the Author)
The authors perform multi-omic profiling of bladder tumors from a rapid autopsy cohort accrued and analyzed at their institution. Notably, the cohort is enriched in variant histologic subtypes, which occur in a subset of bladder cancer cases, but which are generally understudied in terms of biology and clinical trials. The authors leverage a variety of techniques including WGS, bulk and single cell RNA-sequencing, and cfDNA analyses to investigate important features of metastatic disease that are only addressable with this type of autopsy cohort in which multiple samples from patients at a specific timepoint are available. Specifically, the phylogenetic reconstructions identify multiple interesting examples of tumor-to-met, met-to-met, and polyclonal patterns of seeding. Similarly, patterns of acquisition of pathogenic alterations seemed to vary across patients and histologic subtypes. Perhaps not surprisingly given the end-stage nature of the cohort, the majority of driver alterations, and an impressive percentage of all mutations, could be observed from cfDNA, with nucleosomal profiling identifying known features of specific subtypes (eg ASCL1 positioning in NE patient). The single cell RNA sequencing identifies tumor cell features reflective of biology captured in part by the consensus subtypes defined and validated using bulk RNA sequencing. Immune and stromal cell features vary across histologic subtypes, with immune-enriched TME in PUC and immune-suppressive TME in UCSD, both of which have been described in some fashion albeit not at single cell resolution. Overall this comprehensive effort applying state-of-the-art approaches represents a significant advance and will be of immediate broad interest and serve as a resource for the field. I have some comments that the authors can hopefully address prior to potential publication.

More detail regarding histology-based tumor assignments should be provided. For example, is the definitive UC/PUC/UCSD/etc identify for each patient made based only on H&E/IHC analysis of the primary tumor? In addition, for all tumors with variant histology, the % of variant vs conventional histology (as assessed by the pathologist from review of primary tumor at diagnosis) should be provided (ie, were these 100% plasmacytoid tumors or UC with some % of plasmacytoid component)? Given the emphasis on properties of variant subtypes, it should be clearly stated how each of these cases would align with the way these subtypes are typically defined in routine clinical practice.

The projection/MIP-like images in Fig 2A-C are of limited value since the lesions being referenced cannot be observed. Would recommend using individual axial/coronal/sagittal CT images instead (as are used in Sup Fig 2).

Direct comparison/description of WGS features the from initial diagnostic/pre-treatment biopsy (or RC specimen) of the primary bladder tumor to any residual/recurrent bladder tumor harvested at autopsy should be performed when possible. Similarly, at least some of these patients likely had biopsy of a metastatic site while they were alive that was later harvested/analyzed at autopsy. How similar/different are features from the same metastatic site in these cases?

How was the value of 2.3 clones/seeding event chosen for analysis in Fig 2D?

For analysis in Fig 2G, did some of the ICI-treated patients get chemo before (or with) ICI? Is the comparison really chemo-only vs chemo-then-ICI?

For the founder analyses in Figure 3, it would be interesting to compare founder profiles of metastases that did vs didn't seed additional metastases. Along these lines, an asterisk should be added to denote cases for which the analyzed bladder tumor was the tumor collected at time of diagnosis/presentation (rather than at time of autopsy)….it would be reasonable to assume that the primary may resemble metastases to greater/lesser extent depending on when the bladder tumor was harvested/analyzed.

Were platinum signatures identified in patients who did not receive platinum-based chemo? This should be stated explicitly.

The sentence in lines 196-199 needs to be corrected to state that no differences in gene expression of the assessed pathways were noted. It remains possible that any/all of these pathways could be biologically altered in the tumor, but just not as defined by changes at the transcript level. Also, there was a $p<0.05$ effect for GSH (Sup Fig 9), but this was not chosen for further analysis while the authors did choose to focus on the difference in FA pathway with $p=0.071$. There would be some biological plausibility for altered GSH/redox signaling as a potential cisplatin resistance mechanism.

Does FANC pathway expression correlate with cisplatin sensitivity in bladder cancer cell lines in publicly available databases such as DepMap and/or COSMIC? This should be checked and reported.

Cisplatin causes a variety of DNA lesions including intra- and interstrand crosslinks. The FANC pathway is specialized for repairing interstrand crosslinks; therefore, it would be useful to test an agent such as mitomycin-C that specifically creates interstrand crosslinks in the assays resulted in Fig 4F-H.

Are there other tumor settings (beyond bladder) in which the FANC signature has been associated with cisplatin signatures or (more likely) cisplatin sensitivity? There are some tumor types such as HNSCC, ovarian cancer, and some NSCLCs that would receive cisplatin-based chemo as standard of care and likely have RNA-seq data sets available.

For the cfDNA analysis, the expected differences between WGS and targeted panel (TP) should be discussed briefly because the rationale (assuming its sequencing depth) for using both is not currently clear from the main text or Figure 7.

The nature of the x-axis values for Fig 7F is not clear. Tumor purity (from each tumor/met? As a fraction between 0-1? times tumor volume (of which metastasis? Or combined across all gross/radiologic mets?)

The following sentence in the Discussion is unclear: "Remarkably, increased transcriptional heterogeneity was associated with longer survival in patients. These findings suggest that, in cases where the original tumor is less aggressive, heterogeneity that accumulated over time led to lethality." I'm not following the logic, and in any case, its not possible from the data to know whether heterogeneity is actually driving mortality.

(Remarks on code availability)
I reviewed the code at a high level and it looks to have sufficient detail to reproduce results, but I don't have sufficient expertise to comment on more subtle aspects.

Referee #2

(Remarks to the Author)
A. Summary of the key results
The authors performed a very interesting and broad multi-omic analysis on a bladder cancer rapid autopsy cohort of tumor/normal samples from 20 metastatic patients, including analysis of aggressive rare histological subtypes. Their main objective was to provide a comprehensive characterization of metastatic tumor evolution and molecular heterogeneity for these histological subtypes, which is currently limited. They performed whole genome or exome sequencing to study genomic tumor evolution, heterogeneity, and metastatic seeding. Bulk RNA-seq and single-nucleus RNA-seq to study transcriptional heterogeneity and the tumor microenvironment cfDNA targeted and whole genome sequencing from plasma or serum was performed to evaluate genomic heterogeneity, clonal contribution, and transcriptional activity. A cohort of N=20 patients with N=120 samples (primary tumors N=20, metastatic sites N=80; N=20 benign) was used for analyses (N=47 UC, N=22 plasmacytoid, N=18 UC + squamous diff, N=8 NE and N=5 sarcomatoid).

The authors start with mapping the clonal tumor evolution to metastatic growth and sequence of seeding by combining WGS/WES, phylogenetic analyses and radiological imaging. They show that divergent clonal seeding is associated with aggressive histological variants and treatment with ICI.
They show the importance of multiple tumor sampling to be able to fully capture genomic alterations for treatment guidance and show that mBLCA progression is characterized by early clonal driver events and continued evolution through instances of increasingly complex genomic structural alterations. Within the histological variants, they show that pathogenic genomic driver alterations in the founder clone at disease initiation promote early aggressiveness in PUC and NE tumors. In UC and UCSD, pathogenic alterations acquired throughout tumor evolution likely contributed to progression later in the disease course. Interestingly, their data supports a mechanism by which PUC tumors have increased activity of the FANC pathway and ability to repair cisplatin-induced crosslinks compared to UC/UCSD tumors, which may underlie the difficulty in treating this aggressive subtype that often progresses quickly on platinum-based therapies and this is functionally validated in cell line experiments.

The second part focuses on transcriptome analyses, and they are the first to show that the variant histology PUC metastases were luminal-unstable while the primary tumors were stroma-rich, linking tumor subtype heterogeneity to tumor

aggressiveness. They are the first to study the TME of variant histologies at single-cell resolution and show that differing levels of immune activation and immunosuppression across mBLCA histological subtypes and metastatic sites has potential implications for immunotherapy response in end-stage disease.

In the last part, they show that most early and driver alterations can be readily captured from cfDNA, while detection of later-evolving SNVs is influenced by clonal burden, tumor volume and purity, and cfDNA tumor fraction (TFx).

B. Originality and significance: if not novel, please include reference
The work presented is very relevant to the field and has not been performed by other groups. Urothelial cancer with variant histology represents a challenge in clinical-decision-making and treatment selection. Although the cohort size is limited, the findings are very relevant and important to the field. The techniques used are not novel to the field, but still very relevant.

Furthermore, the study is unique, being a rapid autopsy program on urothelial cancer and the authors have to be congratulated that they have been able to include 20 patients within a 5-year time frame. The comprehensive characterization of primary tumors and matched metastases further enforces the importance of the study.

C. Data & methodology: validity of approach, quality of data, quality of presentation
The authors used a very comprehensive approach which is valid for the posed research question/research gap: WGS/WES, bulk RNA-seq, snRNA-seq (all on tissue) and detection of ctDNA in blood.
Some point to consider:
- Although in some cases the authors validated their findings in external cohorts, in most cases their broad conclusions are based on comparisons of relatively small groups of patients (N = 16).
- This study identified instances of alterations in key mBLCA genes (e.g. ARID1B, PIK3CA/B, and NECTIN4) that were absent in the primary tumor but acquired later in metastases, and conversely others were found only in the primary tumor but not in metastases (e.g. KMT2D in patient 19-007). Can they confirm this claim by analyzing the HMF and TCGA data or by referring to relevant studies, e.g. PMID: 28988769, PMID: 31645765?
- Purity of non-conventional UCs may affect results regarding polyphyletic events and survival, as the proportion of non-conventional UC versus conventional UC has been linked to survival. Can the authors discuss whether differences in % of non-conventional UC may have affected interpretation, especially for PUC?
- Are there differences in survival between patients who developed liver metastases and those without? In general, patients with liver metastases have poorer outcomes than patients with lymph node metastases.
- Platinum chemotherapy may affect clonal selection and induce new mutations that are classified as subclonal. Were there significant time differences between chemotherapy and sample collection across patients and tumor subtypes? Shorter intervals may hinder the discovery of new mutations because of low VAF, specifically if this is true for PUC tumors.
- From the methods, it appears that metastatic samples were obtained at the time of death. Were the primary samples obtained before autopsy was performed and could the authors elaborate how this was done? If primary samples were not obtained at autopsy, new subclonal populations in primary tumors (if still present during metastatic development) may have not been captured in the analysis, especially upon selective pressure of therapy, and the metastases-to-metastases seeding may be overestimated.
- Did all 20 patients receive a CT-scan of thorax and abdomen at 3 and 6 months before death? Due to the nature of a rapid autopsy program, it seems unlikely to have all patients undergo radiological imaging at fixed time points before death. This is of importance because the authors use imaging to corroborate ordering of the computationally inferred metastatic seeding, line 95 – 106. Were all CT-scan centrally reviewed by an independent radiologist and were all metastatic sites confirmed? As CT-scanning is a snapshot, small metastases at t= -3 mo or t = -6 mo, might have been missed and they may have become large metastases at the moment of death.
- Although Figure 1A demonstrates the origin of the primary tumor and metastases, the authors are encouraged to provide additional information per individual patient and show how many metastatic sites per patient were harvested and what was primary histology of the primary tumor versus those of the harvested metastatic sites? In addition, what was the origin of the 20 benign samples?
- Independent pathology review of all primary tumors with pure conventional UC and metastases with variant histology would improve the quality of the study. In addition, it is important to discriminate between urothelial carcinoma with variant histology, like plasmacytoid or micropapillary UC, while small cell neuro-endocrine carcinoma of the bladder or squamous cell carcinoma of the bladder are different histology. Were all tumors with squamous or NE differentiation in the study predominant urothelial carcinoma? Please clarify. Suggest using variant histology instead of histological subtypes. In addition, not all variant histologies in bladder cancer correlate to poor prognosis, i.e. glandular, lympho-epitheliod. Furthermore, the poor prognosis of VH is predominantly caused by metastatic spread, such as small cell neuro-endrocrine bladder cancer or micropapillary urothelial carcinoma. However, plasmacytoid urothelial bladder cancer typically is characterized by local spreading of tumor, which is clinically not apparent leading to a very high risk of positive surgical margins in patients undergoing radical surgery. I would suggest adjusting the abstract and taking these remarks into account.
- Please provide justification for the cutoff used for highly polyclonal seeding (2.3) as this is correlated to poor survival, line 107-110 and Figure 2D. In addition, t=0 is the time of diagnosis, but some patients were diagnosed with primary metastatic disease whereas others had MIBC but were cM0 at moment of diagnosis. Can the authors explain how they conducted the survival analysis shown in Fig 2?

D. Appropriate use of statistics and treatment of uncertainties
Line 1813 briefly mentions the statistical tests used but from the information provided it is not possible to judge their appropriate use and the treatment of uncertainties.

E. Conclusions: robustness, validity, reliability
Although a limited number of patients was analyzed, methods used and data analyses are very comprehensive and robust. Whenever a validation was possible (on other cohorts), the authors performed the validation and also set out to perform a functional validation by using cell lines.

F. Suggested improvements: experiments, data for possible revision
In general, there is a need for check of figures/tables for completeness and accurate numbers.
For example:
- Discrepancy: Figure 1 right panel: #tumors for WGS/WES N=89, text line 66 states “all” (N=100)
- Supp Table 1 sheet 1 should contain NGS info from all samples but only contains N=8 patients
- Supp Table 3 sheet 1 should contain counts of seeding events for all analyzed metastatic samples, now only contains N=2

G. References: appropriate credit to previous work?
Yes

H. Clarity and context: lucidity of abstract/summary, appropriateness of abstract, introduction and conclusions
- Good structure, good readability though the authors are encouraged to check that past tense is used throughout the entire manuscript. See for examples line 47, 62, and 118-120.
- The authors use histological variation and histological subtype throughout the abstract. Did the authors considered using variant histology?
- Limitations of the study are lacking in the abstract and main text.
- Only 5 authors have reported COI, which seems limited.

Prof. dr. J.L. Boormans
Dr. T.C.M. Zuiverloon
Dr. J.N. Nakauma - Gonzalez

(Remarks on code availability)
Our bioinformatician has reviewed the code and was onsidered appropriate. The data presented in the paper are reproducible and a usable resource to the community.

Referee #3

(Remarks to the Author)
Itagi et. al. present data from a rapid autopsy program that has collected primary and metastatic tumors from bladder cancer patients, specifically enriching for histologic subtypes. They go on to complete comprehensive molecular profiling of both the tumors and mets and relate these findings back to the histologic subtypes and clinical features. This study representing an enormous effort by all the investigators involved and should be commended, not only for their findings but for the high-quality data they have generated.

The true strength of this manuscript is the comprehensiveness of the molecular profiling and the amount of data that was generated, which I am sure will aid in numerous subsequent discoveries across the research community. However, there is an overall lack of integration between omic platforms and tissue sources (primary/met/normal). While the focus on histologic subtypes is interesting and unique feature of this work, the layering of more clinically relevant questions, such as clonal evolution and adaptation in response to therapy could have added to the broad impact of this work (specific comments below).

In total, the study as currently presented, does lack the paradigm shifting impact typically seen in a Nature publication, however, it represents an outstanding compilation of high quality data, which as a resource, would be of considerable interest to the Nature readership.

Specific comments:
1) Regarding the relationship between ICI and clonal evolution. Using imaging and clinical record, can the authors compare the clonal composition of mets that that were present prior to ICI versus those that developed after ICI (e.i. ICI did not impose pressure on the met itself but rather the tumor that seeded the met). Does ICI change which cells are able to migrate and where they migrate to or does it selectively effect specific populations within the tumor?

2) The authors state that PUC and NE are driven by early events as represented by an increased proportion of founder mutations. Is this a reflection of PUC and NE having histologic variant specific driver events, such as CHD1 loss for PUC and/or >75% of the tumor displaying PUC (whereas the UCSD is focal). More broadly, how does the varying extent of histologic subtypes component of the UC effect the analysis and conclusions?
3) I appreciate the authors trying to functionally link the FANC pathway to PUC cisplatin resistance. However, this needs to be done in a more rigorous fashion if this section is to remain in the paper. Specifically, does knockdown or overexpression of the pathway in the given cells reverse the phenotype. Evidence of DNA repair modulation (such as gammaH2AX staining) would bolster the conclusions.

4) In tumors that displayed mix phenotypes (75% PUC or 5% UCSD), is there similar proportionality represented in the

snRNAseq and do the transcription pattern vary between the populations? How does treatment, ICI or chemo interact with the heterogeneity and by extension survival?

5) By identifying met specific TFBS signatures, can you link cfDNA back to specific mets. Are specific locations of metastasis more likely to release cfDNA into the circulation?

6) Does time until autopsy contribution to the levels of cfDNA detected?

(Remarks on code availability)
Code is appropriately accessible and annotation.

Referee #4

(Remarks to the Author)
I co-reviewed this manuscript with one of the reviewers who provided the listed reports.

(Remarks on code availability)
The code is well structured and documented. It contains a README file and each folder for a specific analysis is well documented. The instructions and steps can be followed to reproduce the data. The code can be downloaded and be adapted to run internally.

Referee #5

(Remarks to the Author)
I co-reviewed this manuscript with one of the reviewers who provided the listed reports.

(Remarks on code availability)

Version 1:

Reviewer comments:

Referee #1

(Remarks to the Author)
Thank you to the authors for their comprehensive and organized approach to responding to my comments. Overall, I believe the revisions have strengthened the manuscript and that the core genomic findings are solidly supported and correctly interpreted. The clinical cohort and data sets are highly unique and the same or even similar analyses are unlikely to be available from any other center in the near to intermediate term. Therefore, I believe the findings are of high impact and will be broadly useful and interesting to the bladder cancer and tumor evolution fields. I think the findings regarding the relationship between FANC pathway expression and cisplatin mutational signatures and sensitivity will need to be validated and further mechanistically interrogated in future work, and I have made some suggestions below regarding softening the language and interpretations for these findings.

Regarding responses to specific comments:

1.1: The additional data regarding subtype % is appreciated, and its reassuring to see that, for the majority of cases, the variant histology was quite dominant. For the rare cases with similar % of classic UC and variant histology in some specimens (such as 17-071), was there an attempt to use macro/microdissection to isolate UC and variant components and perform separate analyses on each? For the few SARC and UCSD cases with minimal % variant histology, it feels more difficult to really consider these as reflecting biology of the variant component: for example, 19-004 was annotated as a SARC case, but two samples had 0% sarcomatoid histology, two samples had 5%, and only one had majority (70%) sarcomatoid histology. Changes to the text have been made to describe

1.2: I understand the rationale for keeping the MIPS in Figure 2 and appreciate the effort to included annotated CT slides in the Extended Data.

1.3: I appreciate the effort to include analysis of primary TURBT samples when available, and I think integration of these findings into the manuscript provides important additional insights and context regarding the case-specific relationship among primary bladder tumor, autopsy bladder tumor, and autopsy metastatic sites.

1.4: I agree with the authors that a multivariable Cox model is a more robust method for analyzing the prognostic impact of polyclonal seeding in the context of known clinical prognostic factors.

1.5: Thank you for performing the updated analysis, and I do think the difference in findings in the updated results is notable. An alternative (or perhaps supplementary) interpretation of the differences in ‘pre-ICI’ vs ‘post-ICI’ metastasis properties is that these differences are not driven by ICI pressure directly but rather simply reflect the biology of the more advanced

disease state in which patients would have received ICI. One way to test this might be to separate metastasis from chemo-only patients into “early” vs “late” developing metastasis and comparing frequency of polyclonal polyphyletic events in these two groups. At the least, the potential for both ICI pressure or disease stage to contribute to the differences in pre- vs post-ICI metastasis properties should be noted.

1.6: Similar to response to 1.3 above. It is interesting and perhaps reassuring (from technical perspective) that the source of primary tumor collection (esp TURBT vs surgery) did not seem to impact clonal composition between primary and mets.

1.7: I worry that readers who don’t read the reviewer comments and responses may have the same concern regarding signature specificity that I initially had, especially now that the cisplatin signature has been specifically excluded from analysis of the non-platinum treated patients. Including some version of the response text (“…we found a cis signature in 1 platinum-treated patient…we acknowledge its an artifact likely due to low mutation count…we therefore excluded the cis signatures for the analysis of the non-cis patients…”) in the Methods or Extended Data would be appropriate.

1.8: Explanation and changes based on my comments are reasonable.

1.9: The response and additional analyses are reasonable, particularly in light of the additional experiments performed to address subsequent comments (see below).

1.10: It is slightly disconcerting that the relationship between FANC status and MMC does not hold up as it did with cisplatin, given that MMC is the drug classically associated with exquisite sensitivity in the FANC-deficient setting. I appreciate the potential reasons raised by the authors in their response to my initial comment, but I would suggest being slightly more forthcoming in the text by directly stating that there was not a difference in phenotype between FANC hi and lo lines using the same approach that was used to identify the difference with cisplatin, but that there was a modest difference (in the expected direction) when additional approaches were applied.

It is somewhat surprising that over-expression of a single member of the FANC pathway (FANCF), albeit a critical component, is sufficient to partially overcome cisplatin sensitivity in a FANC-low cell line. Given that the FANC signature is calculated from levels of dozens of FANC gene transcripts, it is not necessarily obvious that over-expressing a single member of the pathway will change pathway activity (unless its known that the level of that specific protein is the activity-limiting feature of the pathway).

(Remarks on code availability)
I reviewed the code but am not an expert and therefore may not appreciate all relevant nuances.

Referee #2

(Remarks to the Author)
We would like to thank the reviewers for their extensive work and structured comments to our review. We believe the manuscript has improved substantially. We have no further comments in addition to our previous comments that were all addressed by the authors.

(Remarks on code availability)

Referee #3

(Remarks to the Author)
I would like to thank the authors for their extensive and detailed revisions and responses. The authors have addressed all my concerns and they should be congratulated for their outstanding manuscript.

(Remarks on code availability)

Referee #4

(Remarks to the Author)
I co-reviewed this manuscript with one of the reviewers who provided the listed reports.

(Remarks on code availability)
The code is well documented and it can be used for replication studies.

Referee #5

(Remarks to the Author)
I co-reviewed this manuscript with one of the reviewers who provided the listed reports.

(Remarks on code availability)

Version 2:

Reviewer comments:

Referee #1

(Remarks to the Author)
The authors have sufficiently addressed my concerns with appropriate updates to the text; I recommend publication.

(Remarks on code availability)
I reviewed the code and it seems appropriate, although I'm not a coding expert.

We thank the reviewers for their thoughtful reading of our manuscript and for providing excellent suggestions. We believe the manuscript has greatly benefited from addressing these comments. Below, we have included a brief summary of the major revisions and additions, followed by point-by-point responses to reviewer comments.

Summary of Key Revisions

1) Addition of TURBT samples for temporal clonal analysis

We performed a comparison of clonal dynamics between primary tumors acquired at autopsy and at initial diagnosis by transurethral resection of the bladder tumor (TURBT). We were able to acquire TURBT specimens for four patients to perform a temporal analysis. We observed distinct evolutionary patterns leading to clonal divergence where *(i)* both primaries (TURBT and autopsy) were more similar to each other than the metastases; *(ii)* metastases were more similar to the TURBT primary than the primary at autopsy; and *(iii)* the autopsy primary tumor exhibited selection and expansion of a minor subclone.

Addresses Reviewer **Comment 1.3**. See **Response 1.3** and **1.6**.

2) New experiments examining Fanconi Anemia DNA repair in bladder cancer cell lines

We performed four new sets of experiments to further support the relationship between the Fanconi anemia pathway and cisplatin resistance in BLCA. By repeating the bladder cancer cell line experiments using mitomycin C (**Response 1.10**), we verified that resistance to chemotherapy in FANC-high cells stemmed from FANC repair of inter-strand crosslinks. Reciprocal knockdown and overexpression experiments of *FANCF* (**Response 3.3.1**) demonstrated that modulating key FANC genes is sufficient to alter cisplatin response. Longitudinal monitoring of γH2AX foci (**Response 3.3.2**) confirmed increased DNA repair in FANC-high cell lines when compared to FANC-low BLCA cells.

Addresses Reviewer **Comments 1.10** and **3.3**. See **Responses 1.10**, **3.3.1**, and **3.3.2**.

3) Acquisition and analysis of additional patient CT scans

We acquired 44 additional computed tomography (CT) scans. These now represent the complete set of clinical scans available for all 20 patients, each evaluated by a radiologist and a radiation oncologist to identify metastases sampled at autopsy. With these additional scans, matched staging studies spanning metastatic evolution were available for two new patients to corroborate metastatic seeding patterns, bringing the total to five (**Figure 2A, Response 2.6**). These scans also allowed us to time the emergence of metastases relative to treatment with immune checkpoint inhibitors (ICI), revealing increased complexity of metastatic seeding and greater clonal expansion in tumors arising post-ICI (**Responses 1.5** and **3.1**). Lastly, additional scans strengthened the analysis between cfDNA and radiological tumor volume (**Figure 7F**).

Addresses Reviewer **Comments 2.6** and **3.1**. See **Responses 1.5**, **2.6**, and **3.1**

4) Clarification of tumor histological subtype purity

All Reviewers brought to our attention the need for further details on the proportion of variant histology in each sample to aid in analysis interpretation. We have performed additional review of the tumor pathology with an independent pathologist (F.V.L.) to quantify the percent of each histological subtype in each tumor (**Supplementary Table 1**). This is now used as a covariate in our analyses (see **Responses 2.2** and **3.2**). Importantly, PUC and NE tumors in our cohort had predominantly pure variant histology.

Addresses Reviewer **Comments 1.1, 2.2, 2.7, 2.8, 2.9, 3.2, and 3.4**.

Referee #1 (Remarks to the Author):

The authors perform multi-omic profiling of bladder tumors from a rapid autopsy cohort accrued and analyzed at their institution. Notably, the cohort is enriched in variant histologic subtypes, which occur in a subset of bladder cancer cases, but which are generally understudied in terms of biology and clinical trials. The authors leverage a variety of techniques including WGS, bulk and single cell RNA-sequencing, and cfDNA analyses to investigate important features of metastatic disease that are only addressable with this type of autopsy cohort in which multiple samples from patients at a specific timepoint are available. Specifically, the phylogenetic reconstructions identify multiple interesting examples of tumor-to-met, met-to-met, and polyclonal patterns of seeding. Similarly, patterns of acquisition of pathogenic alterations seemed to vary across patients and histologic subtypes. Perhaps not surprisingly given the end-stage nature of the cohort, the majority of driver alterations, and an impressive percentage of all mutations, could be observed from cfDNA, with nucleosomal profiling identifying known features of specific subtypes (eg ASCL1 positioning in NE patient). The single cell RNA sequencing identifies tumor cell features reflective of biology captured in part by the consensus subtypes defined and validated using bulk RNA sequencing. Immune and stromal cell features vary across histologic subtypes, with immune-enriched TME in PUC and immune-suppressive TME in UCSD, both of which have been described in some fashion albeit not at single cell resolution. Overall this comprehensive effort applying state-of-the-art approaches represents a significant advance and will be of immediate broad interest and serve as a resource for the field. I have some comments that the authors can hopefully address prior to potential publication.

Comment 1.1) *More detail regarding histology-based tumor assignments should be provided. For example, is the definitive UC/PUC/UCSD/etc identify for each patient made based only on H&E/IHC analysis of the primary tumor? In addition, for all tumors with variant histology, the % of variant vs conventional histology (as assessed by the pathologist from review of primary tumor at diagnosis) should be provided (ie, were these 100% plasmacytoid tumors or UC with some % of plasmacytoid component)? Given the emphasis on properties of variant subtypes, it should be clearly stated how each of these cases would align with the way these subtypes are typically defined in routine clinical practice.*

Response 1.1) We defined histology based on each tumor specimen (both primary and metastases) within a patient. Specifically, we defined the patient-level histology as variant histology (PUC, UCSD, NE, or UC-Sarc) if there is evidence of the non-UC histology in at least one tumor in the patient. Similarly, tumor-specific histology was defined as variant if there was any percentage of non-UC morphology in the tumor. The presence and proportion of each histological subtype in each specimen (primary and metastases) was determined by pathological assessment of H&E sections by a board-certified pathologist (F.V.L.). Neuroendocrine histology was further verified by positive synaptophysin staining. These methods are consistent with the clinical classifications outlined by the WHO Classifications of Tumours of the Genitourinary System and Male Genital Organs (*5th edition*).

These details have been clarified in the Methods and the Results. The proportion of each histological subtype in each primary and metastatic tumor has been added to **Supplementary Table 1** (1st sheet: columns hist_detailed, UC_percent, UCSD_percent, PUC_percent, SARC_percent, and NE_percent), in addition to the annotation of both patient-level and tumor-level histology (hist_patient and hist_sample).

Methods, lines 847-861:

> ***"Histology was defined both at the patient level and the tumor (sample) level. All classifications were based on pathology assessment of FFPE H&E specimens by***

pathologist (F.V.L.) review based on the WHO Classifications of Tumours of the Genitourinary System and Male Genital Organs (5th edition)[25]. Neuroendocrine histology was further verified by synaptophysin positivity. PUC, UC-sarcomatoid, and UCSD tumors are urothelial carcinoma with plasmacytoid, sarcomatoid, or squamous differentiation, respectively. Patients and tumors were designated as non-UC if there was any evidence of variant histology. For patient-level histology, the histology was defined as a variant if there was evidence of subtype histology in any tumor in that patient (e.g., if a patient had any tumor exhibiting any squamous differentiation, they were classified as UCSD). Patients 16-070, 17-030, 18-101, and 19-022 were designated UCSD by having a mix of UC and UCSD tumors, while all tumors in UCSD patients 16-097 and 17-026 exhibited UCSD histology. Sample-level histology was defined for each tumor individually (e.g., 16-070's primary tumor is UCSD, while their metastases are UC at the sample level). Further details on the percentage of histological subtypes in each tumor are given in Supplementary Table 1 (1st sheet)."

Results, lines 60–65:

"Tumors represented a spectrum of histological subtypes[25], including 50 with conventional urothelial carcinoma (UC) and an enrichment of subtypes: 24 plasmacytoid UC (PUC), 19 UC with squamous differentiation (UCSD), 8 neuroendocrine (NE), and 3 UC with sarcomatoid subtype (UC-Sarc). PUC and NE tumors were predominantly variant histology (mean 96% PUC and 98% NE, respectively), whereas UCSD and UC-sarcomatoid tumors had variable subtype histology ranging from focal to extensive (Supplementary Table 1)."

Comment 1.2) *The projection/MIP-like images in Fig 2A-C are of limited value since the lesions being referenced cannot be observed. Would recommend using individual axial/coronal/sagittal CT images instead (as are used in Sup Fig2).*

Response 1.2) We appreciate the reviewer making this suggestion. In most cases, individual axial/coronal/sagittal CT slices did not capture all the lesions we wished to illustrate, due to their non-coplanar locations. Because the metastases are not all on the same plane, a single CT slice will only show certain lesions and miss others; we did not have adequate space in the main figure to display all the necessary slices. While we elected to keep the 2D projections (DRR's generated from the CTs) in **Figure 2A**, we agreed with the reviewer that the complete images were more informative; therefore, we have expanded **Extended Data Fig. 2** to include detailed axial, coronal, and sagittal CT images capturing every metastatic lesion shown in **Figure 2A.** These slices are color matched and annotated to clearly show all metastatic lesions and their relationship to the 2D projections. We also edited the **Figure 2A** legend to clarify that these images are 2D projections and that individual CT slice images that can be found in the supplement:

Figure 2A legend:

"2D projection images of computed tomography (CT) scans show the ordering of metastatic development from the patient's first to last clinical staging scans. Individual axial, coronal, and sagittal cross-sectional images of the CT scans are shown in Extended Data Fig. 2A-E."

Extended Data Fig. 2A-E includes detailed axial, coronal, and sagittal CT images for each of the 5 patients in **Figure 2**. Additionally, **Extended Data Fig. 2F-G** display cross-sectional images for the patients whose order of metastatic seeding was not able to be determined by CT images and for the patients treated with immunotherapy (**see Response 3.1**), respectively, such that all

analysis involving CT scans is represented by individual images. Here is an excerpt of the first patient from **Extended Data Fig. 2A**:

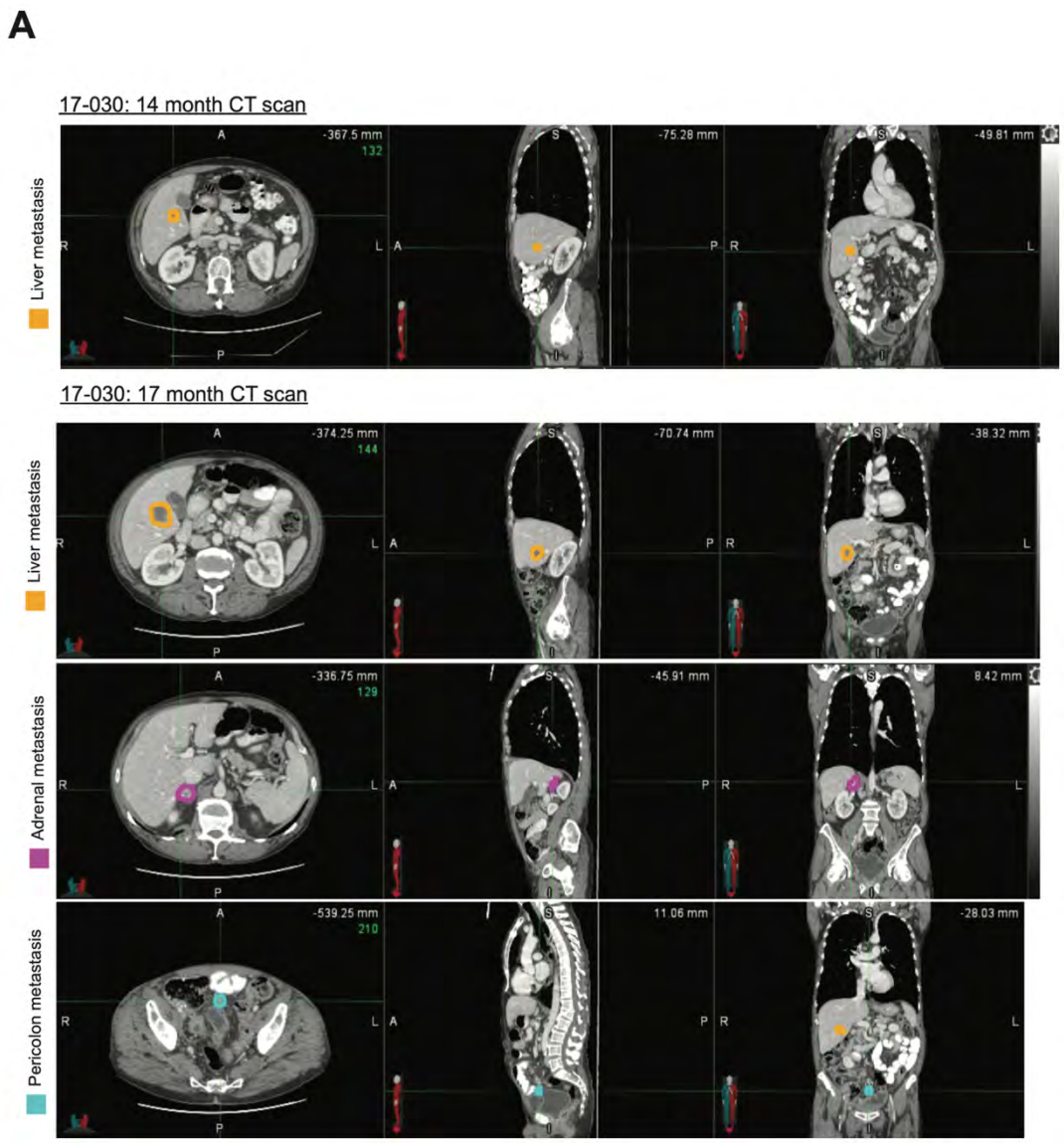

Extended Data Figure 2. A) *Coronal, sagittal, and axial CT cross-sections from all CT scans shown in Figure 2A as two-dimensional projections for patients 17-030.*

Comment 1.3) *Direct comparison/description of WGS features the from initial diagnostic/pre-treatment biopsy (or RC specimen) of the primary bladder tumor to any residual/recurrent bladder tumor harvested at autopsy should be performed when possible. Similarly, at least some of these patients likely had biopsy of a metastatic site while they were alive that was later harvested/analyzed at autopsy. How similar/different are features from the same metastatic site in these cases?*

Response 1.3) We thank the reviewer for these important suggestions. The IRB protocol for the rapid autopsy program did not include acquiring metastatic biopsies while the patients were alive and thus we do not have access to these samples. However, we were approved to retrieve diagnostic tissue from transurethral resection of bladder tumor (TURBT). Of the eight patients whose sequenced primary tumor sample was from autopsy, we obtained additional archival

TURBT specimens from diagnosis for four (17-020, 17-026, 18-016, 19-007). The remaining four patients' TURBT samples could not be retrieved; they had been discarded since it had been over 10 years since these patients' diagnosis. We performed whole genome sequencing (WGS) on these archival FFPE samples, analyzed genomic alterations, and refined our seeding analysis for these cases. The details for these four TURBT samples are included in the Results, Methods, **Figure 1A**, and **Supplementary Table 1**.

Results, lines 56-59:

> ***"Primary tumors were obtained at diagnosis from transurethral resection of bladder tumor (TURBT, n=5), from surgery (n=11), or at the time of autopsy (n=8); four patients had samples from both TURBT and at autopsy."***

Methods, lines 834-836:

> ***"In accordance with IRB-approved study protocols, no metastatic biopsies collected from living patients were obtainable for use in this analysis."***

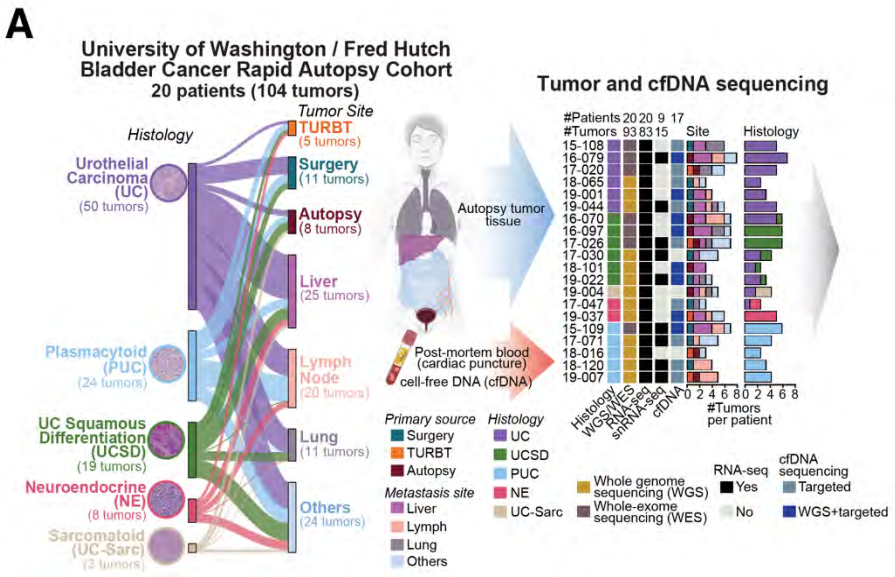

Figure 1. A) Schematic and description of the UW/Fred Hutch rapid autopsy cohort, involving 20 patients from 2015-2020. Sankey diagram shows histological subtype classification and anatomical sites of all 104 primary and metastatic tumors (left panel). Middle panel shows sequencing performed for each patient (bulk DNA and RNA sequencing, snRNA-seq, and cell-free DNA sequencing) and the number, tumor site, and histology of all primary and metastatic samples for each patient (see also **Supplementary Table 1**). Right panel summarizes the analyses undertaken for this study. Dx, diagnosis; ICI, immune checkpoint inhibitor; Met, metastasis; TURBT, transurethral resection of bladder tumor.

Response 1.3 cont'd) To compare between primaries taken from TURBT (early diagnostic) and at autopsy for each of these four patients, we performed three types of analyses:

(i) *Genomic pathogenic alterations:* We compared pathogenic alterations between TURBT and autopsy primaries, as well as how the primaries compared to metastases. In patient 17-026, nine pathogenic copy number alterations, including *TP53* loss and *EGFR* gain, were shared between the TURBT sample and the metastases but not with the autopsy primary. In patient 17-020, driver events in *BRCA1* and *NECTIN4* were shared only among metastatic samples and absent from both primaries. In patient 19-007, a *KMT2D* frameshift deletion was observed only in the primary at autopsy (**Extended Data Fig. 4D),** suggesting continued evolution in the intact primary. In

patient 18-016, all pathogenic alterations were observed in both primaries. These results for all four patients are shown in **Fig. 3A** and discussed in lines 150-153 and 165-169 of the results.

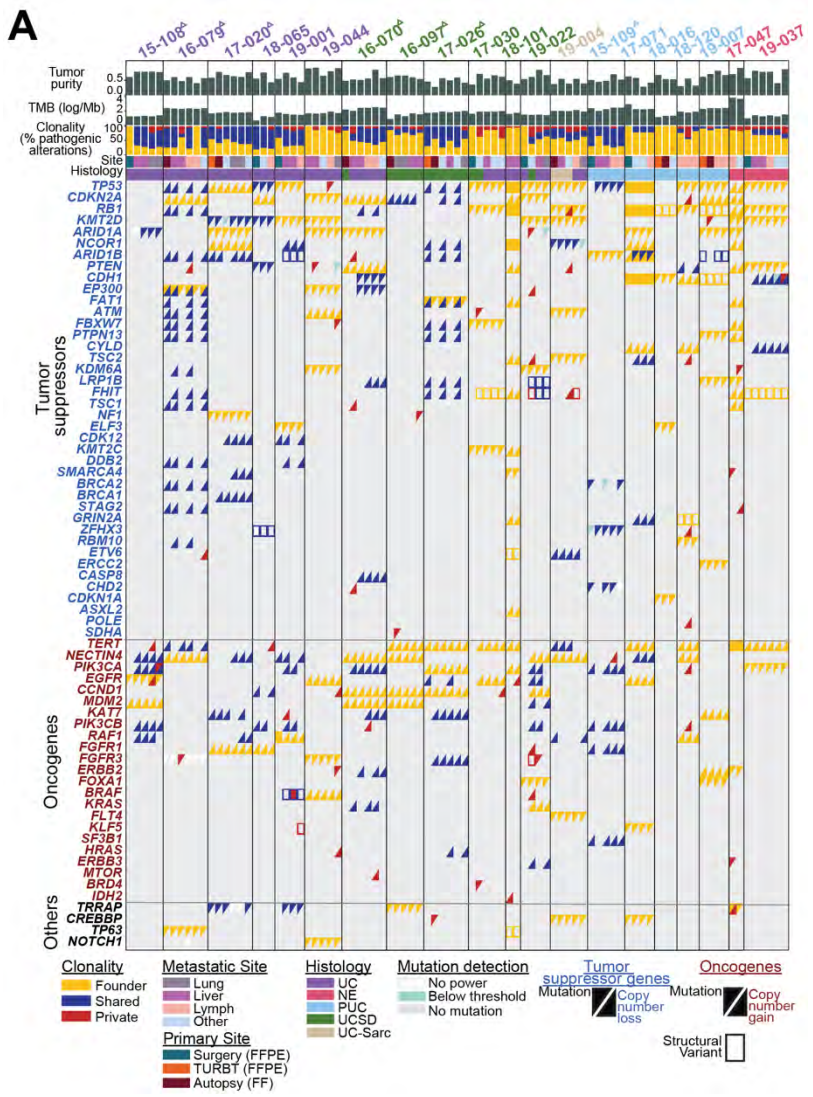

Figure 3. A) A genomic landscape plot showing pathogenic alterations in a subset of driver genes including mutations (SNVs and indels, upper triangles), copy number alterations (CNAs, lower triangles), and structural variants (SVs, open rectangles) by founder, shared, and private status. Mutations clustered by Pyclone-VI but not meeting high-confidence criteria are shown in light blue ("below threshold", see **Methods**). White triangles represent mutations with < 80% power for detection (see **Methods**). Other absent mutations with sufficient detection power are shown in grey. Tumor purity, tumor mutational burden (TMB, exonic missense/nonsense and splicing mutations per megabase), proportion of pathogenic alterations in BLCA driver genes, tumor site, and sample histology is denoted above the landscape plot. Δ denotes whole exome sequencing (WES), all others were WGS.

(ii) *Clonal composition:* We compared the clonal composition of each primary sample to the metastases, observing that the TURBT and autopsy primaries each shared an equal overlap with clones present in the metastases in patients 17-020 and 18-016. However, for patients 17-026 and 19-007, the TURBT sample was more polyclonal and contained more clones present in the metastases, suggesting that the metastases share a more similar clonal lineage with the TURBT primary in these patients (**Extended Data Fig. 6B**).

(iii) *LOH-based analysis of clonal selection and divergent evolution:* We compared chromosomal regions of loss of heterozygosity (LOH) between the primary samples, as well as the metastases,

to assess clonal differences. In 17-020, we observed two LOH events in chromosomes 6p and 19p that were only in the metastatic tumors but in neither of the primaries. Together with the metastasis-specific mutations, these events further support the divergent evolution in the metastases **(Extended Data Fig. 6A**).

Evaluating LOH also provides an interesting approach to infer selection of distinct clones because LOH is an irreversible event. It is not possible for an LOH region to regain heterozygosity after a copy loss of a large chromosomal region; a subsequent copy gain at the region would lead to copy neutral LOH, which is still homozygous. In patient 17-026, we observed an LOH event in chromosome 6q that was found in the TURBT sample and all matched metastases, supporting a common clonal origin (**Extended Data Fig. 6C)**. Interestingly, this LOH event was not detected in the primary at autopsy. Further single-nucleus analysis of copy number confirmed that the primary at autopsy predominantly contained cells that were heterozygous at 6q (**Extended Data Fig. 7A-B**). Together, these results suggest that the primary in the intact bladder at autopsy involved the selection and subsequent expansion of a distinct minor subclone (without LOH) **(Extended Data Fig. 7C**).

Extended Data Fig. 7C illustrates the unique evolutionary patterns for each of the cases with paired primary tumors and their clonal relationships with the metastases. It is important to note that the TURBT samples were typically treatment-naïve and may capture a broader, potentially polyclonal tumor representation, as the TURBT procedure collects tissue in fragments that are sequenced as a pool. For autopsy samples, the single contiguous lesion is collected, from which a distinct section is sequenced.

Results, lines 151 – 154:

> ***"We observed examples of known potentially druggable mutations in private clones for FGFR3 (R248C, patient 19-022), PIK3CA (E545K, patient 15-108), and KMT2D (frameshift deletion, patient 19-007), suggesting divergent evolution (Figure 3A, Extended Data Fig. 4B-D)."***

Results, lines 165-178:

> ***"For the patients with paired primary samples collected at TURBT and autopsy, we observed multiple distinct evolutionary patterns. In patient 17-020, both primary samples had more similar clonal composition and alterations to each other than to the metastases, indicating divergent metastatic evolution (Figure 1B, Figure 3A, Extended Data Fig. 6A). In patients 19-007 and 17-026, the metastases shared more clones and had a closer lineage with the TURBT sample than with the autopsy primary (Extended Data Fig. 6B). Additionally, in patient 17-026, loss of heterozygosity (LOH) of chromosome 6q was observed in all four metastases and the TURBT sample, while 6q was predominantly heterozygous in the autopsy primary (Extended Data Fig. 6C and 7A-B). These results suggest that the autopsy primary tumor likely included the selection and expansion of a minor subclone without 6p LOH in the early bladder, leading to its divergent clonal composition compared to the metastases (Extended Data Fig. 7C). Despite these various evolutionary trajectories, the source and timing of primary tumor collection (TURBT, surgery, or autopsy) did not lead to systematic differences in clonal composition between primary and metastatic tumors in the cohort (Extended Data Fig. 7D-E)."***

Results, lines 186-189:

> ***"By contrast, in patient 19-007, ERBB2 was amplified via ecDNA in shared clones present in the lymph node metastases and TURBT sample, which were confirmed to***

have higher HER2 protein expression, while the event was absent in the primary tumor at autopsy (Figure 3D, Extended Data Fig. 10).”

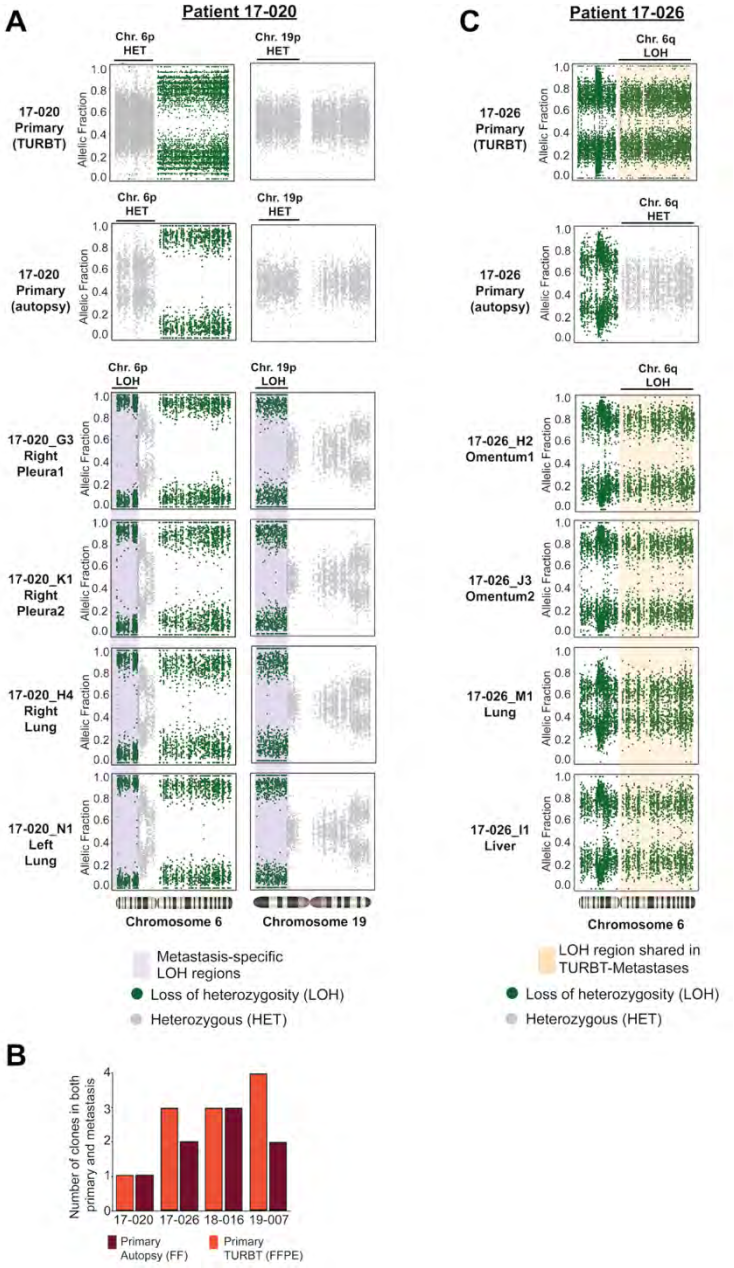

Extended Data Figure 6

A) Loss of heterozygosity (LOH) profiles for chromosomes 6p and 19p in patient 17-020. The autopsy and TURBT primaries remain heterozygous in these regions, whereas all four metastases exhibit loss of heterozygosity (LOH). Shared LOH regions across metastatic tumors are highlighted in purple, suggesting a common metastatic origin.

B) Bar plot of the number of clones shared between primary and metastatic samples, compared between autopsy and TURBT (diagnostic) primary samples. Number of clones refers to the overlapping clones present in the primary tumor and detected in one or more metastases.

C) Loss of heterozygosity (LOH) profiles for chromosome 6q in patient 17-026. The primary at autopsy remains heterozygous compared to the LOH status in the TURBT primary and metastases at this region. A shared LOH region between the TURBT primary and metastatic tumors is highlighted in yellow, suggesting a common clonal origin. Because it is not possible for an LOH region to regain heterozygosity after a copy loss of a large chromosomal region, the primary at autopsy likely has involved a selection of a distinct subclone (without LOH) that expanded as the disease progressed.

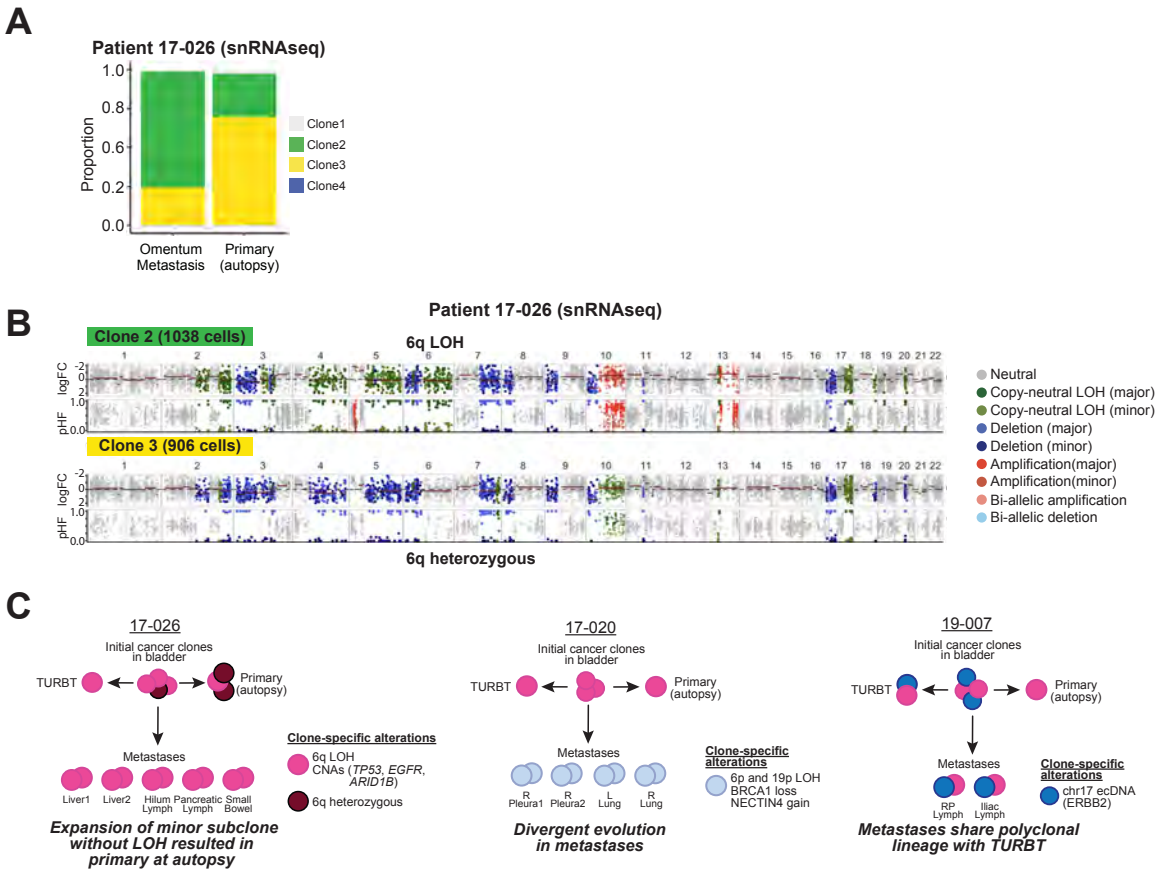

Extended Data Figure 7

A) Proportion of cells in patient 17-026's omentum and autopsy primary tumors assigned to each of four CNA clones by Numbat on snRNA-seq data.

B) Copy number results for Clone2 and Clone3 for patient 17-026 from the Numbat analysis of snRNA-seq data. Log ratio (log_2 fold change, logFC) and phased haplotype fraction (pHF) are shown, with colors indicating copy number status. LOH is shown with blue and green. All other colors are used to represent states that include both alleles (heterozygosity).

C) Schematic illustrating tumor evolution patterns in three patients (17-020, 17-026, and 19-007), comparing paired primary tumors from TURBT and autopsy and their clonal relationships with metastases. Patient 17-020 shows metastasis-specific divergent evolution. Patient 19-007 exhibits high polyclonality in the TURBT sample, including a chr17 ecDNA-containing subclone shared with metastases, consistent with a common lineage, which is absent in the autopsy primary. Patient 17-026 shows shared genomic alterations between the TURBT sample and metastases that are not present in the autopsy primary. In this case, the autopsy primary displays heterozygosity at chr6q, whereas TURBT and metastatic samples show LOH, suggesting expansion of a minor subclone lacking LOH.

Response 1.3 cont'd) In addition to obtaining these new insights, the inclusion of the early TURBT diagnostic samples led to a full re-analysis of all clonality and metastatic seeding for these four patients. Therefore, analysis and figures related to clonal composition, phylogenetic trees, and metastatic seeding have been updated for patients 17-020, 17-026, 18-016, and 19-007. Seeding patterns for two (17-026 and 19-007) of the four patients changed from met-to-met to primary-to-met, while 17-020 remained met-to-met and 18-016 remained primary-to-met. Patients 17-026 and 19-007 previously had equivalent counts of primary-to-met and met-to-met seeding events, but changes to 17-026_Liver and 19-007_Right-Iliac-Lymph-Node now make primary-to-met seeding events predominant in these patients. These two samples were originally predicted

to be seeded from metastases, but new shared clones in common with their respective TURBT samples suggest they could be seeded directly from the primary tumor (**Figure 1B**).

Overall, we continue to observe the majority of patients to have predominantly metastasis-to-metastasis seeding compared to primary-to-metastasis seeding (9 versus 5), with at least one met-to-met event occurring in 13/16 patients. Additionally, metastasis-to-metastasis seeding is corroborated by CT scans in the two patients (16-070 and 19-004) for whom we were unable to obtain a TURBT specimen in addition to their autopsy primary due to technical limitations (see **Response 2.6**, **Figure 2A**).

Results, lines 95-98:

"In the majority (9/16, 56%) of patients, a single early metastatic tumor seeded all other metastases, and 13 (81%) patients had at least one metastasis-to-metastasis seeding event. Five (31%) patients had a primary tumor that was predominantly involved in seeding all metastases."

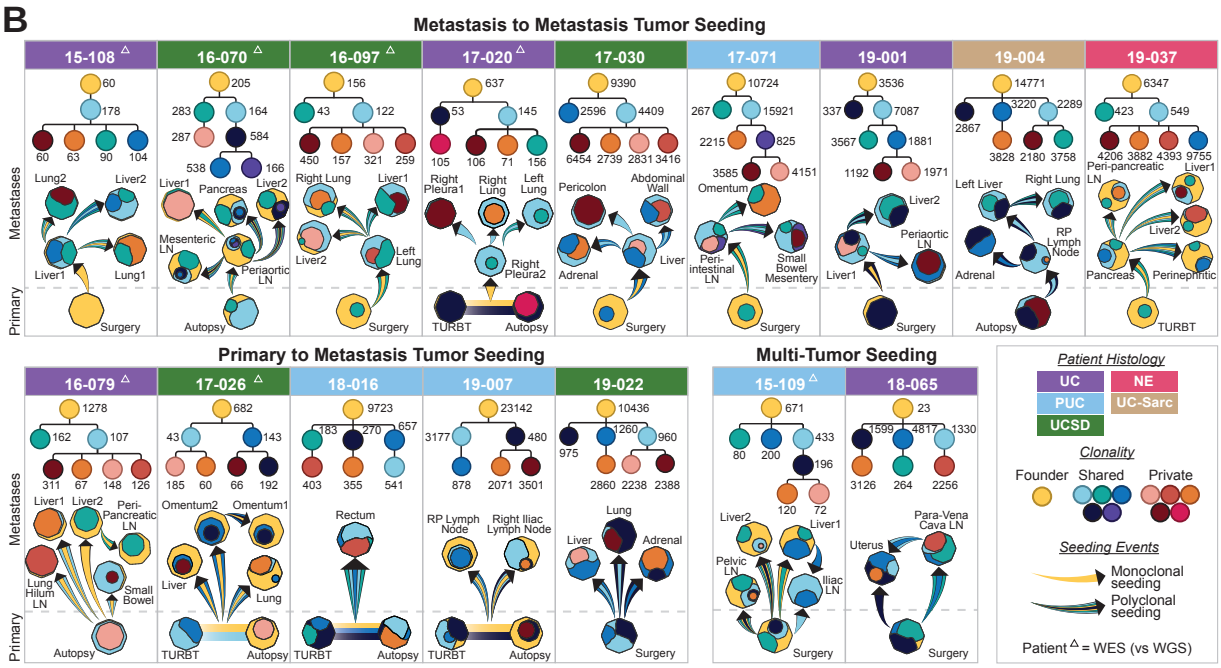

Figure 1. B) Clonal phylogenies and metastatic seeding patterns for 16 patients with high quality matched primary(s) and metastatic DNA sequencing. Patient histological subtype indicated by the colored banner. The mutation-based clonal phylogenetic tree was inferred from PyClone-VI and LICHeE. Each circle in the phylogeny is a cluster of mutations, with clonal status indicated by color shading (founder, yellow; shared, blue; private, red) and the number of mutations in the cluster annotated. Octagonal CloneMaps display the relative proportion of each clone in a tumor. Arrows indicate the inferred seeding events between tumors (directionality), as well as which clones were involved (colors). Δ denotes whole exome sequencing (WES) of the tumor, otherwise whole genome sequencing (WGS) was performed. TURBT, transurethral resection of bladder tumor; LN, lymph node; RP, retroperitoneal.

We have updated the methods to reflect new information regarding the TURBT samples:

Methods, lines 1017-1034:

"TURBT WGS library preparation and sequencing

Sample processing for FFPE TURBT specimens was performed similarly to other FFPE primary samples. Tumor regions were macrodissected to achieve >80% tumor content, and dual DNA/RNA extraction was carried out at the Fred Hutchinson Cancer Center

core facility. For two patients (17-020 and 17-026), normal tissues that were originally sequenced with WES were re-processed for WGS to serve as controls for the WGS TURBT samples, following the same protocol. FFPE tumor DNA and gDNA/FF DNA were quantified using the Invitrogen Qubit 2.0 Fluorometer (Thermo Fisher Scientific, Waltham, MA). For library preparation, 100 ng of DNA per sample was fragmented to a target size of 400 bp using a Covaris LE220-plus Focused Ultrasonicator. Sequencing libraries were then prepared from the fragmented DNA using the IDT xGen cfDNA & FFPE DNA Library Prep v2 MC kit in combination with xGen UDI Indexing Primers (Integrated DNA Technologies, Coralville, IA). Library quantification was performed using the Invitrogen Qubit 2.0 Fluorometer, and fragment size distribution was assessed with an Agilent 4200 TapeStation (Agilent Technologies, Santa Clara, CA). Individual libraries were pooled in 8-plex at weighted molar concentrations based on DNA type. Sequencing was conducted on an Illumina NovaSeq X Plus system (Illumina, San Diego, CA) across two lanes of a 25B-300 flow cell using a paired-end 150 bp read configuration with average sequencing output per library of 837 million read pairs (range 711M-1107M).”

Methods, lines 825-827:

“Archival FFPE primary tumor samples (n=16) include diagnostic (pre-treatment) TURBT (n=5) and surgical primary specimens (n=11) (Supplementary Table 1).

Methods, lines 834-836:

“In accordance with IRB-approved study protocols, no metastatic biopsies collected from living patients were obtainable for use in this analysis.”

Comment 1.4) *How was the value of 2.3 clones/seeding event chosen for analysis in Fig 2D?*

Response 1.4) The cutoff between high and low polyclonal seeding (2.3 clones per seeding event) for the survival analysis in (previous) **Figure 2D** was set as the median value of this metric across patients, ensuring an approximately equal split of the cohort. Upon further consideration, we now avoid dichotomization entirely by employing a multivariate Cox regression model that uses the seeding polyclonality metric (the mean number of migrating clones across all metastatic seeding events in each patient) as a continuous variable (new **Figure 2B**). We included histology, age, and sex as covariates known to be associated with bladder cancer patient survival (**Extended Data Fig. 3A**). Seeding polyclonality did not reach significance as an independent predictor of survival in the updated analysis but still displayed a high hazard ratio (HR = 6.78, p=0.09). Additionally, this multivariate Cox regression model was able to stratify patients into distinct high- and low-risk groups (**Figure 2C**) with greater separation than the base model of only histology, age, and sex (**Extended Data Fig. 2B**). See also **Response 2.10**. Note that the seeding results have also been updated with the addition of new TURBT samples (see **Response 1.3**). We have updated the Results, **Figure 2**, and **Extended Data Fig. 3** to reflect these changes.

Results, lines 115-120:

“The polyclonality of seeding, defined as the mean number of migrating clones across all metastatic seeding events in a patient, trended with increased mortality risk (HR = 6.8, p=0.09, Figure 2B, Extended Data Fig. 3A). This polyclonality metric improved risk stratification (log-rank p=0.0007, Figure 2C) beyond histology, age, and sex alone (log-

rank p=0.008), while the purity of variant histology did not contribute to survival risk (log-rank p=0.06) (Extended Data Fig. 3B-C).

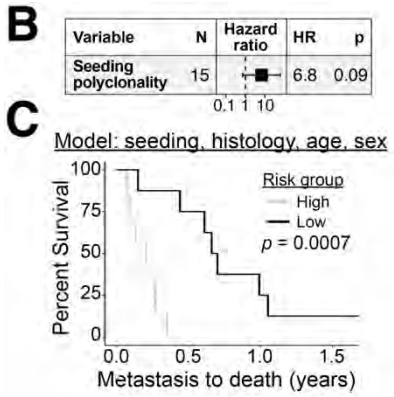

Figure 2
B) Cox proportional hazards model with survival time defined as the interval from first metastasis to death. For each metastasis, the number of clones required to seed the tumor was determined (equivalent to the number of distinct colors in seeding arrows of Figure 1B). The mean of this metric was calculated across all metastases in the patient and used as a predictor of survival in a multivariate model controlling for histological subtype, age at diagnosis, and sex. Full model with covariates shown in Extended Data Fig. 3A. Patient 16-070 was excluded due to being a statistical outlier in survival (see Methods).
C) Patient survival from first metastasis as stratified by the median risk score produced by the multivariate Cox model of seeding polyclonality, histology, age, and sex. Statistics from log-rank test.

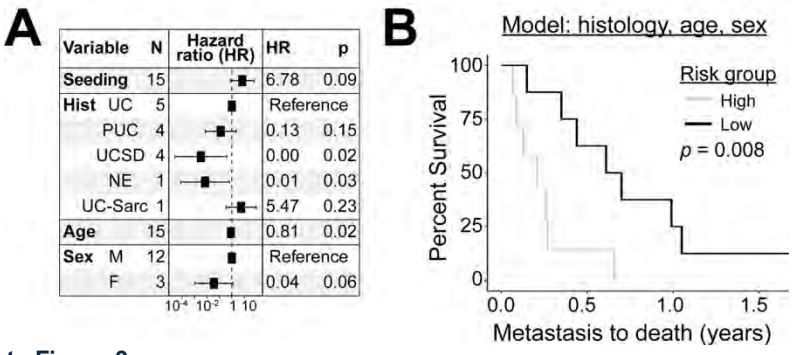

Extended Data Figure 3
A) Cox proportional hazards model with survival time defined as the interval from first metastasis to death. Polyclonality of seeding as a predictor of survival in a multivariate model controlling for histological subtype, age at diagnosis, and sex. Patient 16-070 was excluded due to being a statistical outlier in survival.
B) Patient survival from first metastasis as stratified by the median risk score produced by the multivariate Cox model of only the histology, age, and sex. Statistics from log-rank test.

Comment 1.5) *For analysis in Fig 2G, did some of the ICI-treated patients get chemo before (or with) ICI? Is the comparison really chemo-only vs chemo-then-ICI?*

Response 1.5) Yes, 7 of the 10 ICI-treated patients analyzed in the original Figure 2G were treated with chemo as well as ICI (6 chemo then ICI, 1 ICI then chemo, **Extended Data Fig. 1A**). This analysis has been updated after the addition of TURBT samples for four patients made changes to the seeding results (see also **Response 1.3**). A more detailed comparison considering treatment combinations now finds that there was no significant difference in seeding patterns between patients treated with chemotherapy-only, ICI-only, both, or neither (**Extended Data Fig.**

3C), partially due to the overall increase in polyclonal polyphyletic events now observed with the addition of TURBT samples in ICI-naïve patients.

Upon further consideration of these changes and the complex interactions that may occur between patients with combined treatment histories, we devised a new way of assessing the effect of ICI on metastatic seeding based on the suggestions of Reviewers 1 and 3 (see also **Response 3.1**). We now compare between metastases that were **seeded** before (pre-ICI) versus after ICI (post-ICI) by referencing CT scans to confirm the timing of metastases relative to ICI treatment. Six patients (12 tumors) had at least one metastasis seeded before ICI treatment. Four of these patients (11 tumors) additionally had at least one metastasis after ICI, thereby having metastases seeded *both* before and after ICI. Interestingly, in this analysis, we saw an increase in polyclonal polyphyletic events that occurred post-ICI in the four patients with both pre-ICI and post-ICI metastases (p=0.029, **Figure 2F, Extended Data Fig. 3E**). The number of clones that seed the post-ICI metastases and the cellular prevalence of clones in post-ICI metastases were also higher than in pre-ICI metastases (**Figure 2G**, **Extended Data Fig. 3F**). To further reduce confounding from patient-specific treatment histories, we performed comparisons directly within each patient or used linear mixed-effects models to account for inter-patient variability.

This updated analysis, as well as the finding of no seeding difference between patients with different treatment regimes, is included in the Results, Methods, **Figure 2F-G**, and **Extended Data Fig. 3D-F**.

Results, lines 125 – 131:

> ***"We observed no differences in seeding patterns between patients treated with chemotherapy and immune checkpoint inhibitors (ICI) (Extended Data Fig. 3D). However, in patients treated with ICI, we found that tumors arising after ICI (confirmed by CT scan) were seeded via more migrating clones (p=0.11) and polyclonal polyphyletic events (p=0.029) when compared to pre-ICI metastases (Figure 2F, Extended Data Fig. 3E-F, Methods). These ICI-persistent clones did not preferentially migrate to specific metastatic sites, but they exhibited greater expansion within the post-ICI metastases (p=0.022) (Figure 2G, Extended Data Fig. 3G)."***

The Methods describes the approach used for the ICI timing and seeding analysis references CT imaging and clinical records to determine the timing of metastases prior to ICI treatment.

Methods, lines 890-903:

> ***"Determination of pre- versus post-ICI metastasis***
>
> ***For each patient who underwent at least one full cycle of immune checkpoint inhibitors (ICI, n=9, Supplementary Table 2), the CT scan that immediately preceded start of ICI treatment was assessed for visible tumors. The time between the CT scan preceding ICI and the start of ICI is variable (median 16 days, range 2 - 260 days). For patient 19-022, the most recent CT scan available before ICI was 260 days prior, but clinical records confirmed that only the lung metastasis was observed before starting ICI treatment. The metastases already in place before ICI were designated as "pre-ICI metastases", while metastases collected and sequenced at autopsy but not visible by CT before ICI were designated "post-ICI metastases". Of the 9 ICI-treated patients, there were 3 for whom all metastases were visible by CT prior to start of ICI therapy. Six patients had both metastases visible pre-ICI and metastases that only appeared post-ICI. In total, 17 metastases were designated "pre-ICI" and 15 were "post-ICI" (Supplementary Table 3). Clonal composition (number and CP of clones), metastatic***

seeding, and metastatic site were compared between metastases seeded pre- versus post-ICI."

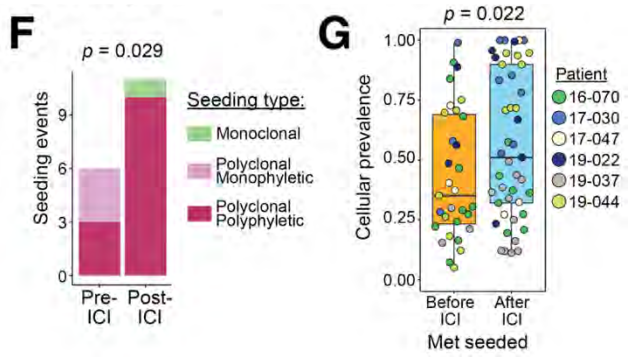

Figure 2
F) Number of pre- versus post-ICI seeding events of each type in patients that have both pre- and post-ICI metastases and seeding analyses (n=4 patients). Per patient breakdown in Extended Data Fig. 3E, p-value from Fisher's exact test.
G) Cellular prevalence for each shared or private clone, compared between clones in metastases seeded pre- versus post-ICI. Each point is a clone in a tumor. Statistics from linear mixed effects model with both patient and cluster ID as random effects.

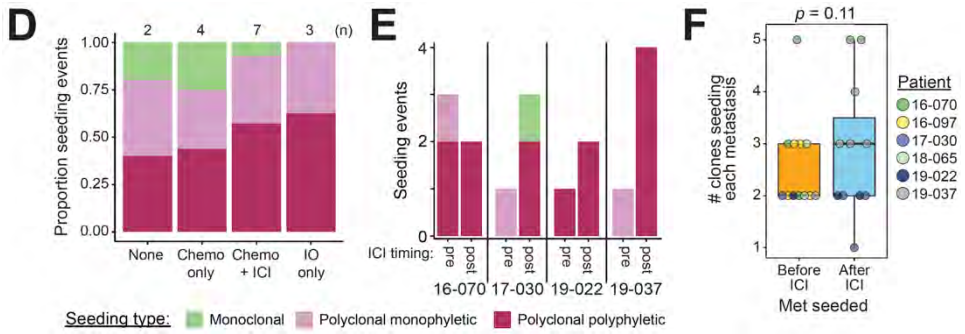

Extended Data Figure 3
D) Proportion of each type of seeding event in patients treated with only chemotherapy, only immune checkpoint inhibitors, both, or neither (n patients in each category labeled above).
E) Number of pre- versus post-ICI seeding events of each type in each patient that has both pre- and post-ICI metastases and seeding analysis. Timing of metastases relative to ICI were determined from CT scans.
F) The number of clones that seeded each metastasis (equivalent to number of colors in Figure 1 migration arrows) for pre-ICI versus post-ICI metastases (n = 12 tumors/6 patients pre-ICI; n = 11 tumors/4 patients post-ICI). Patients without seeding analysis not included. Statistics from linear mixed effects model with patient as a random effect.

Comment 1.6.1) *For the founder analyses in Figure 3, it would be interesting to compare founder profiles of metastases that did vs didn't seed additional metastases.*

Response 1.6.1) Thank you for this suggestion. The founder profile for a patient is the same across all their tumors; therefore, we performed this suggested analysis across patients. We compared the founder profiles between patients in which the metastases never or rarely seed (primary-to-metastasis or multi-tumor seeding patterns) versus patients in which metastases extensively seed additional metastases (metastasis-to-metastasis seeding pattern). We hypothesized that the founder profile of patients in which the primary seeds all or most metastases may confer higher metastatic seeding ability than the founder profile of patients in which the primary only seeded once. Therefore, we compared the founder driver alterations (deleterious

SNVs, indels, CNAs, and SVs in BLCA driver genes, **Figure 3A**) in metastasis-to-metastasis seeding patients (n=9; met-to-met) versus primary-to-metastasis and multi-tumor seeding patients (n=7; pri-to-met/multi-tumor).

We observed that BLCA driver genes such as *TP53* and *TERT* tended to be more frequently altered in met-to-met compared to pri-to-met patients, although the sample size was small and underpowered for statistical testing (**Extended Data Fig. 5F**). *CDKN2A* was the gene most enriched in founder alterations (primarily deletions) in the patients where the primary was the dominant seeder (pri-to-met/multi-tumor cases). *CDKN2A* downregulation and/or deletion is known to be associated with poor prognosis, muscle-invasiveness, and shorter progression-free survival (PMID: 22422578, 17612565, 25092538, 27199504), so it could be contributing to an increased ability of the founder/primary to metastasize in these patients. Additionally, *CDKN2A* was observed to be altered in 49% of metastatic BLCA patients (Hartwig dataset, PMID: 35086719), but only 22% of non-metastatic MIBC patients (TCGA dataset, PMID: 28988769) further suggesting that this alteration may be associated with increased metastatic capacity. Interestingly, *TP53* and *CDKN2A* alterations have been reported to be mutually exclusive in MIBC (PMID: 28988769), supporting their enrichment in distinct metastatic settings.

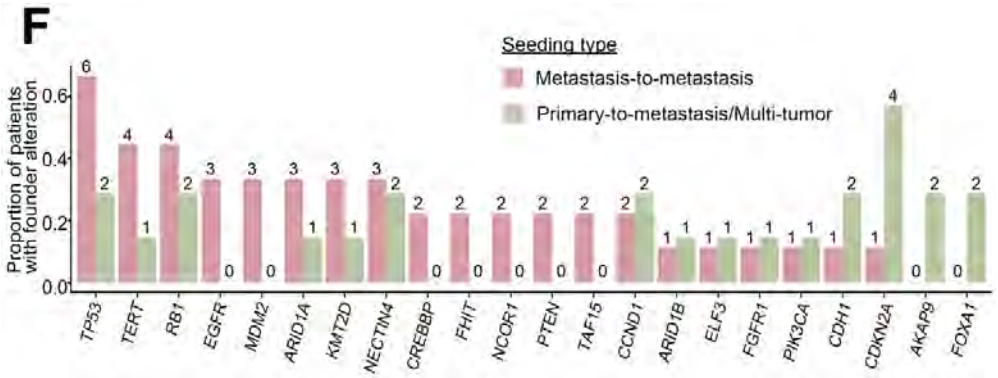

Extended Data Figure 5. F) Proportion (y-axis) and count (number above each bar) of patients with any pathogenic founder alteration (mutation, CNA, or SV) in each BLCA driver gene, separated by patients' metastatic seeding pattern.

Results, lines 159-164:

> ***"We also observed that founder alterations of TP53 and TERT were enriched in patients with metastasis-to-metastasis seeding, while founder CDKN2A alterations were enriched in primary-to-metastasis seeding (Extended Data Fig. 5F). These results are consistent with previous reports that CDKN2A alterations were mutually exclusive of TP53 loss in MIBC[32], enriched in metastatic[1] (49%) versus localized[32] (22%) BLCA, and associated with high metastatic capacity[33–36]."***

Comment 1.6.2) *Along these lines, an asterisk should be added to denote cases for which the analyzed bladder tumor was the tumor collected at time of diagnosis/presentation (rather than at time of autopsy)….it would be reasonable to assume that the primary may resemble metastases to greater/lesser extent depending on when the bladder tumor was harvested/analyzed.*

Response 1.6.2) To clarify the source and collection timing of each primary tumor, we have changed the "Site" annotation row in **Figure 3A** to distinguish between TURBT, surgery, and autopsy.

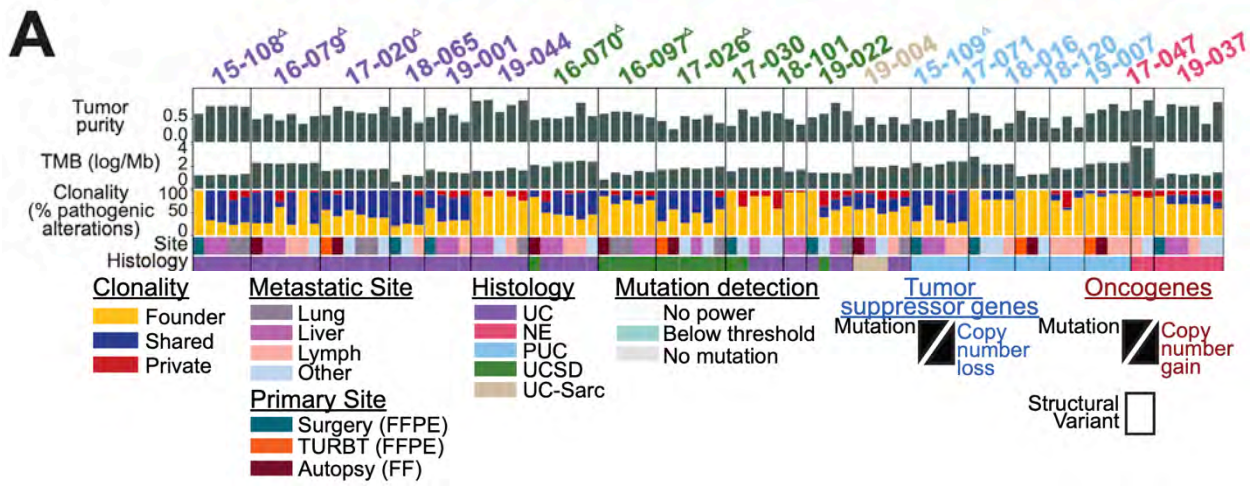

Figure 3. A) Tumor purity, tumor mutational burden (TMB, exonic missense/nonsense and splicing mutations per megabase), proportion of pathogenic alterations in BLCA driver genes, tumor site, and sample histology is denoted above the landscape plot. Δ denotes whole exome sequencing (WES), all others were WGS.

We also thank the reviewer for their suggestion to consider how the different primary collection sources may affect our genomic analyses. With the addition of new TURBT samples, we have performed extensive comparison of the TURBT and autopsy primary samples, finding that patients can have multiple evolutionary patterns (**see Response 1.3**). For example, 17-020's primaries (both from TURBT and at autopsy) are more similar to each other than the metastases, while in 19-007 and 17-026, the TURBT primary was more similar to the metastases than to the primary at autopsy.

In addition to comparing the TURBT and autopsy primaries within patients, we also compared primary to metastatic evolution between different patients whose primary tumors were collected at surgery versus autopsy. We compared the clonal composition of primary versus metastases in each patient, both in terms of the number of shared clones (**Extended Data Fig. 7D**) and the cellular prevalence of these shared clones (**Extended Data Fig. 7E**). We focused the analysis on shared clones since private clones are more challenging to detect in FFPE samples (TURBT or surgery), and the founder clone is the same across all tumors in a patient. Across patients, the similarity between the metastases and the primaries did not vary systematically based on the source of the primary tumor. For example, patient 19-022's surgery primary tumor was very similar to the metastases, while patient 19-001 and 17-071's surgery-derived primaries were quite dissimilar to their metastatic samples (**Figure 1B**). Overall, we conclude that, while the similarity between the primary tumor and metastases can vary widely, there was no systematic trend as to the timing and source of the primary tumor collection and its effect on the degree of similarity.

Results, lines 175–178:

> ***"Despite these various evolutionary trajectories, the source and timing of primary tumor collection (TURBT, surgery, or autopsy) did not lead to systematic differences in clonal composition between primary and metastatic tumors in the cohort (Extended Data Fig. 7D-E)."***

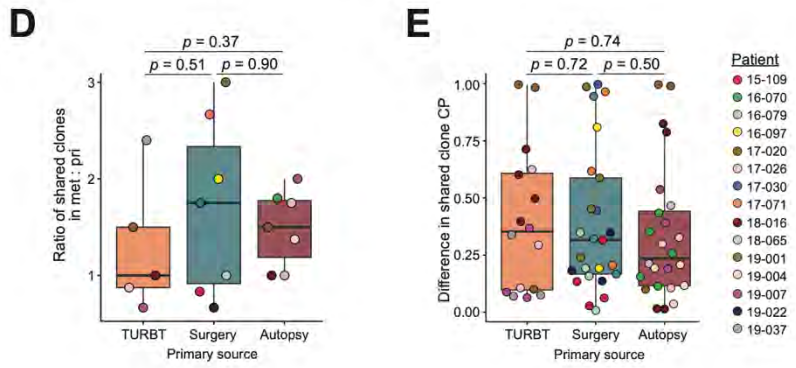

Extended Data Figure 7
D) Per-patient ratio of the average number of shared clones in metastatic tumors verses the number of shared clones in the primary tumor, separated by the source of the primary tumor (p-values from Mann-Whitney U-test).
E) For each shared mutation clone, the difference between the clone's average CP (cellular prevalence) in the metastases versus the CP in the primary tumor is shown (p-values from Mann-Whitney U-test).

Comment 1.7) *Were platinum signatures identified in patients who did not receive platinum-based chemo? This should be stated explicitly.*

Response 1.7) Seven patients in our cohort did not receive any platinum-based chemotherapy (cisplatin or carboplatin). Of these 7 patients, we identified a platinum signature (SBS31) only in the founder clone of patient 15-108 (27% of founder mutations). This instance is likely due to the challenge in identifying signatures from the small number (n=60) of mutations in this clone. We acknowledge that this is a technical artifact of the analysis. Therefore, we have re-analyzed mutation signatures for these 7 patients by removing SBS31 and SBS35 from the reference signature set, as was done previously by Nguyen et al. 2024 (PMID: 39385020); the analysis for patients who received platinum-based therapy remain unchanged. These changes are reflected in the Methods, **Figure 4A**, and **Extended Data Fig. 12A-C**. All of the conclusions remain the same.

Methods, lines 1492-1495:

> ***"For the subset of seven patients who did not receive platinum-based chemotherapy, platinum-associated signatures (SBS31+SBS35) were additionally excluded and refitting was performed separately, yielding a final set of 49 signatures used for downstream analysis in this group (Supplementary Table 5)."***

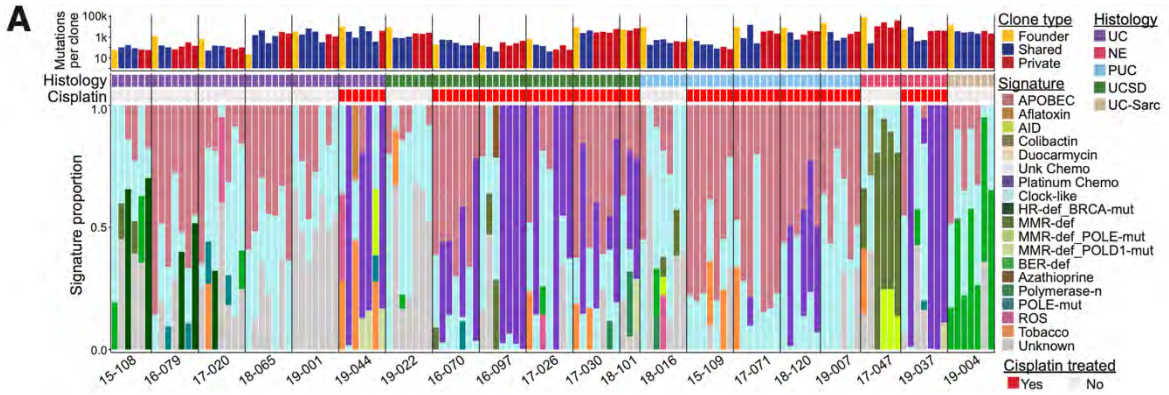

Extended Data Figure 12. A) Proportion of COSMIC SBS signatures (grouped by etiology) across mutation clones per patient. Annotations indicate cluster clonality, mutation count, patient histology, and cisplatin treatment status. SBS31 and SBS35 were excluded in patients without platinum treatment. Histology is shown at the patient level for each clone. Abbreviations: AID, activation-induced cytidine deaminase; Unk, unknown; Chemo, chemotherapy; HR-def_BRCA-mut, homologous recombination–deficient BRCA mutant; MMR-def, mismatch repair–deficient; BER-def, base excision repair–deficient; ROS, reactive oxygen species.

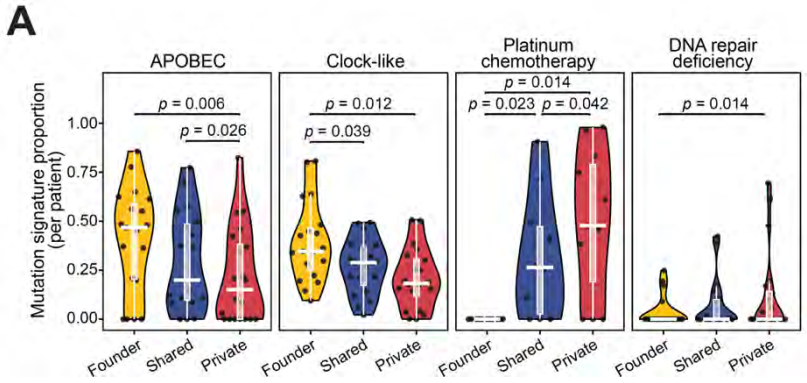

Figure 4. A) Clonality of single-base substitution (SBS) mutations assigned to different mutation signature groups: APOBEC (SBS2 + SBS13), Clock-like (SBS1 + SBS5), Platinum chemotherapy (SBS31 + SBS35), and DNA repair deficiencies (SBS3, SBS6, SBS14, SBS15, SBS20, SBS21, SBS26, SBS30, SBS36, SBS44). Each point is the proportion of founder, shared, or private mutations in a patient that were assigned to the indicated etiology (n = 20 patients, (p-values from Wilcoxon signed-rank test). See Methods for details on signature selection and assignment.

Comment 1.8) *The sentence in lines 196-199 needs to be corrected to state that no differences in gene expression of the assessed pathways were noted. It remains possible that any/all of these pathways could be biologically altered in the tumor, but just not as defined by changes at the transcript level. Also, there was a p<0.05 effect for GSH (Sup Fig 9), but this was not chosen for further analysis while the authors did choose to focus on the difference in FA pathway with p=0.071. There would be some biological plausibility for altered GSH/redox signaling as a potential cisplatin resistance mechanism.*

Response 1.8) Thank you for pointing out this distinction, we have updated the text to clarify that no differences in *gene expression* of these pathways were observed that could explain the difference in cisplatin signatures between patients. We agree that gene expression of the pathway is not always concordant with activity of that pathway in the tumor. This is why we decided to further investigate the initial analysis of RNA-sequencing with cell line studies where we could directly measure pathway activity (i.e. ubiquitinated FANCD2).

Despite a more significant difference in expression of the glutathione pathway, the decrease observed in the PUC tumors was not consistent with the expected biology. Gene expression in the glutathione pathway has been observed to be increased in cisplatin-resistant cells, both in bladder and other cancer types (PMID: 15839938, 25356874), as GSH can reduce the efficacy of cisplatin by both sequestration in the cytoplasm and reduction of cisplatin-induced oxidative stress (PMID: 21892204). Therefore, we would expect that a decrease of GSH expression in PUC tumors should allow more cisplatin-induced signatures, but this is not what we observed. As a result, we decided to prioritize our investigation on the expression difference in the FANC pathway. We have edited the Results to clarify this point.

Results, lines 232-237:

> ***"The limited presence of platinum chemotherapy signature mutations in cisplatin-treated PUC tumors was not explained by altered gene expression of cisplatin import and export, cytoplasmic glutathione (GSH) metabolism of cisplatin, or nucleotide excision repair (NER) (Extended Data Fig. 12H)[40–42]. Though decreased expression of the glutathione pathway was observed in PUC, this would be expected to increase cisplatin-induced mutations[43], inconsistent with our observations in PUC tumors."***

Comment 1.9) *Does FANC pathway expression correlate with cisplatin sensitivity in bladder cancer cell lines in publicly available databases such as DepMap and/or COSMIC? This should be checked and reported.*

Response 1.9) We explored both the DepMap and COSMIC publicly available datasets to find cisplatin sensitivity data for bladder cancer cell lines. While the COSMIC Cell Lines Project does not have drug screening data, the GDSC2 (Genomics of Drug Sensitivity in Cancer 2) dataset from DepMap does report cisplatin sensitivity for BLCA cell lines, allowing us to investigate the correlation between cisplatin sensitivity and FANC pathway expression across a broader set of BLCA cell lines. We calculated the Fanconi anemia pathway expression score for these additional cell lines in the same way as for the initial four tested in the manuscript and used AUC (area under the dose-response curve) as a measurement of cisplatin sensitivity, as suggested by the DepMap project team. There are 14 BLCA cell lines with both RNA expression and cisplatin sensitivity data available in the DepMap dataset, and we observe a moderate positive association (Spearman rho = 0.43, p = 0.12) between AUC and FA score across these cell lines.

We have included this result in **Extended Data Fig. 13A** and the Results.

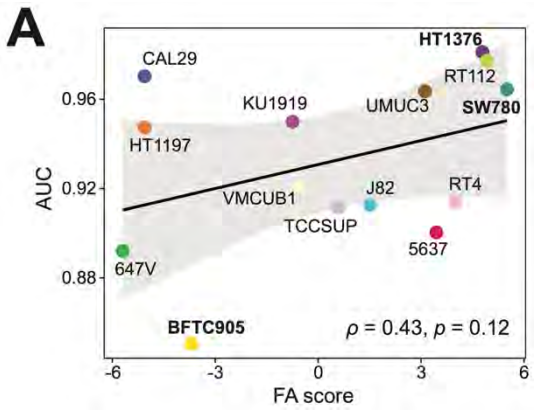

Extended Data Figure 13. A) Spearman correlation between FA score and cisplatin sensitivity for 14 bladder cancer cell lines from the DepMap Genomics of Drug Sensitivity in Cancer 2 dataset. Cisplatin sensitivity represented by the area under the dose-response curve.

Results, lines 249-254:

> ***"There are currently no cell line or mouse models of PUC; however, analysis of publicly available cisplatin sensitivity data from the Genomics of Drug Sensitivity in Cancer (GDSC) database[48] suggested that FANC gene expression is positively correlated with cisplatin resistance within UC-derived BLCA cell lines (Extended Data Fig. 13A). Therefore, we tested UC-origin BLCA cell lines with either high (SW780 and HT1376) or low (UBLC1 and BFTC905) FANC gene expression levels (Extended Data Fig. 13B)."***

Comment 1.10) *Cisplatin causes a variety of DNA lesions including intra- and interstrand crosslinks. The FANC pathway is specialized for repairing interstrand crosslinks; therefore, it would be useful to test an agent such as mitomycin-C that specifically creates interstrand crosslinks in the assays resulted in Fig 4F-H.*

Response 1.10) Thank you for this suggestion. The similarities between mitomycin-C (MMC) and cisplatin-induced DNA damage, as well as published response data for BLCA cell lines to MMC, suggest that the FANC-high cell lines that were resistant to cisplatin would also be more resistant to MMC than the FANC-low cell lines. The GDSC2 (Genomics of Drug Sensitivity in Cancer 2) dataset from DepMap, in addition to having response data for cisplatin (**Response 1.9**), also has MMC response data for three of the four cell lines used in our original experiments. The FANC-high lines SW780 and HT1376 were among the most resistant BLCA cell lines tested in this database, with IC50s of 7.4μM and 1.8μM respectively, whereas FANC-low cell line BFTC905 was much more sensitive to MMC (IC50 = 107nM).

Based on this preliminary published data, we repeated the experiments shown in **Figure 4F-H**, treating each of the four BLCA cell lines with 0-10μM of MMC. To determine whether MMC activated the FANC pathway more in FANC-high lines (SW780 + HT1376) than FANC-low lines (BFTC905 + UBLC1), we treated cells with 1μM MMC for 24 hours, then assessed FANCD2 ubiquitination. As with cisplatin treatment, MMC treatment significantly increased FANCD2-ub in FANC-high lines, whereas it did not significantly activate FANCD2-ub in FANC-low lines (**Extended Data Fig. 13E**). FANC-high lines treated with MMC had double the FANCD2-ub as compared to low FANC cells. Additionally, we assessed cell growth dynamics in response to MMC. Here, we observed no significant difference in IC50 between the high and low FA lines (**Extended Data Fig. 13F**). However, when analyzing cell death, we observed that FANC-low lines UBLC1 and BFTC905 are significantly more sensitive to MMC treatment, with higher number of cells dying in response to treatment (**Extended Data Fig. 13G**). The IncuCyte Cytotox dye directly measures cell health, while confluence can be influenced by a variety of factors, including cell health, growth, and size. Therefore, we conclude that high FANC expression in these cell lines does increase both FANC pathway activity and cells' resistance to MMC, similarly to cisplatin, though there may be other factors (e.g., other resistance pathways or differential mechanisms of cell death) that make the relationship between cisplatin response and FANC stronger than that between MMC response and FANC expression.

Results, lines 262 – 265:

> ***"FANC-high lines also responded to mitomycin C, another crosslink-inducing chemotherapy, with increased FANCD2 ubiquitination and resistance to cell death (Extended Data Fig. 13E-G), confirming that sensitivity stemmed from FANC repair of inter-strand crosslinks."***

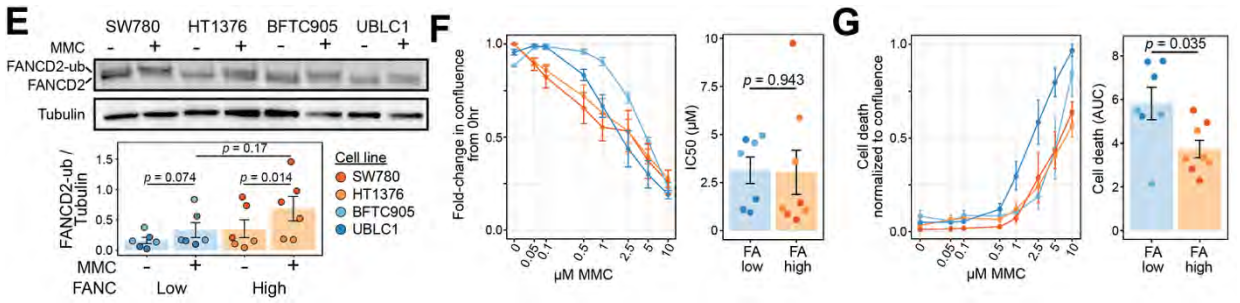

Extended Data Figure 13
E) Western blot of FANCD2 and ubiquitinated FANCD2 protein expression in BLCA cell lines with and without 24 hours of 1 μM MMC treatment, with tubulin loading control. For gel source data, see **Supplementary Figure 1**. Quantification of FANCD2-ub band at bottom (n = three biological replicates). Bars show mean value, with error bars indicating SEM (p-values from paired t-tests between +MMC versus -MMC conditions and unpaired t-test between High versus Low +MMC conditions).
F) Left: Dose response growth curve of 48 hours of MMC treatment on four BLCA cell lines. Y-axis is the fold change from 0 to 48 hours of treatment, scaled within each cell line so the maximum equals 1. Solid lines connect the average response at each cisplatin dose across 3-4 biological replicates (5 technical replicates per dose per experimental replicate), with error bars displaying SEM. **Right**: Half-maximal inhibitory concentration (IC50) values for each biological replicate per cell line were calculated by fitting non-linear regression curves to the baseline-normalized confluence at 48 hours of 0-10μM MMC treatment. Bars show mean IC50, with error bars indicating SEM (p-value from t-test on 3-4 biological replicates per cell line).
G) Left: Dose response cell death curve of 72 hours of MMC treatment on four BLCA cell lines. Dead cell count determined by IncuCyte Cytotox dye, normalized using matched well confluence, and scaled within each biological replicate such that the maximum equals 1. Solid lines connect the average response at each cisplatin dose across 3-4 biological replicates, with error bars displaying SEM. **Right**: Area under the curve (AUC) values for each biological replicate per cell line were calculated using the metric to the left. Bars show mean AUC, with error bars indicating SEM (p-value from t-test on 3-4 biological replicates per cell line).

Comment 1.11) *Are there other tumor settings (beyond bladder) in which the FANC signature has been associated with cisplatin signatures or (more likely) cisplatin sensitivity? There are some tumor types such as HNSCC, ovarian cancer, and some NSCLCs that would receive cisplatin-based chemo as standard of care and likely have RNA-seq data sets available.*

Response 1.11) We appreciate the suggestion to determine whether the observed link between Fanconi anemia (FANC) pathway expression and cisplatin signature and sensitivity is specific to BLCA, or whether this association extends to other cancers. Previous reports have shown that the relationship between Fanconi anemia DNA repair and cisplatin sensitivity varied across cancers. In ovarian and breast cancer cell lines, inhibition of the FANC pathway by a small molecule sensitized cells to cisplatin (PMID: 16648566). Furthermore, activation of the FANC pathway in FANC-deficient ovarian cells led to cisplatin resistance (PMID: 12692539), establishing the dependence of ovarian cancer on the FANC pathway for cisplatin response. However, FANC activation has not been found to be associated with cisplatin sensitivity in NSCLC patients (PMID: 15694018). These studies demonstrated that, while the FANC pathway is known to repair the DNA damage caused by cisplatin, correlation of FANC activation and response is cancer type dependent.

The above studies established the link between FANC activation and platinum sensitivity in ovarian cancer. To directly determine whether the correlation between FANC pathway gene expression and SBS31/SBS35 mutational signature that we observed in BLCA extends to other cancers, we analyzed the ovarian and lung cancer datasets from the Hartwig Medical Foundation

(HMF). The HMF database consists of metastatic samples with detailed pre- and post-biopsy treatment metadata. Most of the ovarian cancer samples in the HMF dataset received carboplatin, as that is the standard of care for ovarian cancer (PMID: 12860964). Because carboplatin and cisplatin are platinum-based agents, they have similar mechanisms of action in creating inter-strand crosslinks repaired by the FANC pathway. Therefore, we analyzed both carboplatin- and cisplatin-treated samples.

We analyzed the correlation between platinum chemotherapy mutational signatures (SBS31+35) and FANC expression score (11 FANC genes) in the ovarian metastases that had been treated with platinum prior to biopsy (n=115). We observed a significant negative correlation between SBS31+35 and FANC expression score (Pearson r=-0.19, p=0.039, **Extended Data Fig. 12l**). This correlation was somewhat less strong as that observed in the HMF metastatic BLCA cohort (n=52, Pearson R=-0.31, p=0.025, **Figure 4E**). Note that the HMF BLCA cohort size increased with additional samples in a recent database update.

We also analyzed cisplatin-treated metastatic lung tumors from HMF (n=130). There was a large number of lung tumors that lacked the SBS31+35 mutation signature despite being treated with cisplatin (91/130, 70%), which was consistent with previous observations in other lung cancer cohorts receiving platinum, such as TRACERx (25/34, 73%; PMID:37046095) and a study from the University of Cologne (16/24, 67%; PMID:38480884). In these HMF samples, there was a weak negative correlation between FANC expression and SBS31+35 that was not statistically significant (Pearson R=-0.083, p=0.35; see panel below). Due to the lack of correspondence between platinum treatment and mutation signatures, we decided to not include the lung cancer results in the manuscript.

Overall, previously published literature and new analysis of the HMF metastatic dataset demonstrate that the FANC pathway is associated with platinum chemotherapy response and mutation signature in ovarian cancer. We have added the results from the HMF ovarian analysis in **Extended Data Fig. 12l** and the Results.

Results, lines 239-244:

> ***"Furthermore, we observed that higher FANC pathway expression was significantly associated with lower burden of late-acquired platinum chemotherapy signature (Figure 4D, ρ = -0.7, p=0.024). We observed similar trends in independent cohorts[1,47] of mBLCA patients treated with cisplatin (n=52, r = -0.31, p=0.025, Figure 4E) and ovarian cancer patients treated with platinum (n=115, r = -0.19, p=0.039, Extended Data Fig. 12l, Supplementary Table 5)."***

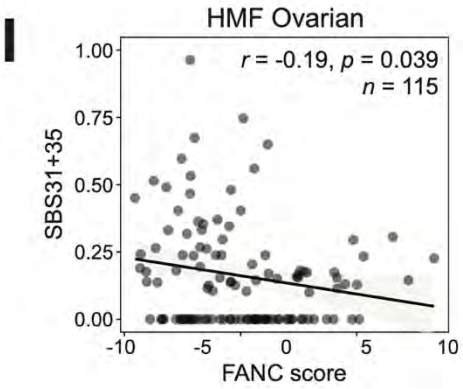

Extended Data Figure 12. I) Pearson correlation between Fanconi anemia (FANC) expression score and proportion of platinum chemotherapy mutation signature for each cisplatin and carboplatin treated patient in the Hartwig Medical Foundation (HMF) ovarian cancer cohort (n=115 patients). Scores were calculated as a sum of z-scores (normalized tpm across patients within each gene) for 11 key FANC genes.

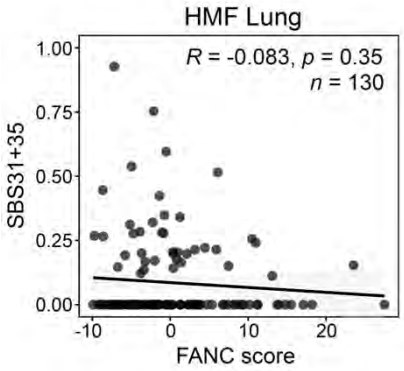

Figure. Pearson correlation between Fanconi anemia (FANC) expression score and proportion of platinum chemotherapy mutation signature for each cisplatin-treated patient in the Hartwig Medical Foundation (HMF) lung cancer cohort (n=130). FANC score and correlation were computed the same as for Extended Data Fig. 12I.
This panel was not included in the manuscript.

***Comment 1.12**) For the cfDNA analysis, the expected differences between WGS and targeted panel (TP) should be discussed briefly because the rationale (assuming its sequencing depth) for using both is not currently clear from the main text or Figure 7.*

Response 1.12) Thank you for pointing out the need to clarify the rationale for performing WGS and TP sequencing of cfDNA. The *first* goal for the cfDNA studies was to assess the ability to capture genomic alterations. In particular, it is not known how accurately either approach captures clonal versus subclonal mutations and the overall clonal composition of multiple tumors in a patient. To evaluate the clonality capture performance of using the breadth (WGS) vs. the depth (TP) of cfDNA sequencing, we performed TP (~3000x fragment coverage) sequencing on all 17 samples and WGS (~70x fragment coverage) on 8 samples that had at least moderate levels of ctDNA fraction (TFx ≥ 8%). It is expected that the ultra-deep TP will have higher statistical power to capture subclonal, low VAF mutations in lower TFx cfDNA samples, due to having ~50x higher sequencing depth. However, the breadth of WGS has been proposed as advantageous for ctDNA detection due to the higher number of variants that can be observed genome-wide (PMID: 32483360), increasing the power to detect a tumor overall (**Figure 7C**). Interestingly, for samples that had higher TFx (≥ 8%), we did not observe a difference in the proportion of tumor mutation capture by TP or WGS for the eight samples sequenced by both platforms (**Figure 7A-B**). To evaluate the capture of copy number alterations and structural variations, we used the WGS data.

The *second* goal was to assess tumor phenotype and detection of tissue damage by using cfDNA fragmentation pattern analysis, which we and others have shown is possible by analyzing WGS data.

We have incorporated additional explanation of the rationale between WGS and TP sequencing, and some of the observed differences in the Results and Methods.

Methods, lines 1574-1588:

"Overview and rationale for cfDNA sequencing

Whole genome sequencing (WGS, ~70x fragment coverage) and targeted panel (TP, ~3000x fragment coverage) were performed on post-mortem plasma cfDNA samples. Each sequencing data type provides unique molecular features for assessment of cfDNA. WGS of cfDNA allowed for whole-genome assessment of copy number. WGS also enabled the assessment of tumor phenotype and detection of tissue damage by using cfDNA nucleosome profiling analysis, which we and others have utilized previously[78,79,144,145]. The breadth of WGS has been proposed as advantageous for ctDNA detection due to the higher number of variants that can be observed genome-wide, increasing the power to detect the presence of tumors[146]. However, the depth of coverage for WGS data was limiting for samples with low ctDNA fraction (i.e. tumor fraction, TFx < 8%). Ultra-deep TP sequencing provided the statistical power to detect mutations in samples with lower TFx (< 8%), although it is limited to interrogating mutations and indels only in the targeted regions. For samples with higher TFx (≥ 8%), we had the opportunity to compare both WGS and TP to evaluate their ability to capture mutation clonality from the primary and metastatic tumors."

Results, lines 377-383:

"To assess the utility of cfDNA sequencing breadth versus depth for capturing mutation clonality, we performed deep WGS (mean 73x fragment coverage, n=8) for samples with higher TFx (≥ 8%) and ultra-deep targeted panel (TP) capture of 397 cancer genes (mean 3,469x target consensus coverage, n=17) for all samples (Supplementary Table 1, Methods). TP is expected to provide adequate statistical power to capture mutations at lower TFx (< 8%) where it may be more challenging with WGS[71]."

Results, lines 390-393:

Notably, every tumor with a private clone was detected in cfDNA WGS at a higher rate than explained by sequencing error, suggesting that the breadth of genome-wide mutation analysis was advantageous in capturing notable representation of every profiled tumor (Figure 7C, Extended Data Fig. 20F)."

Results, lines 414-415:

"The analysis of nucleosome occupancy from cfDNA WGS data can be used to assess differential transcriptional activity between tumor subtypes[76–78]."

Comment 1.13) *The nature of the x-axis values for Fig 7F is not clear. Tumor purity (from each tumor/met? As a fraction between 0-1? times tumor volume (of which metastasis? Or combined across all gross/radiologic mets?)*

Response 1.13) The x-axis in **Figure 7F** displays the multiplication product of tumor purity and tumor volume for an individual tumor, making a *tumor-specific* metric of tumor burden. The ability to make these calculations on a tumor-specific level is key to the correlation with that tumor's private mutation detection in cfDNA.

The tumor purity component of this metric is the same as is used in **Figure 7E** x-axis – the average tumor cellularity across all sections of the individual tumor, with purity determined by a pathologist on histological sections as a proportion between 0 and 1. These pathological tumor purity measurements are reported in **Supplementary Table 2** sheet *"Pathology_byBlock"* – a reference to this table has been added in the legend.

Tumor volume (in cubic centimeters) for the individual tumor is determined by a radiologist from CT scans, as described in the methods section "Radiological assessment of tumor volume". These pathological tumor purity measurements are reported in **Supplementary Table 2** sheet "CT_volumes" – a reference to this table has been added in the legend.

We have reworded the **Figure 7E** and **7F** legends and added text in the results section to enhance clarity and emphasize that these correlations/metrics are tumor-specific:

Results text lines 398-402:

> ***"However, the detection rates of private SNVs were not well explained by clone abundance, nor metastatic site, but rather by sample-specific tumor purity (from histology, ρ=0.59, p=0.0049 for WGS) and volume (from CT, ρ=0.53, p=0.02 for TP) of the individual tumor harboring each private clone (Figure 7E-F, Extended Data Fig. 20H-J, Methods)."***

Figure 7E legend:

> ***"E) Tumor purity of an individual tumor correlates with the detection of that tumor's private SNVs in WGS cfDNA. Tumor purity is determined as a proportion 0-1 by a pathologist on each histological section, then the mean of all sections of a given tumor is calculated (see Supplementary Table 2 and Methods). Each point is a private clone in a tumor, with Spearman correlation statistics shown. For legend refer to A."***

Figure 7F legend:

> ***"F) The product of an individual tumor's histological tumor purity (as in E) and radiological tumor volume (determined by a radiologist from the last CT scan prior to death for 12 patients, see Supplementary Table 2 and Methods) correlates with detection of that tumor's private SNVs in targeted panel cfDNA. Each point is a patient tumor. If a single metastatic site (e.g. liver) had multiple sequenced samples, the mean of the private clone capture in each sample and the mean histological purity across samples was used. Spearman correlation statistics shown. For legend refer to A."***

Comment 1.14*) The following sentence in the Discussion is unclear: "Remarkably, increased transcriptional heterogeneity was associated with longer survival in patients. These findings suggest that, in cases where the original tumor is less aggressive, heterogeneity that accumulated over time led to lethality." I'm not following the logic, and in any case, its not possible from the data to know whether heterogeneity is actually driving mortality.*

Response 1.14) We agree that these statements were not well worded and overstated possibilities regarding lethality. We have rephrased it to more simply state that patients who had

prolonged survival may have experienced more accumulation of transcriptional heterogeneity in their tumors.

Discussion, lines 510-511:

> ***"Patients who survived longer had tumors with increased transcriptional heterogeneity, likely due to greater accumulation over the longer time span."***

Referee #1 (Remarks on code availability):

I reviewed the code at a high level and it looks to have sufficient detail to reproduce results, but I don't have sufficient expertise to comment on more subtle aspects.

Referee #2 (Remarks to the Author):

A. Summary of the key results

The authors performed a very interesting and broad multi-omic analysis on a bladder cancer rapid autopsy cohort of tumor/normal samples from 20 metastatic patients, including analysis of aggressive rare histological subtypes. Their main objective was to provide a comprehensive characterization of metastatic tumor evolution and molecular heterogeneity for these histological subtypes, which is currently limited. They performed whole genome or exome sequencing to study genomic tumor evolution, heterogeneity, and metastatic seeding. Bulk RNA-seq and single-nucleus RNA-seq to study transcriptional heterogeneity and the tumor microenvironment cfDNA targeted and whole genome sequencing from plasma or serum was performed to evaluate genomic heterogeneity, clonal contribution, and transcriptional activity. A cohort of N=20 patients with N=120 samples (primary tumors N=20, metastatic sites N=80; N=20 benign) was used for analyses (N=47 UC, N=22 plasmacytoid, N=18 UC + squamous diff, N=8 NE and N=5 sarcomatoid).

The authors start with mapping the clonal tumor evolution to metastatic growth and sequence of seeding by combining WGS/WES, phylogenetic analyses and radiological imaging. They show that divergent clonal seeding is associated with aggressive histological variants and treatment with ICI.
They show the importance of multiple tumor sampling to be able to fully capture genomic alterations for treatment guidance and show that mBLCA progression is characterized by early clonal driver events and continued evolution through instances of increasingly complex genomic structural alterations. Within the histological variants, they show that pathogenic genomic driver alterations in the founder clone at disease initiation promote early aggressiveness in PUC and NE tumors. In UC and UCSD, pathogenic alterations acquired throughout tumor evolution likely contributed to progression later in the disease course. Interestingly, their data supports a mechanism by which PUC tumors have increased activity of the FANC pathway and ability to repair cisplatin-induced crosslinks compared to UC/UCSD tumors, which may underlie the difficulty in treating this aggressive subtype that often progresses quickly on platinum-based therapies and this is functionally validated in cell line experiments.

The second part focuses on transcriptome analyses, and they are the first to show that the variant histology PUC metastases were luminal-unstable while the primary tumors were stroma-rich, linking tumor subtype heterogeneity to tumor aggressiveness. They are the first to study the TME of variant histologies at single-cell resolution and show that differing levels of immune activation and immunosuppression across mBLCA histological subtypes and metastatic sites has potential implications for immunotherapy response in end-stage disease.

In the last part, they show that most early and driver alterations can be readily captured from cfDNA, while detection of later-evolving SNVs is influenced by clonal burden, tumor volume and purity, and cfDNA tumor fraction (TFx).

B. Originality and significance: if not novel, please include reference
The work presented is very relevant to the field and has not been performed by other groups. Urothelial cancer with variant histology represents a challenge in clinical-decision-making and treatment selection. Although the cohort size is limited, the findings are very relevant and important to the field. The techniques used are not novel to the field, but still very relevant.

Furthermore, the study is unique, being a rapid autopsy program on urothelial cancer and the authors have to be congratulated that they have been able to include 20 patients within a 5-year time frame. The comprehensive characterization of primary tumors and matched metastases further enforces the importance of the study.

Thank you for these positive and encouraging comments on our study.

C. Data & methodology: *validity of approach, quality of data, quality of presentation The authors used a very comprehensive approach which is valid for the posed research question/research gap: WGS/WES, bulk RNA-seq, snRNA-seq (all on tissue) and detection of ctDNA in blood. Some points to consider: Although in some cases the authors validated their findings in external cohorts, in most cases their broad conclusions are based on comparisons of relatively small groups of patients (N = 16).*

Response to 2C: Thank you for this comment. We acknowledge the limited cohort size and have noted this as a limitation in the several points within the Discussion, emphasizing it as an important caveat.

Discussion (driver gene alteration clonality), lines 473-475:

> ***"We identified instances of alterations in key mBLCA genes that were only acquired later in metastases or found in a subset of metastases, although associations with specific genes may not be readily generalizable due to the small cohort size."***

Discussion (immune composition and ICI), lines 520-521:

> ***"Despite the smaller sample sizes in our study, these findings suggest the potential for future stratification of patients to immunotherapy by histological subtype[17,105]."***

Discussion (cfDNA), lines 538-542:

> ***"Other considerations for our findings include the small cohort size and single cfDNA time point for each patient. Future studies involving larger cohorts, including more histologic subtypes, and serial plasma collection are needed to validate our approach as a potential clinically useful approach to detect the presence of both pathogenic alterations and mBLCA subtypes linked to aggressive tumor evolution."***

Discussion (overall study), lines 543-546:

> ***"This study has generated a compendium of multi-omic datasets from a unique cohort of rapid autopsy cases. Despite the modest cohort size, which may limit generalizability, it is among the largest of its kind, comprising multiple tumors per patient and representing histological subtypes, and provides a basis for future investigation."***

Comment 2.1) *This study identified instances of alterations (e.g. ARID1B, PIK3CA/B, and NECTIN4) that were absent in the primary tumor but acquired later in metastases, and conversely others were found only in the primary tumor but not in metastases (e.g. KMT2D in patient 19-007). Can they confirm this claim by analyzing the HMF and TCGA data or by referring to relevant studies, e.g. PMID: 28988769, PMID: 31645765?*

Response 2.1: Thank you for this suggestion. We downloaded copy number and mutation call sets from the Hartwig Medical Foundation (HMF, n=116) and TCGA (n=344) bladder cancer studies. For copy number alterations, we assessed *PIK3CA*, *PIK3CB*, *EGFR*, *ARID1B*, and *NECTIN4* to determine whether they were more frequently altered in the metastatic (HMF)

compared to localized primary (TCGA) settings. We found that *NECTIN4* was significantly enriched for copy number gain/amplification in metastatic tumors (χ^2 test, $P < 0.05$), while *PIK3CB* showed a trend toward metastatic enrichment. In addition, a prior study also reported increased expression and activity of *NECTIN4* in metastatic bladder cancer compared to primary (PMID: 37344281). These results are now shown in **Extended Data Fig. 5E**, and the results have been revised to highlight only *PIK3CB* and *NECTIN4*.

Results, lines 154-157:

"CNAs involving PIK3CB* and *NECTIN4* were frequently non-founder events and confirmed as being subclonal from single-nucleus analysis, consistent with previous observations of enrichment in metastases[31] (Figure 3A, Extended Data Fig. 5A-E)."

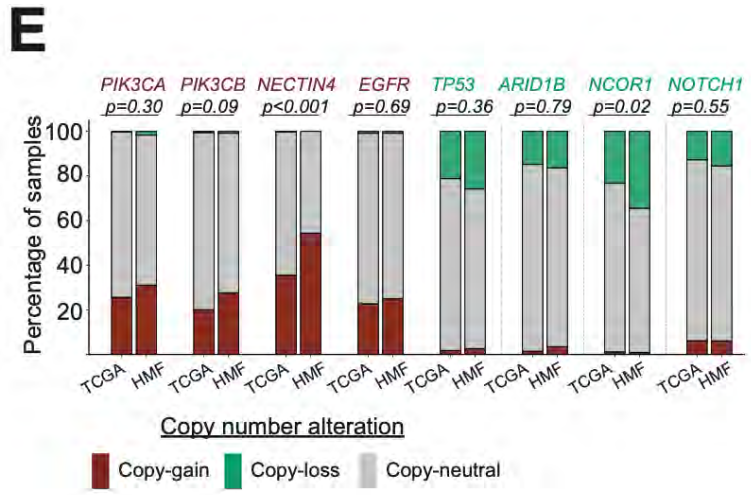

Extended Data Figure 5. E) Comparison of copy number alterations in selected bladder cancer driver genes across HMF (n=116 samples) and TCGA (n=344 samples) cohorts. Bars represent the percentage of samples with copy number alteration. Oncogenes are shown in red and tumor suppressor genes in green. P-values are derived from chi-square tests, comparing copy-number gains in oncogenes and copy-number losses in tumor suppressor genes. Copy number alterations were defined based on ploidy-adjusted copy ratios as described in Methods.

For mutations, we reassessed our initial claim of *KMT2D* being mutated by frameshift deletion in only the primary tumor at autopsy in patient 19-007 because we now have the addition of the TURBT sample taken prior to autopsy. We did not observe this mutation in the TURBT sample, indicating that this event was acquired independently later in only the primary tumor through divergent evolution. These results are now shown in **Extended Data Fig. 4D,** and we have revised text in the Results section to present this event as a private event.

Results, lines 151-154:

"We observed examples of known potentially druggable mutations in private clones for FGFR3 (R248C, patient 19-022), PIK3CA (E545K, patient 15-108), and KMT2D (frameshift deletion, patient 19-007), suggesting divergent evolution (Figure 3A, Extended Data Fig. 4B-D)."

Methods, lines 1561-1572:

"Bladder cancer samples from the cohort described above were used to assess gene-level copy number alterations for genes of interest and compared with the TCGA cohort. Copy number data were normalized and thresholded using a previously described approach (see Gene overlap of tumor CNAs).

The Cancer Genome Atlas (TCGA) data analysis

Copy number data for bladder cancer (BLCA) were obtained from TCGA at the gene level via the Genomic Data Commons (GDC). Associated clinical and sample metadata were curated from previously published sources[32,116]. The analysis was restricted to primary solid tumor samples (N=344). Copy number profiles were processed in the GRCh38 (hg38) reference genome coordinate system and analyzed using a ploidy-aware framework consistent with previously described approaches (see Gene overlap of tumor CNAs) for gene-level CNA normalization and thresholding."

Furthermore, we want to emphasize that we did not intend to claim that these specific gene alterations observed in the metastatic tumors would generalize more broadly. These were examples that we observed as instances of shared and private alterations in known mBLCA genes that were enabled by the unique multi-tumor setting of this cohort and suggests that analyzing multiple metastatic tumors may capture some driver alterations that could be missed by studying the primary tumor only. We have added the limitation of generalizability in the Discussion.

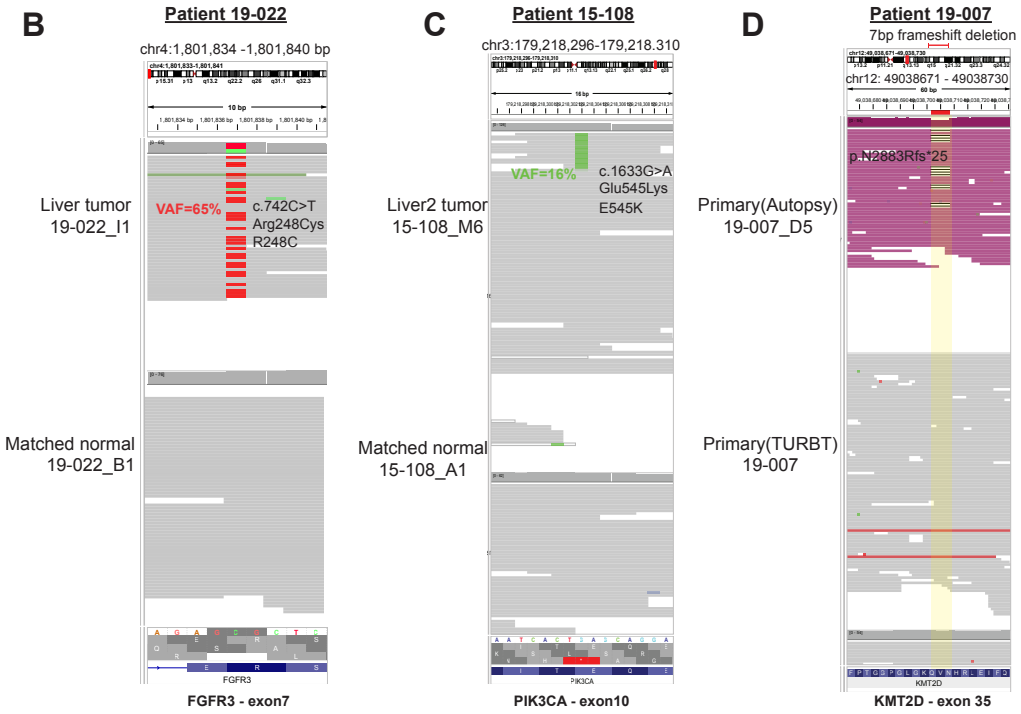

Extended Data Figure 4
B) IGV screenshot showing presence of private mutation in *FGFR3* in patient 19-022 Liver metastasis and absent in matched normal.
C) IGV screenshot showing presence of private mutation in *PIK3CA* in patient 15-108 Liver metastasis and absent in matched normal.
D) IGV screenshot showing presence of private deletion in *KMT2D* in patient 19-007 primary collected at autopsy and absent in primary at TURBT.

Discussion, lines 473-475:

"We identified instances of alterations in key mBLCA genes that were only acquired later in metastases or found in a subset of metastases, although associations with specific genes may not be readily generalizable due to the small cohort size."

Comment 2.2*) Purity of non-conventional UCs may affect results regarding polyphyletic events and survival, as the proportion of non-conventional UC versus conventional UC has been linked to survival. Can the authors discuss whether differences in % of non-conventional UC may have affected interpretation, especially for PUC?*

Response 2.2) We thank the reviewer for bringing up this important matter. We have added further details on the proportion of different histological subtypes in each tumor, as assessed by pathologist F.V.L., in **Supplementary Table 1** (sheet 1 – all_sequencing_detailed) and modified the Results section accordingly. See also **Response 1.1**.

Results, lines 60-65:

"Tumors represented a spectrum of histological subtypes[25], including 50 with conventional urothelial carcinoma (UC) and an enrichment of subtypes: 24 plasmacytoid UC (PUC), 19 UC with squamous differentiation (UCSD), 8 neuroendocrine (NE), and 3 UC with sarcomatoid subtype (UC-Sarc). PUC and NE tumors were predominantly variant histology (mean 96% PUC and 98% NE, respectively), whereas UCSD and UC-sarcomatoid tumors had variable subtype histology ranging from focal to extensive (Supplementary Table 1)."

In the correlative analysis between metastatic seeding and survival (**Figure 2B-C)**, we used histology as a categorical covariate to account for the known influence of histological subtype on patient survival. As the reviewer suggests, the proportion of conventional to non-UC histology may also influence survival. Therefore, we have now additionally performed the same analysis but using % conventional UC morphology as a covariate (**Extended Data Fig. 3C**). We found that % UC morphology itself was not a significant predictor of mortality in the multivariate Cox model ($p = 0.35$) and the corresponding risk score was not able to significantly stratify patient survival, suggesting that it is not likely a confounding factor in the analysis of seeding and survival.

Additionally, in our cohort, PUC tumors did not vary widely in the proportion of PUC histology. 21 of 24 PUC tumors were 100% PUC, with an overall average of 96% PUC. The one patient with mixed PUC morphology is 17-071, which had three 100% PUC tumors and two tumors with 50% and 60% PUC histology. Despite having a lower percentage of PUC histology, patient 17-071 had an overall survival very close to the mean and median survival of the PUC patients (17-071: 1.27 years, mean: 1.11 years, median: 1.1 years, **Supplementary Table 2**) and was similarly enriched in polyclonal polyphyletic seeding events (**Figure 1B**), suggesting that PUC survival was not confounded by purity in our cohort.

Results, lines 115-120:

"The polyclonality of seeding, defined as the mean number of migrating clones across all metastatic seeding events in a patient, trended with increased mortality risk (HR = 6.8, p=0.09, Figure 2B, Extended Data Fig. 3A). This polyclonality metric improved risk stratification (log-rank p=0.0007, Figure 2C) beyond histology, age, and sex alone (log-rank p=0.008), while the purity of variant histology did not contribute to survival risk (log-rank p=0.06) (Extended Data Fig. 3B-C)."

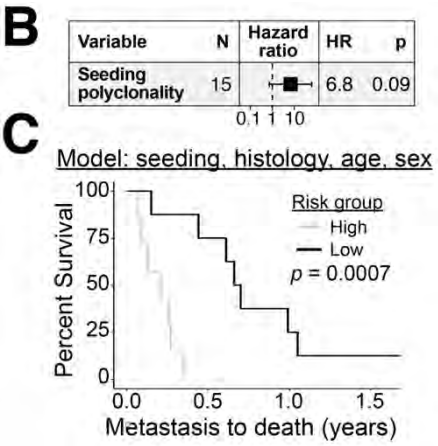

Figure 2

B) Cox proportional hazards model with survival time defined as the interval from first metastasis to death. For each metastasis, the number of clones required to seed the tumor was determined (equivalent to the number of distinct colors in seeding arrows of **Figure 1B**). The mean of this metric was calculated across all metastases in the patient and used as a predictor of survival in a multivariate model controlling for histological subtype, age at diagnosis, and sex. Full model with covariates shown in **Extended Data Fig. 3A**. Patient 16-070 was excluded due to being a statistical outlier in survival (see **Methods**).

C) Patient survival from first metastasis as stratified by the median risk score produced by the multivariate Cox model of seeding polyclonality, histology, age, and sex. Statistics from log-rank test.

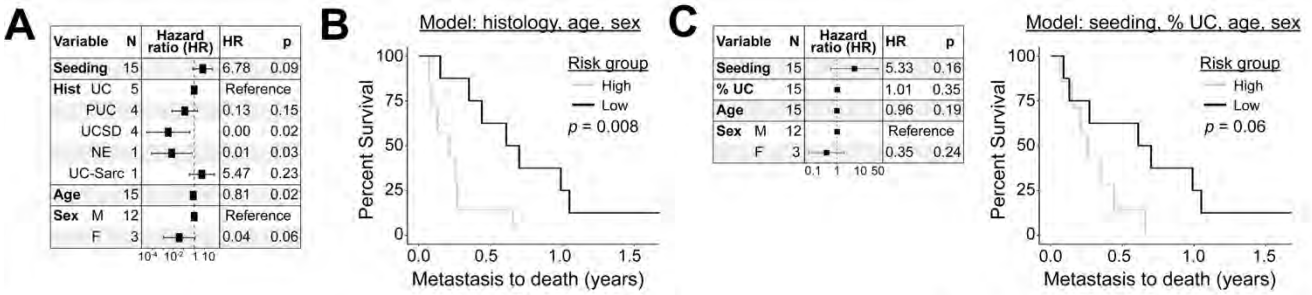

Extended Data Figure 3

A) Cox proportional hazards model with survival time defined as the interval from first metastasis to death. Polyclonality of seeding as a predictor of survival in a multivariate model controlling for histological subtype, age at diagnosis, and sex. Patient 16-070 was excluded due to being a statistical outlier in survival.

B) Patient survival from first metastasis as stratified by the median risk score produced by the multivariate Cox model of only histology, age, and sex. Statistics from log-rank test.

C) Left: Cox proportional hazards model with survival time defined as the interval from first metastasis to death. Multivariate model including polyclonality of seeding, the proportion of UC (versus non-conventional) histology per tumor, age at diagnosis, and sex. **Right**: Patient survival from first metastasis as stratified by the median risk score produced by the multivariate Cox model in the left panel. Statistics from log-rank test, patients stratified by median risk score.

Comment 2.3*) Are there differences in survival between patients who developed liver metastases and those without? In general, patients with liver metastases have poorer outcomes than patients with lymph node metastases.*

Response 2.3) In our cohort, patients with liver metastases tended to have longer survival from diagnosis than patients without liver metastases (**Extended Data Fig. 1C**). While patients with liver metastases have been shown to have worse prognosis than those with other distant sites of metastases, including distant lymph nodes (PMID: 34028594, 29180897), our cohort differs from these published studies due to the inclusion of variant histological subtypes (52% of tumors). The histological subtypes within our cohort are a potential confounder when associating survival with different sites of metastasis because the subtypes themselves differ in metastatic patterns. In

particular, PUC patients have more LN metastases and fewer liver metastases than other subtypes, but have the poorest survival (**Figure 1A, Extended Data Fig. 1B**). In a multivariate ANCOVA analysis, the presence of liver metastases was not significantly associated with survival after adjusting for histological subtype (p=0.88) (**Extended Data Fig. 1C**). Therefore, we conclude that in our cohort, the poor survival of PUC patients and their tendency to only have local lymph node metastatic spread during their short survival times overwhelms the usual trend of liver metastases being associated with poorer outcomes. In other survival analyses, we include histological subtype as a covariate for this reason.

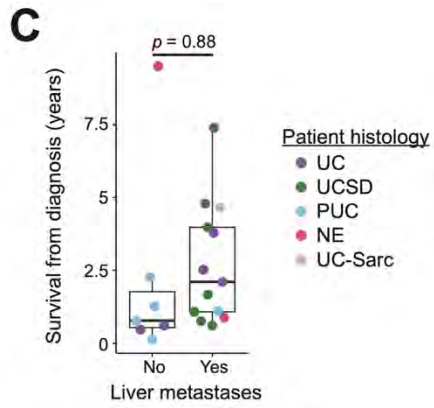

Extended Data Figure 1. C) Survival from diagnosis to death (years) for patients who had versus did not have liver metastasis at autopsy. p-value of the difference in survival by liver met presence with histological subtype as a covariate in an ANCOVA model.

Results, lines 68-70:

> ***"Patients with PUC tumors had the shortest survival from diagnosis (Extended Data Fig. 1B), while the presence of liver metastases was not significantly associated with survival after adjusting for histology (Extended Data Fig. 1C)."***

Comment 2.4*) Platinum chemotherapy may affect clonal selection and induce new mutations that are classified as subclonal. Were there significant time differences between chemotherapy and sample collection across patients and tumor subtypes? Shorter intervals may hinder the discovery of new mutations because of low VAF, specifically if this is true for PUC tumors.*

Response 2.4) This reviewer brings up an interesting point about the time between completion of platinum chemotherapy and collection of samples at autopsy. We had previously examined cisplatin treatment exposure (number of cycles) and found no difference in the number of chemotherapy treatment cycles between histological subtypes (**Extended Data Fig. 12F**). Now, we further assessed the time interval between the completion of cisplatin treatment and death and found no significant difference between PUC and UC/UCSD (p = 0.91, Mann Whitney U test, **Extended Data Fig. 12G**). Together, these analyses indicate that neither duration of cisplatin exposure nor the interval between treatment and death explain the observation that PUC had lower platinum chemotherapy mutational signature. We have added these results to **Extended Data Fig. 12G** and the Results section.

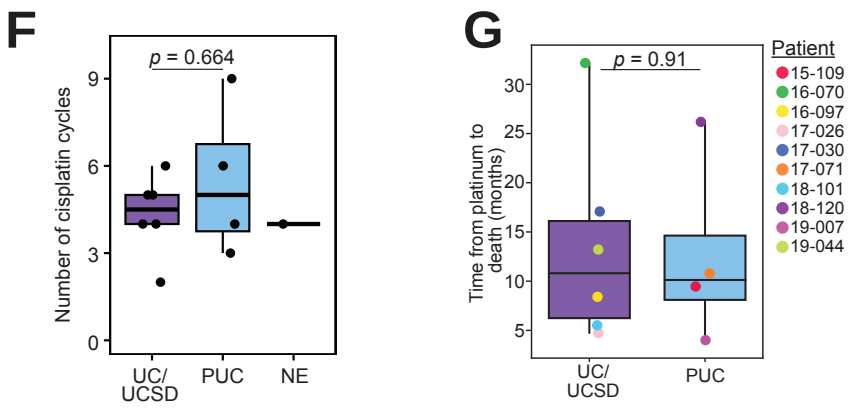

Extended Data Figure 12
F) No significant difference in the number of cisplatin cycles given to UC/UCSD versus PUC patients (p-value from Mann-Whitney U-test)
G) Time from end of cisplatin treatment to death (months) in UC/UCSD and PUC tumors (p-value from Mann-Whitney U-test).

Results, lines 224-229:

> ***"However, PUC tumors displayed significantly lower proportion and total burden (0.73 mutations/Mb) of platinum chemotherapy-induced mutations in shared and private clones compared to tumors of UC or UCSD histology (LME p=0.011, Figure 4B, Extended Data Fig. 12D), despite receiving similar cycles of cisplatin exposure, having comparable time from cisplatin treatment to death, and exhibiting the highest overall TMB (Figure 3E, Extended Data Fig. 12E-G)."***

Comment 2.5.1*) From the methods, it appears that metastatic samples were obtained at the time of death. Were the primary samples obtained before autopsy was performed and could the authors elaborate how this was done?*

Response 2.5.1) Primary samples were collected from autopsy, surgery, and/or transurethral resection of bladder tumor (TURBT) depending on the patient, which we have clarified throughout the revised paper. **Figures 1A** and **Figure 3A** now distinguish between primary tumors taken prior to autopsy by TURBT (n=5) or surgery (n=11), or at autopsy (n=8) using separate colors in the Sankey plot, stacked bar plot, and annotation of the co-mutation plot. Additionally, a column was added to **Supplementary Table 1** to annotate the source of each sample (primary, metastasis, and normal). We have also added information to the Results to clarify how each sample was obtained and in the Methods for the sample processing.

Results, lines 56-60:

> ***"Primary tumors were obtained at diagnosis from transurethral resection of bladder tumor (TURBT, n=5), from surgery (n=11), or at the time of autopsy (n=8); four patients had samples from both TURBT and at autopsy. Normal tissue (n=20), blood (n=17), and metastases (n=80) were collected at autopsy."***

Methods, lines 819-827

> ***"Details of tissue source, location, histology, etc. for each sample can be found in Supplementary Table 1. Autopsy samples (n=108), which included all normal, all metastatic, and 8 primary samples, were obtained within 11.5 hours (median 3.7 hours)***

of death as part of the rapid autopsy program described (Supplementary Table 1). For the logistical framework of the rapid autopsy program, see Figure 1A. A representative selection of the metastases observed at autopsy (excluding bone metastases) was chosen for sequencing, in addition to autopsy-derived primary samples when available. Archival FFPE primary tumor samples (n=16) include diagnostic (pre-treatment) TURBT (n=5) and surgical primary specimens (n=11) (Supplementary Table 1).”

Comment 2.5.2*) If primary samples were not obtained at autopsy, new subclonal populations in primary tumors (if still present during metastatic development) may have not been captured in the analysis, especially upon selective pressure of therapy, and the metastases-to-metastases seeding may be overestimated.*

Response 2.5.2) We thank the reviewer for raising this point. For eight of the nine patients in our cohort with predicted metastasis-to-metastasis seeding, we sequenced a primary tumor sample collected either at autopsy or as part of a radical surgery, meaning the tumor used for seeding analysis was the final state of the primary tumor in the patient's body. For the five patients with radical surgery samples, both CT scans and pathologist assessment at autopsy confirmed the lack of primary tumor or recurrence in the patient following surgery. Therefore, in these patients, there was not a primary tumor present during metastatic development.

The one exception to this, patient 19-037, had their cystectomy aborted due to extensive muscle invasion of their bladder/UVJ primary tumor. While this primary tumor can be observed in CT scans at 6 and 3 months prior to death (**Figure 2A**), pathology found 0% tumor purity when it was sampled extensively at autopsy (**Supplementary Table 2**); therefore, it was not sequenced and the diagnostic TURBT sample was sequenced instead. Due to the aborted surgery in this patient, our analysis may underrepresent clonal evolution of the primary tumor that happened during metastatic development. However, regression of the primary tumor accompanied by growth of the metastases was observed during the time between the last CT scan and death while patient was being treated with paclitaxel. These data suggest that there was divergent evolution between the primary and metastases, supporting the evolutionary reconstruction of multiple metastasis-only shared clones that were observed in the sequenced samples. These metastasis-specific shared clones led to the prediction of a metastasis-to-metastasis seeding pattern, which was further supported by CT scans (**Figure 2A**). There are three other patients (16-070, 17-020, 19-004, who all had an autopsy primary sequenced) who also had a primary tumor remain *in situ* during metastatic development and still show the metastasis-to-metastasis seeding pattern. For these reasons, we continue to classify patient 19-037 as having metastasis-to-metastasis seeding. However, we added a statement of the limitations in the seeding analysis to the Discussion acknowledging the potential uncertainty of our analysis.

Discussion, lines 458-459:

“Our analysis represents the most parsimonious solutions given the available data, although further multi-regional or longitudinal sampling could refine or improve the results.”

Comment 2.6*) Did all 20 patients receive a CT-scan of thorax and abdomen at 3 and 6 months before death? Due to the nature of a rapid autopsy program, it seems unlikely to have all patients undergo radiological imaging at fixed time points before death. This is of importance because the authors use imaging to corroborate ordering of the computationally inferred metastatic seeding, line 95 – 106. Were all CT-scan centrally reviewed by an independent radiologist and were all*

metastatic sites confirmed? As CT-scanning is a snapshot, small metastases at t= -3 mo or t = -6 mo, might have been missed and they may have become large metastases at the moment of death.

Response 2.6) It is correct that patients did not undergo scheduled imaging with respect to autopsy due to the unpredictable timing of a rapid autopsy. As such, in our original analysis, we retrospectively requested scans that were available for patients at approximately 3 months (2-4 months) and 6 months (5-7 months) prior to death (PTD) to assess the ordering of late metastatic growth in the patients with predicted metastasis-to-metastasis seeding. All CT scans were centrally reviewed by an independent radiologist as part of standard of care and the de-identified radiology reports and scans were further evaluated by a radiation oncologist (O.Y.M.) to confirm the presence of the metastatic sites collected at autopsy.

To more thoroughly assess metastatic seeding order without bias towards the availability of certain CT scan time points, we have now requested all available clinical staging CT scans for all patients (**Supplementary Table 2;** see also **Response 1.2**). With these additional scans, of the nine patients with predicted metastasis-to-metastasis seeding, we are now able to corroborate the progression and ordering of metastatic seeding in five patients (**Figure 2A**). For the remaining four patients, we were still unable confirm the ordering of seeding by CT due to either (1) lack of any staging scans (15-108), (2) all sequenced metastases were already present in their first staging scan (16-097 at 13.5m PTD, 19-001 at 1.6m PTD), or (3) the metastases at autopsy could not be reliably matched to CT scan lesions (17-071 at 6m PTD) (**Extended Data Fig. 2F**).

The reviewer is correct that the CT scans are snapshots that may miss small metastases. We understand that this is a limitation of the analysis, particularly if looking only at specific timepoints. Expanding our analysis to additional CT scans may help to reduce the chance that we miss certain metastases; however, some metastases would still be missed even on the latest CT scan prior to death. For example, we sequenced a metastasis collected at autopsy that was not detectable on the last CT scan in each of patients 17-030, 19-004, and 19-037.

For all of these points, we have clarified the results and limitations in the Results, Methods, and Discussion. **Figure 2** now includes updated CT scans corroborating metastatic seeding for five patients.

Methods, lines 880-889:

"Corroboration of metastatic seeding

For each patient with metastasis-to-metastasis seeding (n=9), the first available clinical staging CT scan after diagnosis was assessed for visible tumors to determine whether an initiating metastasis could be identified. For five patients in which the early CT scan identified a first metastasis, subsequent CT scans were assessed to follow metastatic evolution. In patient 19-037, the sequenced peri-pancreatic LN corresponds to a portion of the RP LN visible in the CT scan. The remaining four patients were unable to be assessed further due to either lack of any staging CT scans (15-108), all sequenced metastases visible at first CT scan (16-097, 19-001), or lack of clear correspondence between lesions visible on first scan and metastatic sites collected at autopsy (17-071) (Extended Data Fig. 2F)."

Results, lines 102-113:

"Computed tomography (CT) scans performed prior to autopsy were used to corroborate the ordering of the computationally inferred metastasis-to-metastasis seeding. We evaluated scans for all 20 patients and identified five for whom metastatic

timing could be determined from the pattern of disease progression on staging CT scans (Figure 2A, Extended Data Fig. 2, Supplementary Table 2, Methods). For patients 17-030, 19-004 and 19-037, radiographic imaging detected a single metastatic tumor in the first staging scan that confirmed the first seeded metastasis, while subsequent scans detected additional lesions that developed later. In patients 16-070 and 17-020, the initial scan detected two early metastatic lesions and computational seeding analysis was able to further resolve the clonal constraints to identify the initial seeded metastasis (periaortic lymph node and right pleura, respectively). Metastases of the abdominal wall (17-030), liver (19-004), and perinephritic site (19-037) that were absent in the last scans likely emerged after the scan during the latest stages of disease."

Discussion, lines 455-459:

"Analysis of CT scans corroborated the temporal sequence of metastatic tumor seeding, though it does not preclude the possibility that late-emerging metastases may have seeded earlier below the limit of detection by CT. Our analysis represents the most parsimonious solutions given the available data, although further multi-regional or longitudinal sampling could refine or improve the results."

A

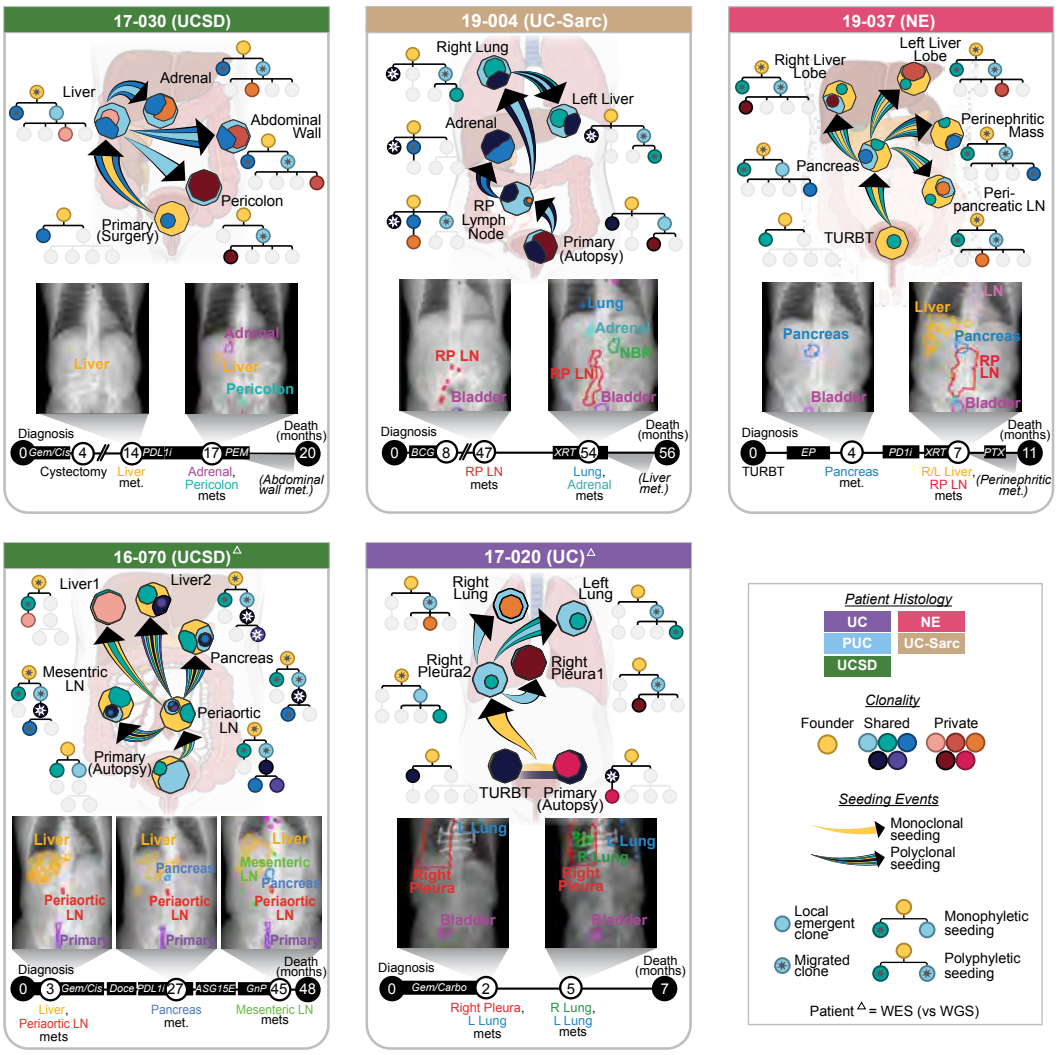

Figure 2. A) Mutation phylogenies and metastatic seeding patterns for patients 17-030, 19-004, 19-037, 16-070, and 17-020. Phylogenetic trees, CloneMaps, and seeding events are shown as described in **Figure 1B**. A star inside a clone in the phylogenetic tree indicates that clone was involved in the seeding event of that metastasis. Clones that emerge within a metastasis after seeding are indicated without a star. Monophyletic seeding is indicated with a single star across clones in the same tree depth; polyphyletic seeding is indicated with two stars in bifurcating branching clones. 2D projection images of computed tomography (CT) scans show the ordering of metastatic development from the patient's first to last clinical staging scans. Individual axial, coronal, and sagittal cross-sectional images of the CT scans are shown in **Extended Data Fig. 2A-E**. Clinical history below each patient indicates months after initial diagnosis for CT scans and death. Standard of care treatments are annotated and other treatments (e.g., clinical trials) denoted by asterisks (see **Extended Data Fig. 1A** and **Supplementary Table 2** for full details).
BCG: Bacillus Calmette-Guérin vaccine; Doce: docetaxel; EP: Etoposide and platinum (cisplatin); Gem: gemcitabine alone; Gem/Carbo: gemcitabine and carboplatin; Gem/Cis: gemcitabine and cisplatin; G/P: Gemcitabine and paclitaxel; L: left; LN: lymph node; Met: metastasis; NBR: nephroureterectomy bed recurrence; PDL1i: programmed death-ligand 1 inhibitor; PD1i: programmed cell death protein 1 inhibitor; Pem: pemetrexed; PTX: paclitaxel; R: right; RP: retroperitoneal; TURBT: Transurethral Resection of Bladder Tumor; XRT: radiation.

Comment 2.7*) Although Figure 1A demonstrates the origin of the primary tumor and metastases, the authors are encouraged to provide additional information per individual patient and show how many metastatic sites per patient were harvested and what was primary histology of the primary tumor versus those of the harvested metastatic sites? In addition, what was the origin of the 20 benign samples?*

Response 2.7) We thank the reviewer for bringing this need for clarification of the patient characteristics and tumor samples. All of these details can be found in **Supplementary Table 1**, which lists each tissue sample used in this study for each patient. We apologize that this table was uploaded incorrectly in our original submission and these details were not clearer. **Supplementary Table 1** lists all primary, metastatic, and normal samples separately for each patient, along with the histology of each individual tumor (column "hist_detailed"). The origin of each normal sample can also be found in column "tumor_site" (n=18 kidney and n=2 liver). In addition to this table, the number of metastatic sites per patient and their histology can be found in the **Figure 1A** (middle panel). The location and histology of each tumor is also annotated in **Figure 3A**. To bring attention to where these details can be found, the table is referred to in the manuscript Results, Methods, and the **Figure 1A** legend.

Results, lines 52-60:

> ***"In this study, 124 tissue samples were collected from 20 patients with carcinomas of the urothelium via rapid autopsy performed within a median of 3.7 hours (range 2.8-11.5) following death (Extended Data Fig. 1A, Supplementary Table 1). Benign (n=20) and tumor tissues (n=104) from primary and metastatic sites were collected for genomic and transcriptomic analyses (Figure 1A, Supplementary Table 1). Primary tumors were obtained at diagnosis from transurethral resection of bladder tumor (TURBT, n=5), from surgery (n=11), or at the time of autopsy (n=8); four patients had samples from both TURBT and at autopsy. Normal tissue (n=20), blood (n=17), and metastases (n=80) were collected at autopsy."***

Methods, lines 817-820:

> ***"Specimens were obtained from 20 patients, including histopathologically normal tissue (n=20, flash-frozen tissue), primary tumor samples (n=24; 16 FFPE and 8 flash-frozen tissue), and 1–7 metastases per patient (n=80, flash-frozen tissue). Details of tissue source, location, histology, etc. for each sample can be found in Supplementary Table 1."***

Figure 1A, legend:

> ***"Figure 1A) Schematic and description of the UW/Fred Hutch rapid autopsy cohort, involving 20 patients from 2015-2020. Sankey diagram shows histological subtype classification and anatomical sites of all 104 primary and metastatic tumors (left panel). Middle panel shows sequencing performed for each patient (bulk DNA and RNA sequencing, snRNA-seq, and cell-free DNA sequencing) and the number, tumor site, and histology of all primary and metastatic samples for each patient (see also Supplementary Table 1). Right panel summarizes the analyses undertaken for this study. Dx, diagnosis; ICI, immune checkpoint inhibitor; Met, metastasis; TURBT, transurethral resection of bladder tumor."***

Comment 2.8*) Independent pathology review of all primary tumors with pure conventional UC and metastases with variant histology would improve the quality of the study. In addition, it is important to discriminate between urothelial carcinoma with variant histology, like plasmacytoid*

or micropapillary UC, while small cell neuro-endocrine carcinoma of the bladder or squamous cell carcinoma of the bladder are different histology. Were all tumors with squamous or NE differentiation in the study predominant urothelial carcinoma? Please clarify.

Response 2.8) All primary and metastatic tumors in the study have been reviewed by an independent pathologist (F.V.L.). Detailed annotation from F.V.L. of whether each tumor was pure versus mixed histology has been added to **Supplementary Table 1** – columns "hist_detailed", "UC_percent", "UCSD_percent", "PUC_percent", "SARC_percent", and "NE_percent". NE and PUC tumors were predominantly variant histology: neuroendocrine tumors were between 90-100% neuroendocrine (90% NE/10% UC in 17-047; 100% NE in 19-037) and 21/24 PUC tumors were 100% plasmacytoid morphology. UCSD tumors ranged from UCSD-focal (5% squamous differentiation, n=10) to UCSD_90 (90% squamous differentiation, n=7). UC-sarcomatoid tumors were also varied, with one predominantly sarcomatoid (70%) and two predominantly UC (5% sarcomatoid).

These additional details and a direct reference to **Supplementary Table 1** have been added to the Results, and further clarification between UC with variant histology (PUC, UC-Sarc, and UCSD) and small cell neuroendocrine histology is included in the Methods.

Results, lines 60-65:

> ***"Tumors represented a spectrum of histological subtypes[25], including 50 with conventional urothelial carcinoma (UC) and an enrichment of subtypes: 24 plasmacytoid UC (PUC), 19 UC with squamous differentiation (UCSD), 8 neuroendocrine (NE), and 3 UC with sarcomatoid subtype (UC-Sarc). PUC and NE tumors were predominantly variant histology (mean 96% PUC and 98% NE, respectively), whereas UCSD and UC-sarcomatoid tumors had variable subtype histology ranging from focal to extensive (Supplementary Table 1)."***

Methods, lines 847-861:

> ***"Histology was defined both at the patient level and the tumor (sample) level. All classifications were based on pathology assessment of FFPE H&E specimens by pathologist (F.V.L.) review based on the WHO Classifications of Tumours of the Genitourinary System and Male Genital Organs (5th edition)25. Neuroendocrine histology was further verified by synaptophysin positivity. PUC, UC-sarcomatoid, and UCSD tumors are urothelial carcinoma with plasmacytoid, sarcomatoid, or squamous differentiation, respectively. Patients and tumors were designated as non-UC if there was any evidence of variant histology. For patient-level histology, the histology was defined as a variant if there was evidence of subtype histology in any tumor in that patient (e.g., if a patient had any tumor exhibiting any squamous differentiation, they were classified as UCSD). Patients 16-070, 17-030, 18-101, and 19-022 were designated UCSD by having a mix of UC and UCSD tumors, while all tumors in UCSD patients 16-097 and 17-026 exhibited UCSD histology. Sample-level histology was defined for each tumor individually (e.g., 16-070's primary tumor is UCSD, while their metastases are UC at the sample level). Further details on the percentage of histological subtypes in each tumor are given in Supplementary Table 1 (1st sheet)."***

Comment 2.9.1*) Suggest using variant histology instead of histological subtypes.*

Response 2.9.1) Thank you for this suggestion. In accordance with the most recent 2022 WHO classification of urinary tract tumors (5th edition), we opt to primarily retain "histological subtypes".

The guideline explicitly replaces the use of “histological variants/variant histology” with “histological subtypes”. In reviewing post-2022 literature (PMID: 40288936, 38321289), we see “histological subtypes” being used for this reason.

Comment 2.9.2*) In addition, not all variant histologies in bladder cancer correlate to poor prognosis, i.e. glandular, lympho-epitheliod. Furthermore, the poor prognosis of VH is predominantly caused by metastatic spread, such as small cell neuro-endrocrine bladder cancer or micropapillary urothelial carcinoma. However, plasmacytoid urothelial bladder cancer typically is characterized by local spreading of tumor, which is clinically not apparent leading to a very high risk of positive surgical margins in patients undergoing radical surgery. I would suggest adjusting the abstract and taking these remarks into account.*

Response 2.9.2) Thank you for pointing out this important distinction. We have adjusted wording throughout the manuscript to remove implications that all non-UC histological subtypes have poor prognosis. We have also added a Kaplan-Meier plot depicting the survival by histological subtype within our cohort, where PUC, but not other subtypes, shows poorer survival than UC (**Extended Data Fig. 1B**).

Introduction, lines 24-30:

“Approximately one in four patients with mBLCA have tumors with subtype histologic features such as squamous, plasmacytoid, neuroendocrine, or sarcomatoid differentiation[5,6]. These histological subtypes often have distinct disease trajectories compared to conventional urothelial carcinoma (UC)[5–8]. However, it is not well understood how genomic, transcriptomic, and microenvironmental heterogeneity evolve in these tumors and shape their distinct natural histories and responses to therapy[9–14].”

Results, lines 68-70:

“Patients with PUC tumors had the shortest survival from diagnosis (Extended Data Fig. 1B), while the presence of liver metastases was not significantly associated with survival after adjusting for histology (Extended Data Fig. 1C).”

Discussion, lines 546-548:

“Our results establish the foundational landscape of tumor evolution and heterogeneity of bladder cancer subtypes, uncovering molecular characteristics that shape the natural history of each subtype as it progresses to end stage disease.”

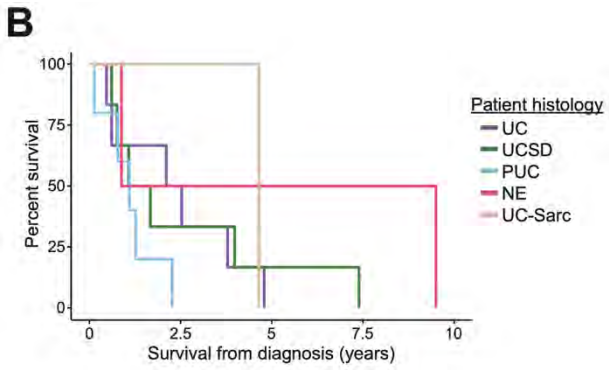

Extended Data Figure 1. B) Survival from diagnosis to death (years) stratified by patient histology.

Comment 2.10*) Please provide justification for the cutoff used for highly polyclonal seeding (2.3) as this is correlated to poor survival, line 107-110 and Figure 2D. In addition, t=0 is the time of diagnosis, but some patients were diagnosed with primary metastatic disease whereas others had MIBC but were cM0 at moment of diagnosis. Can the authors explain how they conducted the survival analysis shown in Fig 2?*

Response 2.10) The cutoff between high and low polyclonal seeding (2.3 clones per seeding event) for the survival analysis in previous **Figure 2D** was set as the median value of this metric across patients, ensuring an approximately equal split of the cohort. Upon further consideration, we now avoid dichotomization entirely by employing a multivariate Cox regression model that uses the seeding polyclonality metric (the mean number of migrating clones across all metastatic seeding events in each patient) as a continuous variable (new **Figure 2B**). We included histology, age, and sex as covariates in the model known to be associated with bladder cancer patient survival (**Extended Data Fig. 3A**). Seeding polyclonality did not reach significance as an independent predictor of survival in the updated analysis but still displayed a high hazard ratio (HR = 6.78, p=0.09). Additionally, this multivariate Cox regression model is able to stratify patients into distinct high- and low-risk groups (**Figure 2C**) with greater separation than a base model of the known variables of histology, age, and sex (**Extended Data Fig. 2B**). Note that the seeding results have also been updated with the addition of new TURBT samples (see **Response 1.3**). We have updated the Results **Figure 2**, and **Extended Data Fig. 3** to reflect these changes. See also **Response 1.4**.

This survival analysis in the previous Figure 2D and now the new **Figure 2B** was performed with respect to survival from first metastasis, since the polyclonal seeding metric quantifies heterogeneity in metastatic evolution. For this reason, we chose to set t=0 to the time a patient's first metastasis was observed on CT scan to avoid confounding analysis of metastatic seeding dynamics in instances of prolonged disease-free survival between diagnosis and first metastasis. For patients who presented with metastases at diagnosis (n=1 in this analysis), time of diagnosis was used as time of first metastasis.

Methods, lines 1337-1350:

> ***"Migration trees and clonal relationships were visualized using Graphviz. MACHINA was run on a high-performance computing cluster using Gurobi version 11.0 with a WLS license. Multivariate Cox regression models including known prognostic factors of age, sex, and histology were used to assess the relationship between polyclonality of seeding (the mean number of migrating clones across all metastatic seeding events in each patient) and patient survival from first metastasis to death. Time that the patient's first metastasis was observed by CT scan was set to t_0 to reduce confounding from the variable interval of disease-free survival from diagnosis to first metastasis. For 1 patient who presented with metastases at diagnosis, we use diagnosis as the time of first metastasis, though there is uncertainty as to when these tumors may have first arisen in the patient. To compute the mean seeding polyclonality metric, we used the following. Let $c_{m,p}$ be the number of clones required to seed metastasis m in patient p. Then, the mean number of clones per seeding event across M total metastases in the patient p was defined as $\overline{C_p} = \left(\sum_m^M c_{m,p}\right)/M$."***

Results, lines 115-120:

> ***"The polyclonality of seeding, defined as the mean number of migrating clones across all metastatic seeding events in a patient, trended with increased mortality risk (HR = 6.8, p=0.09, Figure 2B, Extended Data Fig. 3A). This polyclonality metric improved risk***

stratification (log-rank p=0.0007, Figure 2C) beyond histology, age, and sex alone (log-rank p=0.008), while the purity of variant histology did not contribute to survival risk (log-rank p=0.06) (Extended Data Fig. 3B-C).”

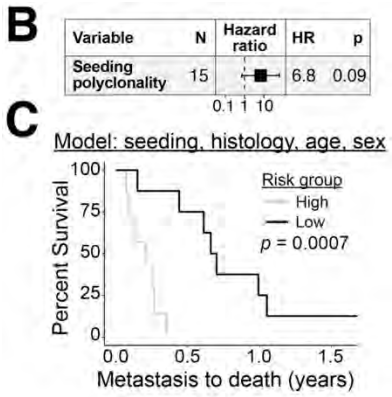

Figure 2
B) Cox proportional hazards model with survival time defined as the interval from first metastasis to death. For each metastasis, the number of clones required to seed the tumor was determined (equivalent to the number of distinct colors in seeding arrows of **Figure 1B**). The mean of this metric was calculated across all metastases in the patient and used as a predictor of survival in a multivariate model controlling for histological subtype, age at diagnosis, and sex. Full model with covariates shown in **Extended Data Fig. 3A**. Patient 16-070 was excluded due to being a statistical outlier in survival (see **Methods**).
C) Patient survival from first metastasis as stratified by the median risk score produced by the multivariate Cox model of seeding polyclonality, histology, age, and sex. Statistics from log-rank test.

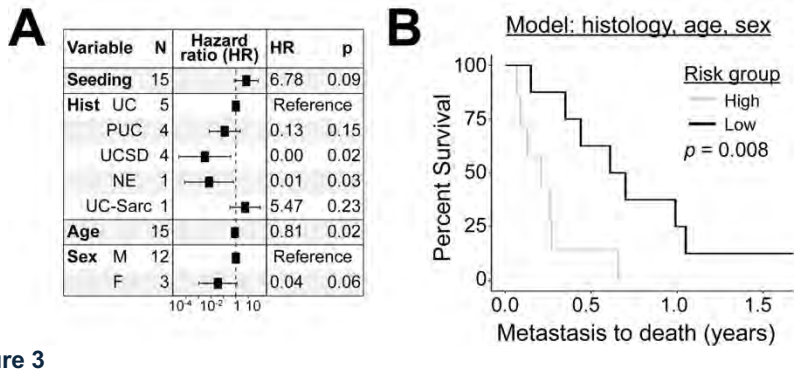

Extended Data Figure 3
A) Cox proportional hazards model with survival time defined as the interval from first metastasis to death. Polyclonality of seeding as a predictor of survival in a multivariate model controlling for histological subtype, age at diagnosis, and sex. Patient 16-070 was excluded due to being a statistical outlier in survival.
B) Patient survival from first metastasis as stratified by the median risk score produced by the multivariate Cox model of only histology, age, and sex. Statistics from log-rank test.

D. *Appropriate use of statistics and treatment of uncertainties*

Comment 2D) *Line 1813 briefly mentions the statistical tests used but from the information provided it is not possible to judge their appropriate use and the treatment of uncertainties.*

Response 2D) We have expanded upon our explanation of statistical testing in the methods, adding a description of when certain tests were used and how they were performed, in addition to listing the specific statistical tests used in each figure panel legend.

Methods, lines 1792-1810:
“Graphing and statistics

A combination of R (v4.4.3) and Python (v3.19, pandas v1.40) was used for scripting, graphs, and statistics. In R, ggplot2 (v3.5.1) was used for graphing, rstatix (v0.7.2) for t-tests and Mann-Whitney U-tests, and lme4 (v1.1-36) for linear mixed effects models. For the snakemake pipelines, Python version 3.7.4 is used. All statistical tests were two-sided unless otherwise specified, with the specific statistical tests used for each analysis are detailed in the respective figure legends.

Linear mixed-effects models were applied for repeated measures within patients (e.g., multiple tumors in a patient), incorporating patient ID as a random effect. For intra-patient comparisons (e.g., proportions of founder, shared, and private alterations), we utilized paired Wilcoxon signed-rank tests. Paired t-tests were used for paired cell line experiments (e.g., siNTC versus siFANCF). All linear fits shown in the figures were obtained using simple linear least-squares regression.

Survival analyses were performed using the Cox proportional hazards model implemented in the R package survival (v0.5.0), with survival time defined as the interval from metastasis to death. Hazard ratios and corresponding P values were derived from the fitted models, and results were presented as forest plots generated with the forestmodel package. For risk stratification, patient-specific risk scores were calculated as the linear predictor from the Cox model and dichotomized at the median into high- and low-risk groups. Kaplan–Meier survival curves were generated using the survminer package"

E. *Conclusions: robustness, validity, reliability. Although a limited number of patients was analyzed, methods used and data analyses are very comprehensive and robust. Whenever a validation was possible (on other cohorts), the authors performed the validation and also set out to perform a functional validation by using cell lines.*

F. *Suggested improvements: experiments, data for possible revision.*

In general, there is a need for check of figures/tables for completeness and accurate numbers. For example:

Comment 2F.1*) Discrepancy: Figure 1 right panel: #tumors for WGS/WES N=89, text line 66 states "all" (N=100)*

Response to 2F.1) We thank the reviewer for this comment. We would like to clarify that the sentence in the Main text reflects the total number of tumor samples profiled by either DNA or RNA sequencing (100 tumors). Of these 100 tumors, 89 tumors have WES or WGS data, while 11 were profiled by RNA sequencing only. In total, 83 tumors had RNAseq performed. Following the addition of four newly sequenced TURBT samples to address **Comment 1.3** (see **Response 1.3**), the total number of unique tumor blocks analyzed increased to 104, and the count of tumors with WES or WGS data is now 93. These numbers are also reflected in the updated **Figure 1** and included in **Supplemental Table 1.**

Comment 2F.2) *Supp Table 1 sheet 1 should contain NGS info from all samples but only contains N=8 patients*

Response to 2F.2) We thank the reviewer for highlighting the incomplete information in Supplementary Table 1 (sheet 1). We had inadvertently used a filter that ended up unintentionally hiding the other rows in the Excel file. We have removed this filter.

Comment 2F.3) *Supp Table 3 sheet 1 should contain counts of seeding events for all analyzed metastatic samples, now only contains N=2*

Response to 2F.3) This table was also inadvertently filtered such that not all the samples were visible. These details are now fully shown in **Supplementary Table 3** (sheet= Metastatic_seeding_summary).

G. References: appropriate credit to previous work? Yes

H. *Clarity and context: lucidity of abstract/summary, appropriateness of abstract, introduction and conclusions*

Comment 2H.1) *Good structure, good readability though the authors are encouraged to check that past tense is used throughout the entire manuscript. See for examples line 47, 62, and 118-120.*

Response to 2H.1) We have carefully reviewed the manuscript and now correctly use past tense throughout.

Comment 2H.2) *The authors use histological variation and histological subtype throughout the abstract. Did the authors considered using variant histology?*

Response to 2H.2) Please see **Response 2.9.1**.

Comment 2H.3*) Limitations of the study are lacking in the abstract and main text.*

Response to 2H.3) We thank the reviewer for this important point. We have revised the manuscript to explicitly address study limitations in two categories. (1) The modest cohort size may limit statistical power and generalizability; however, it represents one of the largest cohorts of its kind, encompassing multiple tumors per patient and histological subtypes, and provides a foundation for future investigation. Additional patients will further refine these findings. (2) Analysis-specific limitations include incomplete assessment of genomic heterogeneity without multiregional tumor profiling of each lesion; in the single-cell analyses, findings such as suppressive myeloid populations require validation in larger cohorts; and in cfDNA analyses, the inability to distinguish clonal hematopoiesis without matched peripheral blood sequencing and reliance on a single time point per patient. These points have now been incorporated into the Discussion.

Discussion, lines 544-545:

> ***"Despite the modest cohort size, which may limit generalizability, it is among the largest of its kind, comprising multiple tumors per patient and representing histological subtypes"***

Discussion, lines 455-459:

> ***"Analysis of CT scans corroborated the temporal sequence of metastatic tumor seeding, though it does not preclude the possibility that late-emerging metastases may have seeded earlier below the limit of detection by CT. Our analysis represents the most parsimonious solutions given the available data, although further multi-regional or longitudinal sampling could refine or improve the results."***

Discussion, lines 479-481:

"While multi-regional sampling of individual tumors could reveal additional insights, our clonality analysis was able to assess genomic heterogeneity both within and across metastases, revealing that the degree of genomic heterogeneity is related to histological subtype."

Discussion, lines 520-521:

"Despite the smaller sample sizes in our study, these findings suggest the potential for future stratification of patients to immunotherapy by histological subtype[17,105]."

Discussion, lines 535-542:

"A limitation of our analysis was the challenge in assessing alterations unique to cfDNA, because clonal hematopoiesis of indeterminate potential (CHIP) mutations could not be distinguished without peripheral blood mononuclear sequencing. Other considerations for our findings include the small cohort size and single cfDNA time point for each patient. Future studies involving larger cohorts, including more histologic subtypes, and serial plasma collection are needed to validate our approach as a potential clinically useful approach to detect the presence of both pathogenic alterations and mBLCA subtypes linked to aggressive tumor evolution."

Comment 2H.4) *Only 5 authors have reported COI, which seems limited.*

Response to 2H.4) COIs for 8 additional authors have been included in the revised manuscript in the COMPETING INTERESTS section.

Referee #2 (Remarks on code availability):

Our bioinformatician has reviewed the code and was onsidered appropriate. The data presented in the paper are reproducible and a usable resource to the community.

We thank the reviewer for testing our code and noting that it is documented appropriately.

Referee #3 (Remarks to the Author):

Itagi et. al. present data from a rapid autopsy program that has collected primary and metastatic tumors from bladder cancer patients, specifically enriching for histologic subtypes. They go on to complete comprehensive molecular profiling of both the tumors and mets and relate these findings back to the histologic subtypes and clinical features. This study representing an enormous effort by all the investigators involved and should be commended, not only for their findings but for the high-quality data they have generated.

The true strength of this manuscript is the comprehensiveness of the molecular profiling and the amount of data that was generated, which I am sure will aid in numerous subsequent discoveries across the research community. However, there is an overall lack of integration between omic platforms and tissue sources (primary/met/normal). While the focus on histologic subtypes is interesting and unique feature of this work, the layering of more clinically relevant questions, such as clonal evolution and adaptation in response to therapy could have added to the broad impact of this work (specific comments below).

In total, the study as currently presented, does lack the paradigm shifting impact typically seen in a Nature publication, however, it represents an outstanding compilation of high quality data, which as a resource, would be of considerable interest to the Nature readership.

Specific comments:

Comment 3.1*) Regarding the relationship between ICI and clonal evolution. Using imaging and clinical record, can the authors compare the clonal composition of mets that that were present prior to ICI versus those that developed after ICI (e.i. ICI did not impose pressure on the met itself but rather the tumor that seeded the met). Does ICI change which cells are able to migrate and where they migrate to or does it selectively effect specific populations within the tumor?*

Response 3.1) We appreciate the reviewer's suggestion to explore the relationship between immunotherapy and clonality further. As suggested, we have significantly expanded our use of clinical imaging (CT scans) to determine which metastases were present prior to ICI versus those that developed after ICI. In our cohort of 20 patients, 12 were treated with immunotherapy (PDL1i or PD1i). Of these 12, three patients died less than one week after beginning ICI treatment, which we considered too brief to assess the effects of ICI. Therefore, we focused on 9 patients who underwent at least 1 full cycle of ICI treatment where we can assess the effects of immunotherapy on clonal evolution (**Supplementary Table 2**). Radiation oncologist O.Y.M. re-reviewed CT scans for each patient to determine which metastases were visible on the scan that immediately preceded the start of ICI treatment (**Extended Data Fig. 2G**). As noted by the reviewer, metastases already present prior to ICI ("pre-ICI metastases") represented the tumors that ICI may have imposed direct selection pressure. Any metastases that were not visible by CT before ICI treatment were considered to be seeded after ICI ("post-ICI metastases"), and therefore ICI did not impose pressure on these metastases directly, but rather on the tumors that seeded these post-ICI metastases. A table showing the designation of all metastases within these 9 patients as before versus after ICI, along with relevant clonality and seeding metrics, has been added as **Supplementary Table 3**. Of these 9 patients, there were 3 who had all metastases that were visible by CT prior to start of ICI therapy, whereas 6 patients had both metastases visible pre-ICI and metastases that only appeared post-ICI. In total, 17 metastases were designated "pre-ICI" and 15 "post-ICI". We have added these details to the Methods.

Methods, lines 890-903:

> ***"Determination of pre- versus post-ICI metastasis***
>
> ***For each patient who underwent at least one full cycle of immune checkpoint inhibitors (ICI, n=9, Supplementary Table 2), the CT scan that immediately preceded start of ICI treatment was assessed for visible tumors. The time between the CT scan preceding ICI and the start of ICI is variable (median 16 days, range 2 - 260 days). For patient 19-022, the most recent CT scan available before ICI was 260 days prior, but clinical records confirmed that only the lung metastasis was observed before starting ICI treatment. The metastases already in place before ICI were designated as "pre-ICI metastases", while metastases collected and sequenced at autopsy but not visible by CT before ICI were designated "post-ICI metastases". Of the 9 ICI-treated patients, there were 3 for whom all metastases were visible by CT prior to start of ICI therapy. Six patients had both metastases visible pre-ICI and metastases that only appeared post-ICI. In total, 17 metastases were designated "pre-ICI" and 15 were "post-ICI" (Supplementary Table 3). Clonal composition (number and CP of clones), metastatic seeding, and metastatic site were compared between metastases seeded pre- versus post-ICI."***

While the suggestion to investigate the clonal composition and timing of metastases affected by ICI is important, we must acknowledge that our cohort may not be ideally positioned to answer it. One limitation to our analysis is that, while we have designated metastases as to whether they were seeded before or after ICI, all metastases were sequenced at the end of life and thus after ICI treatment. Therefore, this comparison does not answer how ICI directly changes the clonal dynamics of tumors, which would require serial sampling of tumors before and after treatment. However, we can compare the different inferred seeding patterns between pre-ICI and post-ICI metastases to gain some insights into the pressure ICI may impose on these tumors. Furthermore, while we have reviewed CT scans and clinical records extensively to determine which metastases were visible before the start of ICI, the clinical record and CT scans were not prospectively timed to compare molecular differences pre- and post-ICI. Therefore, the time between the CT scan preceding ICI and the start of ICI is variable (median 16 days, range 2 - 260 days). With these limitations in mind, we have added new analyses comparing between metastases that were seeded pre- versus post-ICI to determine whether ICI may have exerted selective pressure to affect 1) number of total clones, 2) which clones were able to migrate, 3) where the clones migrated, and 4) overall clonal composition.

Discussion, lines 458-459:

> ***"Our analysis represents the most parsimonious solutions given the available data, although further multi-regional or longitudinal sampling could refine or improve the results."***

(1) First, we found no difference in the number of total clones observed in tumors that were seeded pre- versus post-ICI (median pre = 4, median post = 4, linear mixed effects model p=0.46, **Supplementary Table 3**). **(2)** However, we observed that metastases arising post-ICI were seeded with more clones (higher polyclonality, **Extended Data Fig. 3F**) and polyphyletic events (**Figure 2F, Extended Data Fig. 3E**, fisher's test p=0.029**)**. This indicates that multiple lineages of ICI-resistant clones existed within the metastases in place during treatment that were passed on to those metastases seeded after ICI. **(3)** We found no significant difference between the metastatic sites of tumors that were seeded before ICI, after ICI, or in patients never treated with ICI (**Extended Data Fig. 3G**). We observed variable metastatic locations in each group, indicating that ICI did not impose strong pressure on migration to specific metastatic sites. **(4)** We observed a change in overall clonal composition when analyzing the proportion of tumor cells containing

each clone (as measured by cellular prevalence; CP) in pre- versus post-ICI metastases. The tumors pre-ICI often had smaller subclones that then expanded after seeding to new metastases post-ICI (**Figure 2G**). These results suggest that the ICI-persistent clones that seeded the post-ICI metastases may have been able to expand more during the colonization of new niches than they were in their previously established niche.

Results, lines 126-131:

"However, in patients treated with ICI, we found that tumors arising after ICI (confirmed by CT scan) were seeded via more migrating clones (p=0.11) and polyclonal polyphyletic events (p=0.029) when compared to pre-ICI metastases (Figure 2F, Extended Data Fig. 3E-F, Methods). These ICI-persistent clones did not preferentially migrate to specific metastatic sites, but they exhibited greater expansion within the post-ICI metastases (p=0.022) (Figure 2G, Extended Data Fig. 3G)."

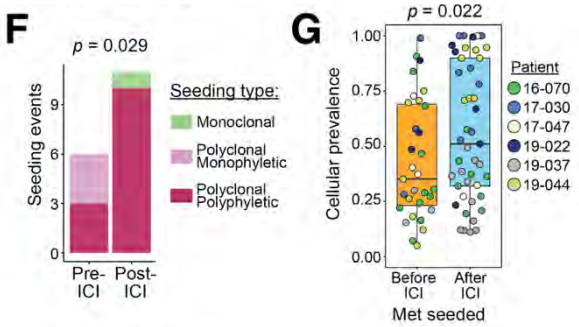

Figure 2

F) Number of pre- versus post-ICI seeding events of each type in patients that have both pre- and post-ICI metastases and seeding analyses (n=4 patients). Per patient breakdown in **Extended Data Fig. 3E**, p-value from Fisher's exact test.

G) Cellular prevalence for each shared or private clone, compared between clones in metastases seeded pre- versus post-ICI. Each point is a clone in a tumor. Statistics from linear mixed effects model with both patient and cluster ID as random effects.

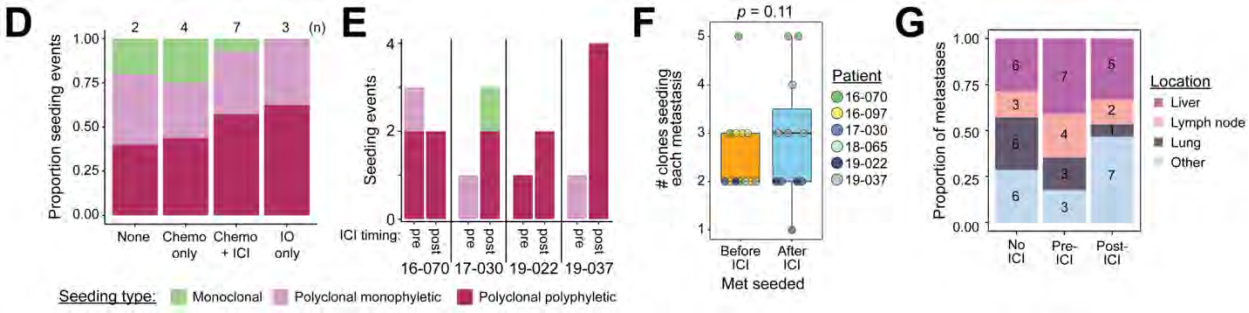

Extended Data Figure 3

D) Proportion of each type of seeding event in patients treated with only chemotherapy, only immune checkpoint inhibitors, both, or neither (n patients in each category labeled above).

E) Number of pre- versus post-ICI seeding events of each type in each patient that has both pre- and post-ICI metastases and seeding analysis. Timing of metastases relative to ICI were determined from CT scans.

F) The number of clones that seeded each metastasis (number of colors in Figure 1 migration arrows) for pre-ICI versus post-ICI metastases (n = 12 tumors/6 patients pre-ICI; n = 11 tumors/4 patients post-ICI). Patients without seeding analysis not included. Statistics from linear mixed effects model with patient as a random effect.

G) Proportion of metastases at different metastatic sites, grouped by patients who did not receive ICI and metastases seeded before versus after ICI in patients receiving ICI treatment. Counts of metastases in each group labeled in each bar. "Other" includes pancreas, pleura, omentum, adrenal, abdominal wall, pericolonic, aortic arch, uterus, perinephritic, and pelvic wall masses

Comment 3.2.1*) The authors state that PUC and NE are driven by early events as represented by an increased proportion of founder mutations. Is this a reflection of PUC and NE having histologic variant specific driver events, such as CHD1 loss for PUC and/or >75% of the tumor displaying PUC (whereas the UCSD is focal).*

Response 3.2.1) We thank the reviewer for raising this interesting question as to whether specific founder driver events or histological purity are related to the increased proportion of founder mutations in PUC and NE. To address the histological purity, we have now included detailed information on the proportion of all histologic components for each tumor in **Supplementary Table 1**. Overall, PUC tumors in our cohort exhibited minimal variability in the proportion of PUC versus UC histology. Of the 24 PUC tumors, 21 had 100% PUC morphology. For the two NE patients, 8/9 tumors had at least 90% NE histology. The UCSD subtype varied from focal to extensive squamous differentiation.

Results, lines 63-65:

> ***"PUC and NE tumors were predominantly variant histology (mean 96% PUC and 98% NE, respectively), whereas UCSD and UC-sarcomatoid tumors had variable subtype histology ranging from focal to extensive (Supplementary Table 1)."***

Regarding histology-defining driver events, we observed that PUC tumors had founder alterations leading to loss of *CDH1* in 4/5 cases (see **Figure 3A**). The addition of the TURBT sample in patient 18-016 changed their *CDH1* mutation from a shared cluster to the founder cluster, increasing this number from 3/5 to 4/5 in the updated analysis. Notably, this includes patient 17-071, who had 2 of their 5 tumors with 50-60% PUC histology and still displayed a high proportion (0.79) of pathogenic alterations in founder clones. In the two patients with NE histology, founder events included loss of major NE drivers *TP53*, *PTEN*, and *RB1*, suggesting the role of founder driver mutations in NE clonal evolution as well **(Figure 3A**). While we do observe both high histological purity and high founder mutations in PUC and NE patients, the same correlation is not observed in UCSD patients. In fact, high proportion of founder events were observed in patients with more focal UCSD (18-101 and 16-097), while low founder proportion was observed in the patient with the highest percent UCSD (17-026) **(Figure 3H**). Though our cohort is small, this may suggest that an increased proportion of founder mutations may be more related to the presence of certain histology-specific founder driver alterations than histological purity.

Results, lines 200-204

> ***"The enrichment of founder alterations in PUC and NE corresponded with inactivating founder alterations of known histology-associated driver genes[38,39]. Patients with PUC tumors harbored inactivating founder alterations of CDH1 (4/5), TP53 (3/5), and RB1 (4/5) and both patients with NE histology harbored founder pathogenic alterations in TP53, PTEN, and RB1 (Figure 3A)."***

Comment 3.2.2) *More broadly, how does the varying extent of histologic subtypes component of the UC effect the analysis and conclusions?*

Response 3.2.2) To quantitatively assess how varying histological composition may affect our other analyses, we examined the percentage of UC component (% UC in **Supplementary Table 1**) in each tumor, summarized for each patient as the mean % UC across their tumors. In the comparison presented in **Figure 3H** for PUC and UCSD subtypes, we now use this mean % UC value as a covariate in the linear mixed effect model to determine whether enrichment of founder alterations was independent of % UC. The initial conclusions still hold – PUC cases had higher proportion of founder alterations, while UCSD cases did not show significant enrichment for founder alterations. For consistency, we also accounted for the mean % UC in the analysis

presented in **Figure 3I**. We conclude that the mean % UC did not influence the association between clonality and survival, with statistical significance remaining p<0.05 for CNAs and private SVs.

Figure 3H and **Figure 3I** now reflect these new statistical analyses using % UC as a covariate, with explanation of this adjustment in the figure legends, Methods, and Discussion sections.

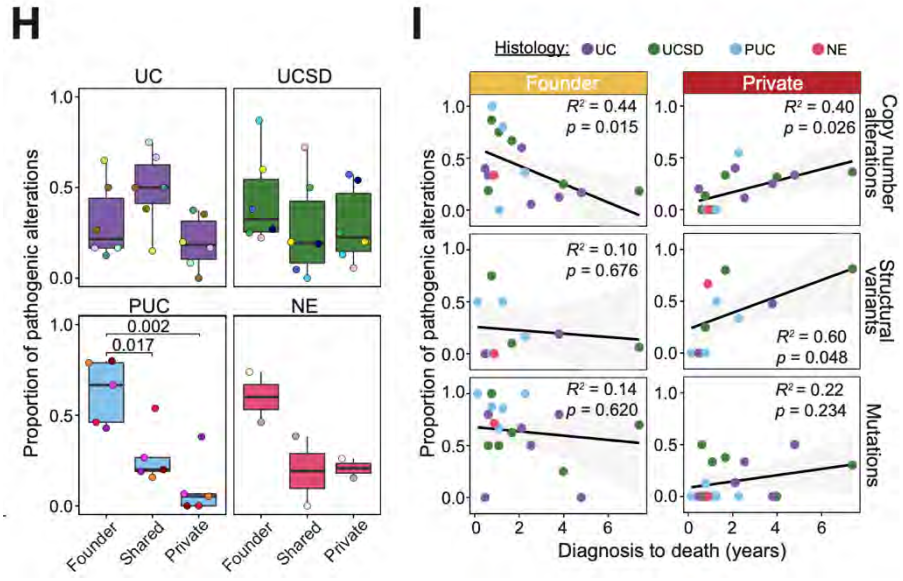

Figure 3

H) Proportion of pathogenic alterations (mutations, CNAs, and SVs) per patient classified as founder, shared, or private, by histologic subtype. Linear mixed-effects models included patient ID as a random effect and were adjusted for covariates: number of tumors and total treatments per patient. For PUC, UCSD, and NE, mean percentage UC histology was also included as a covariate. See legend in E–G for patient IDs.

I) Correlation of the proportion of pathogenic alterations in founder or private clones from diagnosis to death (years) is shown for copy number alterations (n=17 patients), structural variants, (n=10 patients), and mutations (n=18 patients). Linear regression models included patient ID as a random effect and were adjusted for covariates: number of tumors and total treatments per patient and mean percentage UC.

Results, lines 60–65:

> ***"Tumors represented a spectrum of histological subtypes[25], including 50 with conventional urothelial carcinoma (UC) and an enrichment of subtypes: 24 plasmacytoid UC (PUC), 19 UC with squamous differentiation (UCSD), 8 neuroendocrine (NE), and 3 UC with sarcomatoid subtype (UC-Sarc). PUC and NE tumors were predominantly variant histology (mean 96% PUC and 98% NE, respectively), whereas UCSD and UC-sarcomatoid tumors had variable subtype histology ranging from focal to extensive (Supplementary Table 1)."***

Discussion, lines 471-473:

> ***"However, patients with UC and UCSD tumors harbored notably more shared and private pathogenic alterations, independent of histological subtype purity, suggesting their lethal mutations may evolve later in the disease"***

Comment 3.3.1*) I appreciate the authors trying to functionally link the FANC pathway to PUC cisplatin resistance. However, this needs to be done in a more rigorous fashion if this section is*

to remain in the paper. Specifically, does knockdown or overexpression of the pathway in the given cells reverse the phenotype.

Response 3.3.1) Thank you for this suggestion to strengthen our findings connecting the Fanconi Anemia (FANC) pathway to cisplatin resistance. As suggested, we have now performed both knockdown and overexpression experiments to determine whether FANC modulation affects cisplatin response in our bladder cancer cell lines. While the FANC pathway and core complex consists of many proteins that work in concert, we chose to modulate the expression of *FANCF*, a key adaptor protein in the core FANC complex whose knockdown or overexpression alone has been shown to affect sensitivity to other crosslinking agents (PMID: 15802532, 24996439).

We knocked down *FANCF* in SW780 cells, our highest FA-expressing bladder cancer cell line, using siRNA, achieving an average of 84%/57% reduction in gene expression by qPCR and Western (**Figure 4J**, **Extended Data Fig. 14B-C**). Knockdown of *FANCF* resulted in decreased FANC pathway activation, as evidenced by a reduction in the FANCD2-ub to FANCD2 ratio (**Figure 4J, Extended Data Fig. 14C**). Additionally, this decreased activity increased sensitivity to cisplatin in these cells, as shown by both a decrease in confluence (median AUC = 13.5 vs 10.2, p=0.05) and an increase in cell death (median AUC = 32.8 vs 41.9, p=0.0264) as compared to siRNA control cells (**Figure 4K-L, Extended Data Fig. 14D-E**).

Additionally, we overexpressed *FANCF* in our lowest FA-expressing cell line, UBLC1. Stable cell lines with either an empty vector or *FANCF* integrated into the genome were created using lentiviral transfection and G418 selection, resulting in an average of 17x/8.8x overexpression at the RNA and protein levels, respectively (**Extended Data Fig. 14F-G**). This overexpression of *FANCF* resulted in a 22% increase in the FANCD2-ub to FANCD2 ratio, increased growth (median AUC = 11.2 vs 12.6, p=0.0485), and decreased cell death (AUC = 16.1 vs 14.6, p=0.158) compared to empty vector (**Extended Data Fig. 14H-I**).

These experiments demonstrate that in bladder cancer cell lines, modulation of a key component of the FANC core complex is sufficient to drive sensitivity and resistance to cisplatin, supporting the idea that variation in FANC gene expression in bladder cancer such as we observed in PUC versus UC tumors may affect cisplatin response.

See also **Response 1.10** for further experimental validation of the link between the FANC pathway and inter-strand crosslink repair in BLCA cells using Mitomycin C.

Results, lines 272-275:

> ***"Upon FANCF knockdown, FANC-high SW780 cells displayed decreased FANCD2-ubiquitination and increased cisplatin sensitivity (Figure 4J-L, Extended Data Fig. 14B-E). Reciprocally, FANCF overexpression in FANC-low UBLC1 cells increased pathway activity and cisplatin resistance (Extended Data Fig. 14F-I)."***

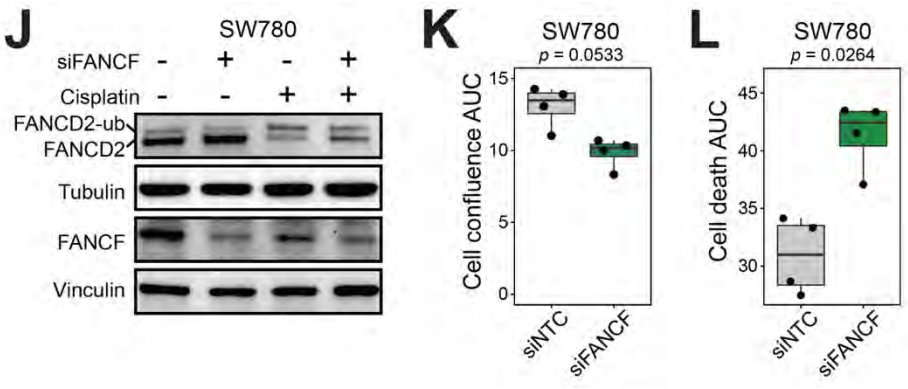

Figure 4

J) Western blot of FANCD2, ubiquitinated FANCD2, and FANCF protein expression in siNTC versus siFANCF SW780 cells with and without 24 hours of 5μM cisplatin treatment. Tubulin used as a loading control for FANCD2 and vinculin for FANCF. Quantification shown in **Extended Data Fig. 14C**. For gel source data, see **Supplementary Figure 1**.

K) Area under the cell confluence dose response curve at 72 hours of 0-20μM cisplatin treatment on siNTC versus siFANCF SW780 cells (p-value from paired t-test of four biological replicates). Confluence values normalized per well to 0hr confluence (**Extended Data Fig. 14D**).

L) Area under the cell death dose response curve at 48 hours of 0-20μM cisplatin treatment on siNTC versus siFANCF SW780 cells (p-value from paired t-test of four biological replicates). Cell death measured as dying cell count normalized to cell confluence (**Extended Data Fig. 14E**).

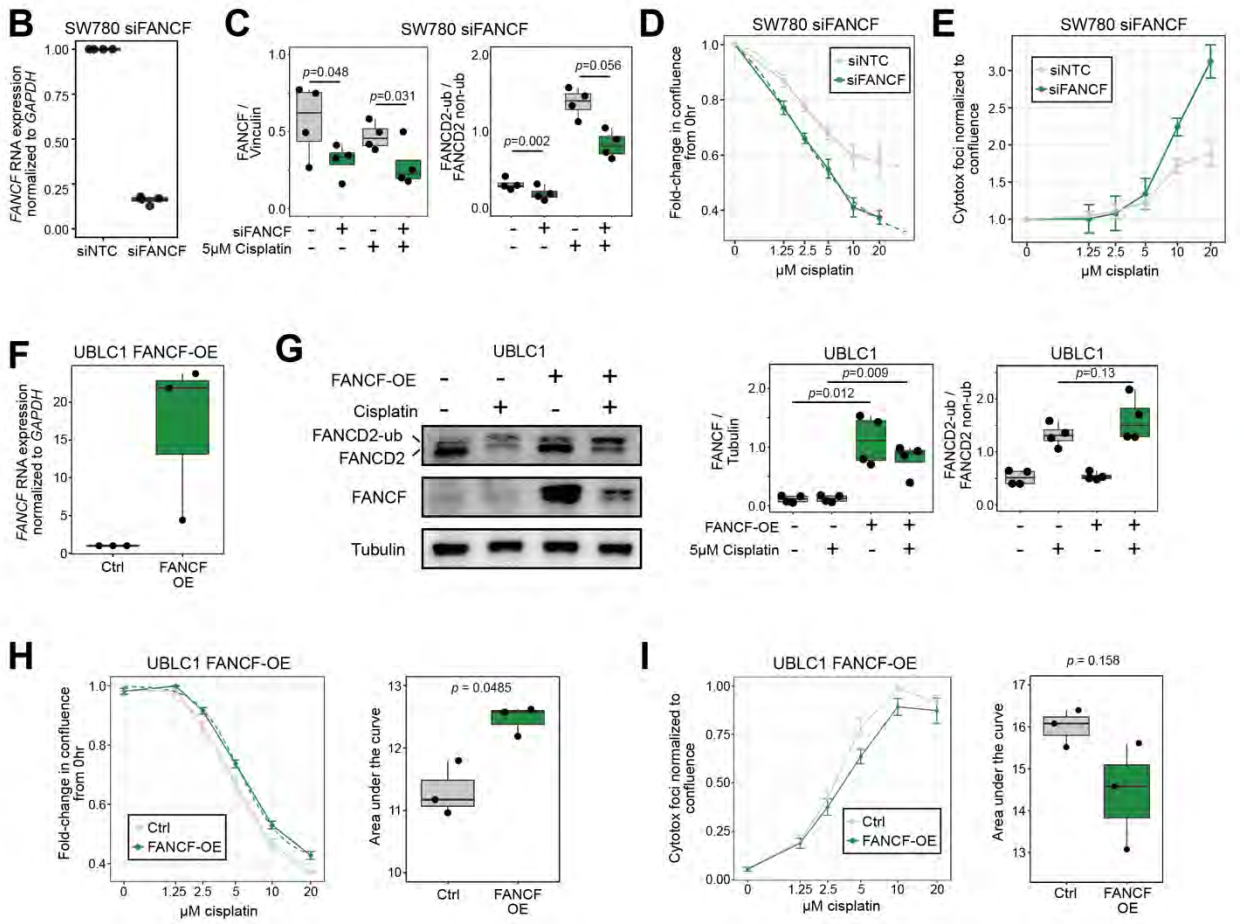

Extended Data Figure 14

B) FANCF mRNA expression (normalized to *GAPDH* housekeeping control) knockdown in siNTC versus siFANCF SW780 cells for four biological replicates.

C) Quantification of SW780 siNTC versus siFANCF Western blots (n = 4 biological replicates, representative shown in Figure 4J). FANCF knockdown observed with vinculin as a loading control. FANCD2-ub activation (as a proportion of total FANCD2) observed to decrease with FANCF knockdown in both cisplatin treated and untreated cells. P-values from paired t-tests.

D) Dose response growth curve of 72 hours of cisplatin treatment on SW780 siNTC and siFANCF cells. Y-axis is the fold change from 0 to 72 hours of treatment, scaled within each cell line so the maximum equals 1. Solid lines connect the average response at each cisplatin dose across four biological replicates, with error bars displaying SEM. Dashed lines display a best-fit polynomial to the data for each cell line. Quantification of corresponding AUC shown in **Figure 4K**.

E) Dose response death curve of 48 hours of cisplatin treatment on SW780 siNTC and siFANCF cells. Y-axis is the number of dead cells at 48 hours normalized to each well's confluence at 48 hours and set such that the DMSO control equals 1. Lines connect the average response at each cisplatin dose across four biological replicates, with error bars displaying SEM. Quantification of corresponding AUC shown in **Figure 4L**.

F) FANCF mRNA expression (normalized to *GAPDH* housekeeping control) in OE-Control versus OE-FANCF UBLC1 cells for three biological replicates.

G) Left: Western blot in OE-Control versus OE-FANCF UBLC1 cells with and without 24 hours of 5mM cisplatin treatment. Tubulin used as a loading control. For gel source data, see **Supplementary Figure 1**. **Right**: Quantification of FANCF overexpression (FANCF/tubulin ratio) and FANCD2-ub activation (FANCD2-ub to FANCD2 non-ubiquitinated ratio) in four biological replicates (p-values from paired t-tests).

H) Left: Dose response growth curve of 24 hours of cisplatin treatment on UBLC1 OE-control versus OE-FANCF cells. Y-axis is the fold change from 0 to 24 hours of treatment, scaled within each cell line so the maximum equals 1. Solid lines connect the average response at each cisplatin dose across three biological replicates, with error bars displaying SEM. Dashed lines display a best-fit polynomial to the data for each cell line. **Right**: Quantification of corresponding AUC for three biological replicates (p-value from paired t-test).

I) Left: Dose response death curve of 72 hours of cisplatin treatment on UBLC1 OE-control versus OE-FANCF cells. Y-axis is the number of dead cells at 72 hours normalized to each well's confluence at 72 hours and set such that the maximum equals 1. Lines connect the average response at each cisplatin dose across four biological replicates, with error bars displaying SEM. **Right**: Quantification of corresponding AUC for three biological replicates (p-value from paired t-test).

Comment 3.3.2*) Evidence of DNA repair modulation (such as gammaH2AX staining) would bolster the conclusions.*

Response 3.3.2) We have performed γH2AX staining to explicitly track the formation and repair of DNA damage in response to cisplatin treatment in the SW780 (FANC-high) versus UBLC1 (FANC-low) BLCA cell lines used above. In keeping with our original results, we hypothesize that higher FANC expression in SW780 cells increases FANC DNA repair of double-strand breaks caused by inter-strand crosslinks. Therefore, we expect a lower amount of γH2AX foci in SW780 cells than UBLC1 cells over time, indicating a more robust DNA repair response in the FANC high cells. To test this, we performed a time course after a 3-hour pulse of cisplatin treatment at each cell lines approximate IC50 (5μM for UBLC1 and 10μM for SW780), staining cell spreads at 0, 4, 24, and 48 hours after treatment (**Extended Data Fig. 14A**). We observed that UBLC1 has higher levels of DNA damage over time than SW780, despite receiving a higher dose of cisplatin (**Figure 4I**). In FANC-low cells, γH2AX foci count continues to rise over the 24-48 hours period, whereas foci count plateaus at 4 hours after treatment in FANC-high cells. This demonstrates that higher FANC RNA expression not only enables increased activation of the FANC pathway (as evidenced by increased FANCD2-ub, **Figure 4F**), but results in increased repair of cisplatin-induced DSBs.

Results, lines 268-272:

> ***"Differential DNA repair activity in these cell lines was confirmed by assessment of γH2AX foci (Extended Data Fig. 14A). FANC-low UBLC1 accumulated more DNA damage over time upon treatment with cisplatin, while SW780 plateaued, indicating more activate DNA repair in the FANC-high cells (Figure 4I)."***

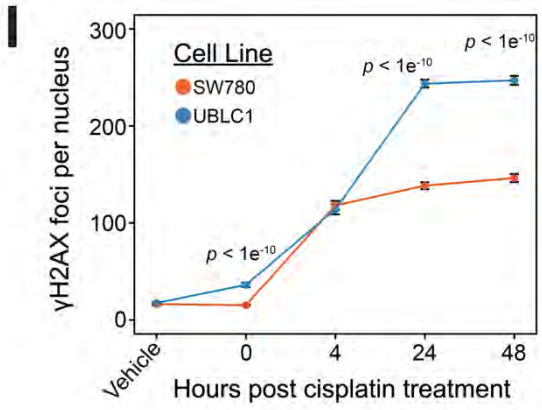

Figure 4. I) Count of γH2AX foci per nucleus in BLCA cell lines treated with cisplatin at the indicated time points after a 3-hour pulse of 5μM (UBLC1) or 10μM (SW780) cisplatin. Points show average foci counts, with error bars indicating SEM (FDR-adjusted p-value from t-test across all nuclei in each image).

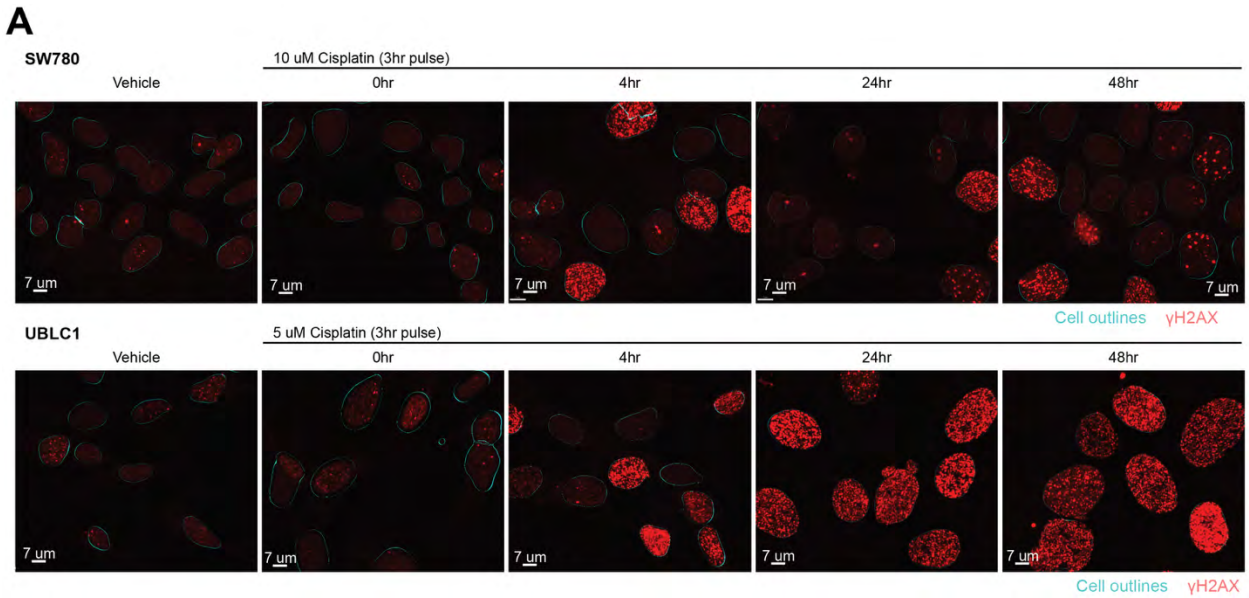

Extended Data Figure 14. A) Representative images of γH2AX staining (red) in SW780 and UBLC1. Cyan outlines denote nuclei borders as segmented by Imaris software on DAPI.

Comment 3.4.1*) In tumors that displayed mix phenotypes (75% PUC or 5% UCSD), is there similar proportionality represented in the snRNAseq and do the transcription pattern vary between the populations?*

Response 3.4.1) Thank you for raising this interesting question. Of the fifteen tumors that had snRNA-seq data, all were of pure histology except for the three UCSD tumors, which were each 90% UCSD/10% UC, and PUC tumor 17-071I1, which was 50% PUC/50% UC (**Supplementary Table 1**).

The mixed histology of PUC tumor 17-071I1 was reflected in the snRNA-seq by the lower proportion of LumU (34%) in this tumor versus the pure PUC histology tumors, with the UC histology portion being represented by LumP (50%) and Ba/Sq (12%) molecular subtypes (**Figure 5I**). The mixed histology of 17-071I1 is also reflected in the UMAP, where it is located between PUC and UCSD samples (**Figure 5G**, **Extended Data Fig. 17C**).

Of the three UCSD tumors with 90% UCSD and 10% UC mixed histology, 19-022H1 displayed a similar ratio of molecular subtypes (87% Ba/Sq:13% LumP), while the other two tumors were fully Ba/Sq (**Figure 5I**). The higher proportion of Ba/Sq molecular subtype than UCSD histology in 17-026K2 and 17-026J3 likely indicates that an early transcriptional change preceded phenotypic alteration towards squamous differentiation in the tumor. This observation is further supported by the bulk RNA-seq subtyping of patients 17-030 and 18-101, where all tumors showed Ba/Sq transcriptional subtype despite only 1-2 tumors having focal squamous histological features (**Figure 5B**).

In conclusion, we observed distinct transcriptomic features and cell populations within a mixed PUC/UC histology tumor, while mixed UCSD/UC histology tumors tended to have predominantly Ba/Sq transcriptomic features. The relationship between mixed histology and molecular subtypes in snRNA-seq analysis is discussed in the Results.

Results, lines 313-322:

"The PUC tumors comprising these "bridges" (samples 15-109G5 and 17-071I1, Extended Data Fig. 17C) were classified as LumP and lacked the PUC hallmarks of ERBB2 overexpression and CDH1 loss[39,57] (Extended Data Fig. 17E-F). These characteristics may indicate the presence of mixed phenotypes or partial trans-differentiation, particularly given the mixed UC/PUC histology in specimen 17-071I1 (Supplementary Table 1). We observed four histologically UC tumors that clustered with the UCSD samples and molecularly subtyped as Ba/Sq, indicating a potentially early transcriptional state change before histological features of squamous differentiation emerged. These mixed cell states were evident in the multiple molecular subtypes observed in UC and PUC tumors (Figure 5I)."

See also **Response 1.1** and **Response 2.8**.

***Comment 3.4.2**) How does treatment, ICI or chemo interact with the heterogeneity and by extension survival?*

Response 3.4.2) It is interesting to examine how treatment influences transcriptional heterogeneity and survival. We previously analyzed the relationship between intra-patient transcriptional heterogeneity (Shannon entropy metric computed from snRNA-seq) and survival (**Figure 5J**). We have now further explored whether treatment affects intra-patient heterogeneity and observed no significant differences in entropy between patients who received different types of treatments (n=6 patients with chemo and ICI, 2 chemotherapy only, and 1 ICI only, **Extended Data Fig. 17J**). Since the snRNA-seq cohort size is limited, we also compared transcriptional heterogeneity to treatment in the broader autopsy cohort using bulk RNA-seq. Here, we compared the proportion of patients that had heterogeneous (mixed) versus homogeneous molecular subtypes across multiple tumors (patients with only one tumor with RNA-seq were excluded from the analysis, **Figure 5B**, **Extended Data Fig. 17K**). Again, with this larger cohort of patients (n=18), we did not see significant enrichment of heterogeneity associated with any treatment type. This observation has been included into the Results and **Extended Data Fig. 17**. Due to the limited sample size within each treatment grouping, we were unable to statistically test whether treatment affected the relationship between snRNA-seq transcriptional heterogeneity and survival from first metastasis.

Results, lines 322-326:

"The higher intra-patient transcriptional heterogeneity in these patients, marked by more widespread distribution of patient cells across UMAP clusters, was correlated with both higher genomic heterogeneity (R^2=0.74, p=0.014) and longer survival from first metastasis (R^2=0.60, p=0.041), while being unrelated to treatment (Figure 5J, Extended Data Fig. 17B,G-K, Methods)."

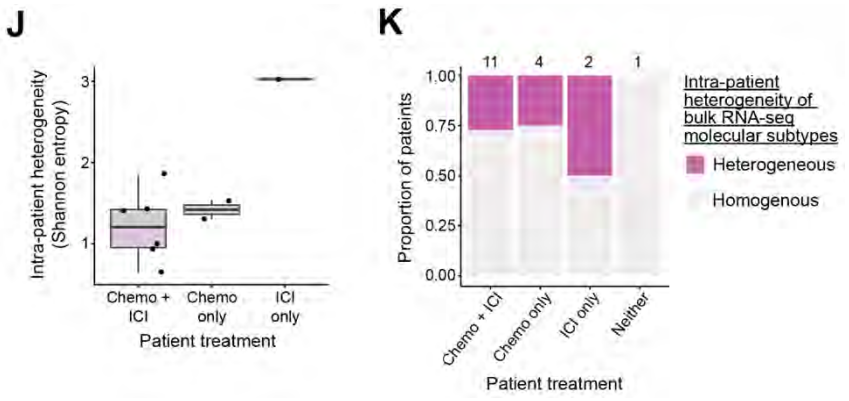

Extended Data Figure 17
J) Shannon entropy of the distribution of cells in each tumor across snRNA-seq epithelial Louvain clusters, differentiated by whether the patient received chemotherapy only (n=2), immune checkpoint inhibitor (ICI) only (n=1), or both (n=6).
K) The proportion of patients within each treatment group that had heterogeneous versus homogenous bulk RNA-seq molecular subtypes across all their tumors. The number of patients in each treatment group is noted above each bar.

Comment 3.5*) By identifying met specific TFBS signatures, can you link cfDNA back to specific mets. Are specific locations of metastasis more likely to release cfDNA into the circulation?*

Response 3.5) These are certainly interesting questions to consider. Previously, we explored the analysis of TFBS signatures in 19-022, who had mixed molecular subtypes and histology. We hypothesized that this patient's ctDNA may display distinct activity of transcription factors (TFs) due to the different phenotypes of their tumors. This patient had two luminal (UC) metastases in the lung and liver that are characterized by increased PPARG and RARG activity in the ctDNA analysis, and a basal/squamous adrenal metastasis characterized by decreased ZNF217 and ZNF146 activity (**Figure 5B**, **Figure 7K-L**). Linking the specific metastases to the TF activity was enabled by virtue of 19-022 having mixed molecular subtypes. For other patients that did not have mixed subtypes, we cannot reliably identify for metastasis-specific TF activity without knowledge of any subtype features that would distinguish the metastases.

Results, in lines 434-438:

> ***"Interestingly, patient 19-022 had a mixed TF activity profile representing both luminal and basal subtypes. Analysis of 19-022 revealed partial activity of luminal TFs (PPARG and RARG), consistent with the presence of two luminal UC tumors, while the decreased activity of ZNF217 and ZNF146, which were also suppressed in basal samples[91], reflects the co-occurrence of the basal squamous tumor in this patient (Figure 7L, Figure 5B)."***

We assessed whether specific metastatic sites released more cfDNA by analyzing mutations that were private to each metastasis (**Extended Data Fig. 20I**) and found no significant differences in mutations detected between the metastatic locations. Despite not seeing a difference in the number of mutations detected between metastatic sites, we found that patients who had 2 or more liver metastases had a higher cfDNA tumor fraction compared to patients with 1 or fewer liver metastasis (p=0.0004, **Extended Data Fig. 20A**). This observation is consistent with other cfDNA studies that report higher tumor fraction in the presence of high burden liver metastases (PMIDs: 36782009, 31340061, and 36681803). Furthermore, we used tissue-of-origin analysis to determine the contribution that normal tissue (including damage of organs harboring metastases)

can make to cfDNA. The observation of hepatocyte transcriptional patterns in patients with liver metastases supports that the liver sheds both tumor and non-tumor DNA into circulation when metastases are present (**Extended Data Fig. 21B**).

Results, lines 398-402:

"However, the detection rates of private SNVs were not well explained by clone abundance, nor metastatic site, but rather by sample-specific tumor purity (from histology, ρ=0.59, p=0.0049 for WGS) and volume (from CT, ρ=0.53, p=0.02 for TP) of the individual tumor harboring each private clone (Figure 7E-F, Extended Data Fig. 20H-J, Methods)."

Results, in lines 415-419:

"Using the Griffin framework[79], we profiled nucleosome patterns to infer the DNA contribution shed by tissue types. This analysis demonstrated that nucleosome occupancy can differentiate BLCA[78] from healthy cfDNA and also identify contribution from immune cells and tissue damage such as hepatocytes in patients with liver metastases (Extended Data Fig. 21A-B, Methods)."

Comment 3.6*) Does time until autopsy contribution to the levels of cfDNA detected?*

Response 3.6) Thank you for bringing up this important question. Since the half-life of cfDNA is estimated to be only minutes to hours (PMID: 30990132), it may be expected that a longer delay between death and autopsy would decrease cfDNA levels. However, tumor and non-tumor cfDNA would likely decay at the same rate. Accordingly, in our patient cohort, we observed a trend towards lower total cfDNA yield in patients with a longer time from death to autopsy (**Extended Data Fig. 20C**), but no correlation between time to autopsy and either cfDNA tumor fraction (**Extended Data Fig. 20B**) or the proportion of tumor mutations captured within cfDNA (**Extended Data Fig. 20D**). Therefore, the clearance of cfDNA after death did not appreciably affect the tumor DNA content within cfDNA or confound the mutation capture analysis. For reference, the time from death to autopsy for each patient is listed in **Supplementary Table 1**.

Results, lines 375-377:

"No relationship was found between the time from death to autopsy and TFx (ρ=0.018, p=0.94), although the total cfDNA yield decreased as the postmortem interval increased (ρ=-0.41, p=0.10) (Extended Data Fig. 20B-C)."

Results, lines 384-386:

"Overall, cfDNA captured a median of 70% of all tumor SNVs in high TFx cfDNA samples (≥ 8% TFx, n=8) and 34% in low TFx samples (< 8%, n=9), independent of time from death to autopsy (Figure 7A, Extended Data Fig. 20D, Supplementary Table 8)."

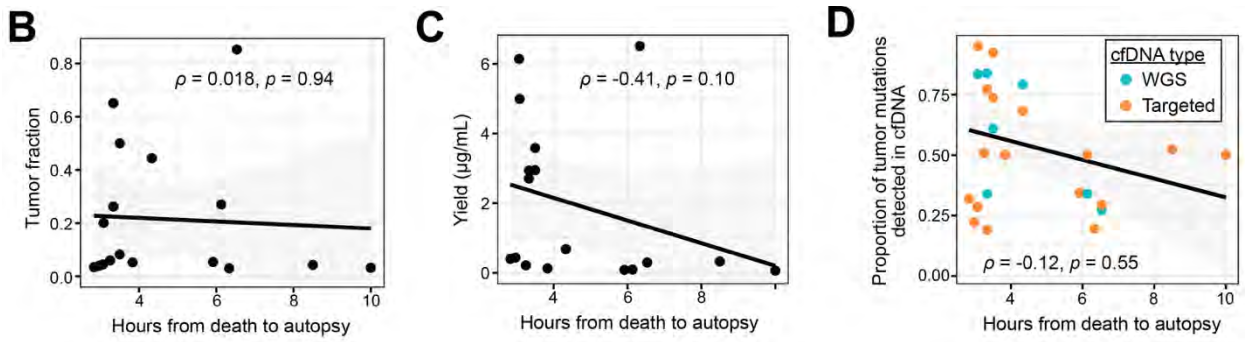

Extended Data Figure 20
B) Spearman correlation between time of death to autopsy and cfDNA tumor fraction for each patient.
C) Spearman correlation between time of death to autopsy and cfDNA yield for each patient.
D) Spearman correlation between time of death to autopsy and the proportion of tumor mutations detected in cfDNA for each cfDNA sample.

Referee #3 (Remarks on code availability):

Code is appropriately accessible and annotation.

We thank the reviewer for noting that the code is appropriately accessible and well-annotated.

Referee #4 (Remarks to the Author):

I co-reviewed this manuscript with one of the reviewers who provided the listed reports.

Referee #4 (Remarks on code availability):

The code is well structured and documented. It contains a README file and each folder for a specific analysis is well documented. The instructions and steps can be followed to reproduce the data. The code can be downloaded and be adapted to run internally.

We thank the reviewer for testing our code and noting that it is documented appropriately.

Referee #5 (Remarks to the Author):

I co-reviewed this manuscript with one of the reviewers who provided the listed reports.

We thank the reviewer for their comments.

Referees' comments:

Referee #1 (Remarks to the Author):

Thank you to the authors for their comprehensive and organized approach to responding to my comments. Overall, I believe the revisions have strengthened the manuscript and that the core genomic findings are solidly supported and correctly interpreted. The clinical cohort and data sets are highly unique and the same or even similar analyses are unlikely to be available from any other center in the near to intermediate term. Therefore, I believe the findings are of high impact and will be broadly useful and interesting to the bladder cancer and tumor evolution fields. I think the findings regarding the relationship between FANC pathway expression and cisplatin mutational signatures and sensitivity will need to be validated and further mechanistically interrogated in future work, and I have made some suggestions below regarding softening the language and interpretations for these findings.

We thank the reviewer for their comprehensive evaluation of our study, and we are pleased that they found it of "high impact" and "broadly useful and interesting to the bladder cancer and tumor evolution fields." We have responded to their comments point-by-point below.

Regarding responses to specific comments:

Comment 1.1: *The additional data regarding subtype % is appreciated, and its reassuring to see that, for the majority of cases, the variant histology was quite dominant. For the rare cases with similar % of classic UC and variant histology in some specimens (such as 17-071), was there an attempt to use macro/microdissection to isolate UC and variant components and perform separate analyses on each? For the few SARC and UCSD cases with minimal % variant histology, it feels more difficult to really consider these as reflecting biology of the variant component: for example, 19-004 was annotated as a SARC case, but two samples had 0% sarcomatoid histology, two samples had 5%, and only one had majority (70%) sarcomatoid histology. Changes to the text have been made to describe*

Response 1.1) We thank the reviewer again for their original suggestion to add quantification of the histological subtype proportions in each tumor; we believe this detail has increased the transparency and robustness of our manuscript. Macrodissection was used to enrich for cancerous regions versus normal tissue when collecting tumor samples for sequencing; however, macro/microdissection was not performed to isolate variant components of the tumor for separate analysis due to the intermixed nature of UC and variant histological components within tumors in this cohort.

We carefully considered how to designate the histological subtype of patients with mixed or minimal variant histology across their tumors. To create consistent and transparent definitions, we categorized histology at both the patient level (for analyses requiring a designation for the patient as a whole) and the tumor level (for more fine-grained analyses). The decision to assign the variant subtype label to patients or tumors if any non-UC histology was observed (A) follows clinical practice, where even small amounts of variant histology can influence clinical decision making, and (B) allows more thorough investigation of how histological subtypes and histological purity affect analyses.

In support of this designation, transcriptomic analysis of our samples revealed that even a minor variant histological component significantly influenced bulk molecular profiles. We found that three of the four patients with less than 10% average UCSD content among their tumors (17-030, 18-101, and 16-097) have exclusively Basal/Squamous molecular subtype tumors (**Figure 5B**),

demonstrating that even a minor UCSD histological component was enough to markedly alter the tumor's transcriptome. Similarly, despite the variation in sarcomatoid component among 19-004's tumors, they all demonstrated the Basal/Squamous molecular subtype and clustered closely together on the RNA-seq UMAP (**Figure 5B** and **Extended Data Figure 15**). For these reasons, patients with any variant histological component were categorized as non-UC at a patient level, particularly in light of the clinical relevance and prognostic implications of the consensus molecular subtypes (PMID: 31563503). We have added text to the discussion to highlight this point.

Discussion, lines 492-495:

"We observed that patients with even a minor component of squamous differentiation in a single tumor often had entirely Ba/Sq tumors, supporting the idea that minimal variant histology can have patient-wide significance."

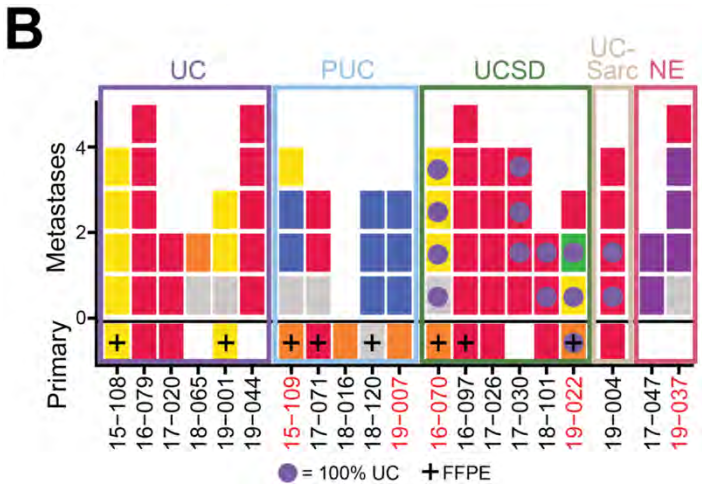

Figure 5B: Intra-patient heterogeneity of consensus molecular subtypes on bulk RNA-seq tumors. Primary tumors, if sequenced, are shown on the bottom row, with metastases above. Plus signs indicate FFPE samples; all others are flash-frozen. Colored boxes group patient-level histology, with 100% UC tumors marked with purple circles. Patients labeled in red text exhibit molecular subtype heterogeneity between tumors.

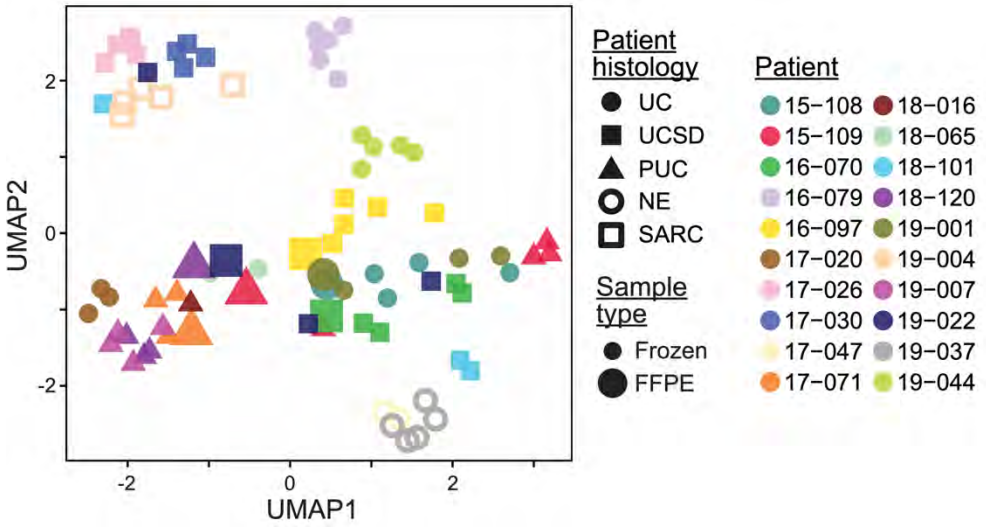

Extended Data Figure 15: UMAP of bulk RNA-seq tumors, with patient identifier indicated by coloring, patient histology indicated by shape, and FFPE versus flash frozen samples indicated by shape size.

Genomic hallmarks of the SARC and UCSD subtypes were more difficult to discern in our patient cohort, and therefore we could not determine how variant purity may have affected genomics of these subtypes. We did not attempt to define genomic features of the UC-sarcomatoid subtype due to the sample size (n=1) as well as mixed histology of this patient. Furthermore, we did not observe any distinct genomic hallmarks of the UCSD subtype. However, as suggested by **Reviewer 3**, we did incorporate the proportion of variant histology into the linear mixed-effects models analyzing genomic clonality across histological subtypes to account for any influence of histological purity (**Figure 3H-I**).

Comment 1.2: *I understand the rationale for keeping the MIPS in Figure 2 and appreciate the effort to included annotated CT slides in the Extended Data.*

Response 1.2) Thank you for the comment and opportunity to clarify the rationale for keeping the MIPS in figure 2; we agree the additional cross-sectional images were a valuable addition.

Comment 1.3: *I appreciate the effort to include analysis of primary TURBT samples when available, and I think integration of these findings into the manuscript provides important additional insights and context regarding the case-specific relationship among primary bladder tumor, autopsy bladder tumor, and autopsy metastatic sites.*

Response 1.3) We thank the reviewer for their recommendation of incorporating the TURBT samples into the analysis, we agree that it has strengthened the paper with new insights unique to this sample set.

Comment 1.4: *I agree with the authors that a multivariable Cox model is a more robust method for analyzing the prognostic impact of polyclonal seeding in the context of known clinical prognostic factors.*

Response 1.4) Thank you, we appreciate your feedback that led to this more robust analysis.

Comment 1.5: *Thank you for performing the updated analysis, and I do think the difference in findings in the updated results is notable. An alternative (or perhaps supplementary) interpretation of the differences in 'pre-ICI' vs 'post-ICI' metastasis properties is that these differences are not driven by ICI pressure directly but rather simply reflect the biology of the more advanced disease state in which patients would have received ICI. One way to test this might be to separate metastasis from chemo-only patients into "early" vs "late" developing metastasis and comparing frequency of polyclonal polyphyletic events in these two groups. At the least, the potential for both ICI pressure or disease stage to contribute to the differences in pre- vs post-ICI metastasis properties should be noted.*

Response 1.5) We thank the reviewer for raising this point. It is true that the inherent difference in timing and disease stage between pre- and post-ICI seeded metastases may be a confounder to the interpretation of this analysis. This is a caveat of performing such analysis in a retrospective, post-mortem cohort. Ideally, this analysis would be performed prospectively, with biopsies before and after each treatment to assess how chemotherapy, ICI, or other therapies differentially affect clonality and metastatic seeding.

As this Reviewer suggested, we explored whether we could perform a similar retrospective seeding analysis for chemotherapy-only patients as we did for ICI treatment. Unfortunately, only three patients in our cohort (15-109, 17-020, 17-026) received chemotherapy alone. Moreover, these 3 patients received chemotherapy early in the disease course, and so no metastases could be confirmed by CT scans prior to treatment.

We have added text to the discussion section addressing the caveat to our analysis:

Discussion, lines 453-457:

> ***"Our analysis revealed features of metastatic spread, including the correlation of highly polyclonal seeding events with poor survival and the higher frequency of divergent (polyphyletic) clonal seeding in histological subtypes. We also observed increased polyphyletic seeding after immunotherapy, although we could not determine whether this reflected therapeutic pressure or natural clonal evolution over time."***

Methods, lines 884-888:

> ***"We explored whether we could perform a similar retrospective seeding analysis for chemotherapy-only patients as we did for ICI treatment. Unfortunately, only three patients in our cohort (15-109, 17-020, 17-026) received chemotherapy alone. Moreover, these 3 patients received chemotherapy early in the disease course, and so no metastases could be confirmed by CT scans prior to treatment"***

Comment 1.6: *Similar to response to 1.3 above. It is interesting and perhaps reassuring (from technical perspective) that the source of primary tumor collection (esp TURBT vs surgery) did not seem to impact clonal composition between primary and mets.*

Response 1.6) We agree, it is reassuring to confirm that differences in clonal composition are driven by biological and not technical reasons. We thank the reviewer for their suggestion that has increased the robustness of our manuscript.

Comment 1.7: *I worry that readers who don't read the reviewer comments and responses may have the same concern regarding signature specificity that I initially had, especially now that the cisplatin signature has been specifically excluded from analysis of the non-platinum treated patients. Including some version of the response text ("…we found a cis signature in 1 platinum-treated patient…we acknowledge its an artifact likely due to low mutation count…we therefore excluded the cis signatures for the analysis of the non-cis patients…") in the Methods or Extended Data would be appropriate.*

Response 1.7) Thank you for raising this concern. As suggested, we have added clarification into the methods section to explicitly state that a low proportion of chemotherapy signature was found in one patient not treated with chemotherapy, and thus these patients were re-fitted to avoid such artifacts.

Methods, lines 1477-1482:

> ***"One of the seven patients who did not receive platinum-based chemotherapy displayed a minor proportion of platinum-associated signatures (SBS31+SBS35), likely an artifact due to low mutation count in this mutation cluster. Therefore, for these seven patients, SBS31 and SBS35 were additionally excluded, and refitting was performed separately to avoid such artifacts, yielding a final set of 49 signatures used for downstream analysis in this group (Supplementary Table 5)."***

Comment 1.8: *Explanation and changes based on my comments are reasonable.*

Response 1.8) We appreciate the reviewer's confirmation that we have satisfactorily addressed the previous comments.

Comment 1.9: *The response and additional analyses are reasonable, particularly in light of the additional experiments performed to address subsequent comments (see below).*

Response 1.9) We thank the reviewer and are pleased that our revisions have addressed their concerns.

Comment 1.10.1: *It is slightly disconcerting that the relationship between FANC status and MMC does not hold up as it did with cisplatin, given that MMC is the drug classically associated with exquisite sensitivity in the FANC-deficient setting. I appreciate the potential reasons raised by the authors in their response to my initial comment, but I would suggest being slightly more forthcoming in the text by directly stating that there was not a difference in phenotype between FANC hi and lo lines using the same approach that was used to identify the difference with cisplatin, but that there was a modest difference (in the expected direction) when additional approaches were applied.*

Response 1.10.1) As suggested, we have modified our wording in the results text to explicitly state that while two of the three experiments originally used to assess cisplatin response (pathway activity via FANCD2-ubiquitination and cell death resistance via IncuCyte cytotox assessment) were observed to respond to MMC similarly as to cisplatin, we did not observe the same in cell growth (confluence) assays. We also mention the caveat that a variety of other pathways that can be involved in either MMC or cisplatin resistance could contribute to the differences observed in sensitivity.

Results, lines 256-262:

> ***"FANC-high lines also responded to mitomycin C, another crosslink-inducing chemotherapy, with increased FANCD2 ubiquitination and resistance to cell death, though no difference was observed in cell confluence (Extended Data Fig. 13E-G). The similarity in pathway activation and cell death resistance between cisplatin and mitomycin C supports that sensitivity stemmed from FANC repair of inter-strand crosslinks, while the expression of other resistance pathways may have contributed to variation in the degree of sensitivity."***

Comment 1.10.2: *It is somewhat surprising that over-expression of a single member of the FANC pathway (FANCF), albeit a critical component, is sufficient to partially overcome cisplatin sensitivity in a FANC-low cell line. Given that the FANC signature is calculated from levels of dozens of FANC gene transcripts, it is not necessarily obvious that over-expressing a single member of the pathway will change pathway activity (unless its known that the level of that specific protein is the activity-limiting feature of the pathway).*

Response 1.10.2) We chose to overexpress FANCF in this context because overexpression of this single FANC component has been shown previously to restore resistance to both melphalan and adriamycin, two other interstrand crosslinking agents (PMID: 15802532, 24996439). Therefore, though it is not known that FANCF is the limiting protein in this pathway, it has been shown to be a critical component whose overexpression can significantly affect pathway activity and drug resistance, potentially due to mechanisms such as increased complex stability (PMID: 22675617). Overexpression of FANCF to the degree achieved in experiments (8.8x increase in protein expression) would increase the 11-gene FANC signature in UBLC1 from its baseline -5.98 to -2.46. While this is still lower than that of the high FANC cell lines SW780 (FANC score = 6.11) and HT1376 (5.51), the experiments demonstrate this increase to be sufficient to partially restore cisplatin resistance (**Extended Data Figure 14G-I**). As expected in such an overexpression system, the increase in resistance upon FANCF overexpression is more moderate than either the difference in sensitivity observed between the original FANC-high and FANC-low cell lines

(**Figure 4F-H**) or that observed upon FANCF knockdown (**Figure 4J-L**). Therefore, we believe the results of these experiments to be in line with expectations from previously published literature and the degree of change observed in the FANC expression signature. We have added this reasoning into the results section.

Results, lines 263-266:

> ***"We further validated the relationship between FANC expression and cisplatin response by knocking down or overexpressing FANCF, a key component of the FANC core complex that has been previously shown to modulate crosslinker sensitivity alone[53–55], in the highest (SW780) and lowest (UBLC1) FANC-expressing cell lines, respectively."***

Referee #1 (Remarks on code availability):

I reviewed the code but am not an expert and therefore may not appreciate all relevant nuances.

Referee #2 (Remarks to the Author):

We would like to thank the reviewers for their extensive work and structured comments to our review. We believe the manuscript has improved substantially. We have no further comments in addition to our previous comments that were all addressed by the authors.

Thank you, we appreciate the reviewer's comments that were able to strengthen the work presented in our manuscript.

Referee #3 (Remarks to the Author):

I would like to thank the authors for their extensive and detailed revisions and responses. The authors have addressed all my concerns and they should be congratulated for their outstanding manuscript.

We thank the reviewer for their kind words. We are glad to have addressed all your comments, which have improved the quality of our manuscript.

Referee #4 (Remarks to the Author):

I co-reviewed this manuscript with one of the reviewers who provided the listed reports.

Referee #4 (Remarks on code availability):

The code is well documented and it can be used for replication studies.

Referee #5 (Remarks to the Author):

I co-reviewed this manuscript with one of the reviewers who provided the listed reports.